

Design-Integrated Urban Heat Island Analysis Tool and Workflow: Development and Application

by

Hellen Rose Anyango Awino

*Bachelor of Architecture
University of Texas at Austin, 2014*

Submitted to the Department of Architecture
in Partial Fulfillment of the Requirements for the Degree of

Master of Science in Architecture Studies
at the
Massachusetts Institute of Technology

June 2019

© Massachusetts Institute of Technology.
All rights reserved.

Signature of Author: _____
Department of Architecture
May 23, 2019

Certified by: _____
Leslie K. Norford
Professor of Building Technology
Thesis Supervisor

Accepted by: _____
Nasser Rabbat
Aga Khan Professor
Chair of the Department Committee on Graduate Students

Committee

Thesis Supervisor:

Leslie K. Norford, PhD
George Macomber Professor in Construction Management
Professor of Building Technology
Associate Head, Department of Architecture

Thesis Readers:

Christoph Reinhart, PhD
Professor of Building Technology

Carlos Cerezo Davila, PhD
Environmental Performance Director at KPF New York

Design-Integrated Urban Heat Island Analysis Tool and Workflow: Development and Application

by

Hellen Rose Anyango Awino

Submitted to the Department of Architecture on May 23, 2019 in Partial Fulfillment of the Requirements for the Degree of Master of Science in Architecture Studies

Abstract

The Urban Heat Island (UHI) effect is a well-studied phenomenon broadly attributed to human activities that transform open terrain into cityscapes. Among global 21st-century concerns, projected trends in population growth, urbanization, and regional climate change could exacerbate the warming in cities and intensify the UHI effect. Yet, microclimate analysis essential to assessing UHI intensity is often neglected, resulting in poor planning practices with adverse effects on health, comfort and energy use within cities. With buildings responsible for substantial quantities of global energy consumption and carbon emissions, this context demands climate-responsive design to achieve better-performing cities.

The UHI effect presents an urban design challenge, but only recently has there been a platform for design workflow integration. Despite existing engines that accurately evaluate UHI intensity in urban environments, architects, designers, and urban planners have often not incorporated such simulation into microclimate studies due to prohibitively expensive computational costs, disconnected workflows within unintuitive or unfamiliar platforms, and uncertainty about difficult-to-obtain urban climatology parameters. These hindrances cause impactful delay within the design feedback loop and often generate a lack of confidence in the simulation process and output.

This thesis proposes a Computer-Aided-Design integrated graphical user interface for the Urban Weather Generator (UWG), an urban-scale climate prediction tool developed by Bruno Bueno to simulate microclimatic conditions of urban sites using operational weather station data. The goal is to make the powerful and computationally cheap engine accessible to design workflows by incorporating it as a plugin within the conventional design software Rhinoceros-3D, and by coupling it with the Local Climate Zone classification scheme developed by urban climate experts Iain Stewart and Timothy Oke to standardize quantitative physical descriptions of cities. The proposed update automates geometric parameter extraction and implements a reliable means of urban morphological parameter estimation. As a case study, an iterative urban-scale design exploration is analyzed for selected climates.

Thesis Supervisor: Leslie Keith Norford

Title: Professor of Building Technology and Associate Head of the Department of Architecture

Contents

| | |
|---|-----------|
| Abstract | 3 |
| Contents | 5 |
| Acknowledgements | 8 |
| List of Figures | 9 |
| List of Tables | 11 |
| Nomenclature | 12 |
| 1. Introduction | 13 |
| 1.1. Objective | 13 |
| 1.2. Context | 13 |
| 1.2.1. Population Growth and Rapid Urbanization | 13 |
| 1.2.2. Urban Heat Island Effect | 14 |
| 1.2.3. Microclimate Analysis | 16 |
| 1.3. Thesis Structure and Scope | 17 |
| 2. Background | 18 |
| 2.1. Urban Weather Generator (UWG) | 18 |
| 2.1.1. Engine | 18 |
| 2.1.1.1. UWG Parameters | 21 |
| 2.1.1.2. Limitations | 22 |
| 2.1.2. User Interfaces | 23 |
| 2.1.2.1. Workflows | 23 |

| | | |
|----------|--|----|
| 2.1.2.2. | Tool Accessibility | 25 |
| 2.2. | Local Climate Zone Classification System | 26 |
| 2.2.1. | Typologies | 27 |
| 2.3. | UWG and LCZ | 30 |
| 3. | Urban Weather Generator for Rhino | 31 |
| 3.1. | Integration into Rhino and Use Interaction | 31 |
| 3.1.1. | Graphical User Interface | 32 |
| 3.1.1.1. | File and Directory Input | 33 |
| 3.1.1.2. | Building and Urban Parameter Input | 34 |
| 3.1.1.3. | Simulation Parameter Input | 35 |
| 3.2. | Workflow | 36 |
| 3.2.1. | Current Workflows | 37 |
| 3.2.2. | Proposed Workflow | 38 |
| 3.2.2.1. | Geometric Parameter Extraction | 38 |
| 3.2.2.2. | Morphological Parameter Extraction | 40 |
| 4. | Design-Integrated Urban Analysis | 41 |
| 4.1. | Overview | 41 |
| 4.2. | Methodology | 42 |
| 4.2.1. | Tested Model Sets | 43 |
| 4.2.2. | Simulation Parameters | 45 |
| 4.3. | Results and Findings | 47 |
| 4.3.1. | Model Results | 47 |

| | |
|--|------------|
| 4.3.2. Climate Impact | 88 |
| 4.3.2.1. Temperature | 88 |
| 4.3.2.1. Rural Reference Location | 88 |
| 4.3.2.3. Wind and Water Observations | 91 |
| 4.3.3. Energy Use Intensity | 93 |
| 4.3.3.1. Vegetation Impact | 95 |
| 4.4. Carbon Intensity and Cost | 100 |
| 5. Conclusion | 103 |
| 5.1. Summary of Contributions | 104 |
| 5.2. Future Work | 105 |
| References | 106 |
| Appendix | 109 |
| A. Tested Model Sets Expanded Information | 109 |
| B. Local Climate Zones Abridged Definitions | 117 |
| C. Local Climate Zone Parameters | 118 |

Acknowledgements

I have had the great privilege to work under respected faculty and with remarkable peers over my two years at MIT. I am forever grateful for this time, and for the knowledge and experiences shared.

First, I would like to thank my advisor, Professor Leslie Norford. I greatly appreciate the time I have spent learning from you and your generous support over the two years. Your advice and wisdom have pushed me to explore beyond my boundaries. I am grateful for the guidance of Professor Christoph Reinhart. Your curiosity and never-ending enthusiasm have inspired me to question everything and trust my intuition. I am very thankful for the advice of Carlos Cerezo Davila. Your insight and mentorship has been an invaluable part of my learning.

To dear Anna Song, this process would not be possible without you. I am forever grateful for your patience, persistence, openness to explore unknown territories and continued interest and effort in making the GUI work.

I would like to thank Chris Mackey, Saeran Vasanthakumar and Ladybug Tools LLC for their continued guidance and support in the development of the UWG for Rhino GUI as well as for the support of the open source code. I would like to thank the Urban Interface and the Environmental Performance teams at KPF for their collaboration and generous contribution of the urban design iterations considered in this study. I am grateful for the work of the Bruno Bueno and all the contributors who followed to further develop and maintain UWG.

A special thank you to dear Andreea O'Connell, Suraiya Baluch and Cynthia Stewart: I can never forget your overwhelming kindness. Thank you for your generous support.

Thank you to my inspiring BT lab colleagues for the supportive community. A special thank you to Nate and Shreshth for your critical advice and refreshing perspectives. A special thank you to Alpha, Moh, and Khadija for your always kind and encouraging words, and for the shared laughter.

To dear Petra Liedl, I am forever grateful for the confidence you have had in me over the years.

To dear Nubianna Aben, Jossie Osellu and Jackie Lieck, I have carried your love and support with me over the years.

Finally, to Judith Millicent Were, Ishmael Jackoyo and Patricia Lohra Atieno: joka Awino, words can never describe the gratitude I have for your unconditional love, support and encouragement. I appreciate your care. Nyar Kobiero odagi loch.

List of Figures

| | |
|--|----|
| Figure 1. Growth Rates of Urban Agglomerations by Size Class, 2018-2013 | 13 |
| Figure 2. Spatial and Temporal Profiles of the UHI Effect and Schematic Description of Urban | 15 |
| Figure 3. UWG Engine Components : | 20 |
| Figure 4. UWG Microsoft Excel Interface | 24 |
| Figure 5. UWG Dragonfly Workflow | 26 |
| Figure 6. LCZ Classification Components | 27 |
| Figure 7. Standard classified LCZs | 28 |
| Figure 8. LCZ Subclasses with combined built and land cover types | 29 |
| Figure 9. UWG for Rhino Input Framework | 32 |
| Figure 10. EPW + STAT File Input | 33 |
| Figure 11. Unit Check | 33 |
| Figure 12. Building Typology Parameters | 34 |
| Figure 13. Rhino 3D Canvas Building Selection | 35 |
| Figure 14. Urban Parameters | 35 |
| Figure 15. Run UWG Window | 36 |
| Figure 16. UWG Simulation Process | 36 |
| Figure 17. Current Design Workflow of Text-based UIs | 37 |
| Figure 18. Rhino 3d replaces textual description of urban sites | 38 |
| Figure 19. Rhino 3d reduced workflow | 39 |
| Figure 20. UWG for Rhino Workflow | 39 |
| Figure 21. LCZ Parameter Extraction | 40 |
| Figure 22. ASHRAE Climate Zones | 42 |
| Figure 23. LCZ Parameter Extraction | 42 |
| Figure 24. Iteration 1 | 43 |
| Figure 25. Iteration 2 | 43 |
| Figure 26. Iteration 3 | 44 |
| Figure 27. Iteration 4 | 44 |
| Figure 28. Traffic Schedule | 47 |
| Figure 29. William P. Hobby Airport, Houston | 89 |
| Figure 30. Hartsfield-Jackson Atlanta International Airport, Atlanta | 89 |

| | |
|--|-----|
| Figure 31. Seattle-Tacoma International Airport, Seattle | 90 |
| Figure 32. O'Hare International Airport, Chicago | 90 |
| Figure 33. LaGuardia Airport, New York | 91 |
| Figure 34. Seattle-Tacoma, Seattle Wind Wheel | 92 |
| Figure 35. LaGuardia, New York Wind Wheel | 93 |
| Figure 36. Net Change in Cooling and Heating EUI | 94 |
| Figure 37. Model Set 1 Cooling EUI | 96 |
| Figure 38. Model Set 1 Heating EUI | 96 |
| Figure 40. Model Set 2 Cooling EUI | 97 |
| Figure 41. Model Set 2 Heating EUI | 97 |
| Figure 42. Model Set 3 Cooling EUI | 98 |
| Figure 43. Model Set 3 Heating EUI | 98 |
| Figure 44. Model Set 4 Cooling EUI | 99 |
| Figure 45. Model Set 4 Heating EUI | 99 |
| Figure 46. Houston CO ₂ Intensity and Electricity Cost | 100 |
| Figure 47. Atlanta CO ₂ Intensity and Electricity Cost | 101 |
| Figure 48. New York CO ₂ Intensity and Electricity Cost | 101 |
| Figure 49. Seattle CO ₂ Intensity and Electricity Cost | 102 |
| Figure 50. Chicago CO ₂ Intensity and Electricity Cost | 102 |

List of Tables

| | |
|---|-----|
| Table 1. UWG Simulation Parameters | 45 |
| Table 2. UWG Building Typology Parameters | 46 |
| Table 3. LCZ Properties for used typologies (I. D. Stewart & Oke, 2012) | 46 |
| Table 4. Local Climate Zones Abridged Definitions | 117 |
| Table 5. Local Climate Zone Parameters | 118 |

Nomenclature

EnergyPlus Weather Data (EPW)
EnergyPlus Weather Data Statistics (STAT)
Microsoft Excel (XLSM)
Extensible Markup Language (XML)
Comma Separated Value (CSV)
Urban Heat Island (UHI)
Urban Cool Island (UCI)
Urban Weather Generator (UWG)
Computer Aided Design (CAD)
The US Department of Energy (DOE)
Rhinoceros 3D (Rhino)
Grasshopper (GH)
MATLAB formatted data (MAT)
Boundary Representation Objects (BREPs)
Local Climate Zones (LCZ)
World Urban Database and Access Portal Tools (WUDAPT)
Urban Modeling Interface (umi)
Design Iterate Validate Adapt (DIVA)
Architecture Engineering Construction (AEC)
Rural Station Model (RSM)
Vertical Diffusion Model (VDM)
Urban Boundary Layer Model (UBLM)
Urban Canopy Layer (UCL)
Urban Canopy – Building Energy Model (UC-BEM)
Floor Area Ratio (FAR)
National Renewable Energy Laboratory (NREL)

1. Introduction

1.1. Objective

The objective of this research is to incorporate Urban Heat Island analysis into a useful design workflow in order to shape urban design practices that affect building performance.

1.2. Context

1.2.1. Population Growth and Rapid Urbanization

The United Nations projects that the world population will reach 8.6 billion by the year 2030, 9.8 billion by 2050, and 11.2 billion by 2100 (UN-DESA Population Division, 2017). The majority of this growth, as illustrated in Figure 1, is foreseen in the developing regions of the world, especially Africa and Asia, which are also set to experience the highest rates of urbanization globally with average growth rates between 3% and 5% (UN-DESA Population Division, 2018a).

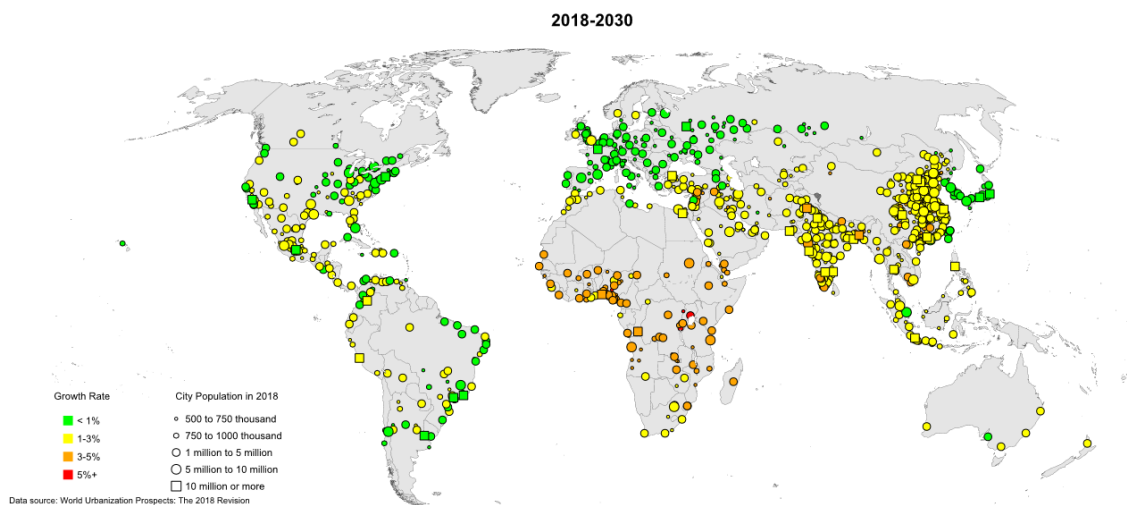


Figure 1. Growth Rates of Urban Agglomerations by Size Class, 2018-2030 (UN-DESA Population Division, 2018b)

In many regions, this growth will occur informally and largely through unstructured densification that will strain local resources and pose major hindrances to governments already struggling to address the various developmental challenges triggered by urbanization (UN-DESA Population Division, 2015)(UN-DESA Population Division, 2014). Issues such as lack of infrastructure and housing, increased density and congestion, and inadequate planning for large-scale energy- and resource efficiency require both urgency and careful consideration in planning.

1.2.2. Urban Heat Island Effect

Characteristically, urbanization imposes significant environmental changes on the urban environments it produces. One such major consequence is the considerable increase of temperatures in urban centers relative to surrounding rural or undeveloped areas due to the transformation of open terrain into dense, urban cityscapes. This phenomenon, known as the Urban Heat Island (UHI) effect, was first proven in early 1800s studies by the pioneer of urban climate studies, Luke Howard (Howard, 1883). It has since been extensively documented in numerous city- and climate-specific field experiments that have demonstrated the UHI effects' magnitude and characteristics.

Causes of the UHI effect lie in the roughness of urban areas along with the artificial materials that blanket these canyons relative to the open, natural terrain of rural surroundings. The differences in morphology disrupt surface energy and radiation balances and cause cities to experience increased temperatures (Oke, 1982). Increased urban surfaces cause greater absorption of solar radiation. The canyons created by the vertical profiles of buildings restrict the surfaces' exposure to the relatively cool sky and reduce wind speeds, thereby respectively decreasing radiative and convective heat removal from the canyons (Oke, 1982). The material choices of urban surfaces cause increased thermal admittance and decreased evapotranspiration due to reduced amount of vegetation (Oke, 1982). Additionally, the waste heat from the combustion of fuels for transportation, industrial processes and building conditioning causes increased anthropogenic heat gain (I. D. Stewart & Oke, 2012).

The UHI effect has both spatial and temporal profiles. In spatial form, the UHI effect is characterized by a sharp rise in the canopy-layer air temperature at the boundary of rural - suburban areas, followed by a slow and often variable increase towards the downtown core of the urban area where the warmest temperatures occur (Figure 2a). In temporal form, the UHI effect has a diurnal

pattern with the highest intensity at night (Figure 2b), expressing a lag in the cooling of cities, and in some situations leading to the opposite “urban cool island” effect during early morning hours.

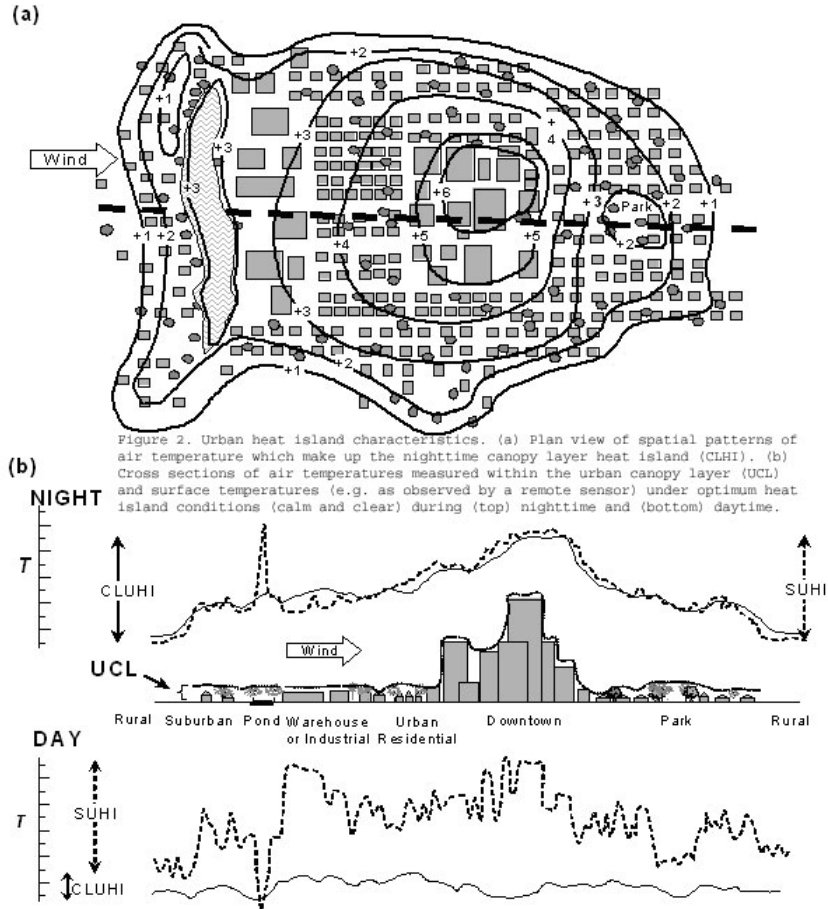


Figure 2. Spatial and Temporal Profiles of the UHI Effect and Schematic Description of Urban Atmosphere Components
(Voogt, n.d.)

The UHI effect implicates some of the most significant challenges of the twenty-first century: the population growth and rapid urbanization discussed in the above section, as well as regional climate change and global warming. These challenges put sustainable urban development as one of the top priorities of the century. However, without proper understanding of and action to properly mitigate the UHI effect, these combined factors could exacerbate the warming in cities and intensify the UHI effect. This becomes highly detrimental to health and comfort within cities, energy use intensity (EUI) and carbon footprints of urban areas and incontestably, the impact of regional climate change on urban systems.

1.2.3. Microclimate Analysis

Microclimate analysis is one of the first steps that architects typically make when approached with a design exercise. This process involves documenting the physical aspects of site context such as neighboring buildings, streets, and vegetation, as well as the environmental factors affecting the site such as wind speeds and direction, sun path and radiation, and temperature ranges and humidity. This process is not only important for creating a design that is contextually responsive, but it is crucial for developing climate-responsive strategies to inform design decisions.

The environmental site factors are available in weather files typically developed for cities globally. The United States Department of Energy (U.S. DOE) funds a database managed by the National Renewable Energy Laboratory (NREL) to collect this information in a format named EnergyPlus Weather (EPW) file that is made available on the EnergyPlus website (<https://energyplus.net/weather>). This file has compiled weather statistics measuring the environmental factors mentioned above on an hourly basis.

The gap between the UHI effect and urban design and building performance lies in microclimate analysis. The difference in temperatures between rural and urban areas is often unaccounted for because the EPW data for a city is typically gathered ten meters above ground at an airport. For most cities, airports are located on the more rural outskirts, but the collected information is still used to describe the urban centers, causing a discrepancy between the provided and actual conditions of the urban area. This oversight often results in design errors for various performance metrics that are useful for benchmarking and establishing environmental performance targets at both building- and urban scales. Ultimately, the design decisions made for urban spaces contribute to global environmental impacts.

1.3. Thesis Structure and Scope

The objective of this research is to incorporate Urban Heat Island analysis into a useful design workflow in order to bridge the gap between the UHI effect analysis and the practices that shape urban design and affect building performance. This thesis is structured in three parts:

1. The proposal of a Computer-Aided-Design (CAD) integrated graphical user interface (GUI) for the Urban Weather Generator (UWG), an urban-scale climate prediction tool developed by Bruno Bueno to simulate microclimatic conditions of urban sites using operational weather station data (Bueno, 2012).
2. The integration of the Local Climate Zone classification scheme developed by urban climate experts Iain Stewart and Timothy Oke to standardize quantitative physical descriptions of cities (I. D. Stewart & Oke, 2012).
3. A demonstration of the workflow in an iterative urban-scale design exploration analyzed for selected climates using UHI intensity to compare cost and carbon intensity.

The goal is to make the powerful and computationally cheap engine accessible to design workflows by incorporating it as a plugin within the conventional design software Rhinoceros-3D (Rhino 3D), and by coupling it with the LCZ scheme. By linking three components, UWG, rhino 3D and the LCZ scheme, the proposed workflow automates geometric parameter extraction and implements a reliable means of urban morphological parameter estimation.

2. Background

2.1. Urban Weather Generator (UWG)

The Urban Weather Generator (UWG) is a physics-based urban-scale climate prediction tool developed by Bruno Bueno (2012) to simulate microclimatic conditions of specific urban sites using operational weather station data. The UWG software takes in meteorological conditions recorded at a rural reference site in the form of an EPW file and morphs the data to output simulated hourly urban air temperature based on specified urban characteristics. The output allows for precise analysis and planning in the design process, as well as for accurate predictions of energy performance at building and neighborhood scales.

2.1.1. Engine

UWG uses energy balance equations to evaluate the two-way interactions between buildings and the climate by implementing four components (Figure 3): rural station model (RSM), vertical diffusion model (VDM), urban boundary-layer model (UBLM), and urban canopy and building energy model (UC-BEM) (Bueno 2012; Bueno et al. 2012). The engine takes into consideration local surface radiation exchanges, sensible heat fluxes from building operations and from building surfaces to output urban-scale building and climate information including building energy consumption, urban air and surface temperatures, surface solar irradiation, local wind speeds as well as urban heat island intensity (Bueno et al., 2012; Yang, 2016).

The RSM is based on an energy balance at the soil surface; a transient heat diffusion equation that represents the storage and release of heat from the ground is solved via finite differences. The RSM collects hourly-recorded meteorological data from a rural reference site, calculates the sensible heat fluxes, and provides the solutions to the VDM and UBLM.

The VDM applies a heat diffusion equation to calculate vertical air temperature profiles above the reference weather station. It uses the air temperatures and velocities read from the reference weather station and the sensible heat fluxes calculated at the RSM as input. The computed air temperatures are forwarded to the UBLM.

The UBLM uses an energy balance for a designated control volume within the urban boundary layer to calculate air temperatures above the urban canopy layer. The calculation uses air temperatures at the different heights provided by the VDM and the rural and urban sensible heat fluxes provided by the RSM and the UC-BEM as input. The UBLM distinguishes the daytime boundary layer from the nighttime boundary layer, as well as the urban-sea breeze circulation, which is induced by the UHI effect and radial in form, from the advection effect of measured wind, which is horizontal and directional in flow.

The UC-BEM calculates urban canopy air temperatures and humidity levels using radiation, precipitation, air velocity and humidity data recorded at the reference weather station, as well as the air temperatures calculated by the UBLM. The model is based on the town energy balance (TEB) scheme developed by Masson (2000) to simulate turbulent fluxes within urban areas, and an integrated building energy model incorporated to more precisely capture the effects of buildings on the urban climate and the urban climate's effects on urban-scale energy consumption (Bueno, et al., 2012). The energy balance considers heat fluxes from building surfaces and roads, waste heat from HVAC equipment and other anthropogenic heat sources, and the radiant exchange between the urban canyon air and the sky. In order to maintain a low computational cost for simulations, the building energy model takes in assumptions and geometric representations of buildings simplified to a level of achieving a comprehensive BEM; it accounts for solar radiation, heat conduction through the envelope, ventilation and internal gains, as well as indoor humidity and air temperature fluctuation.

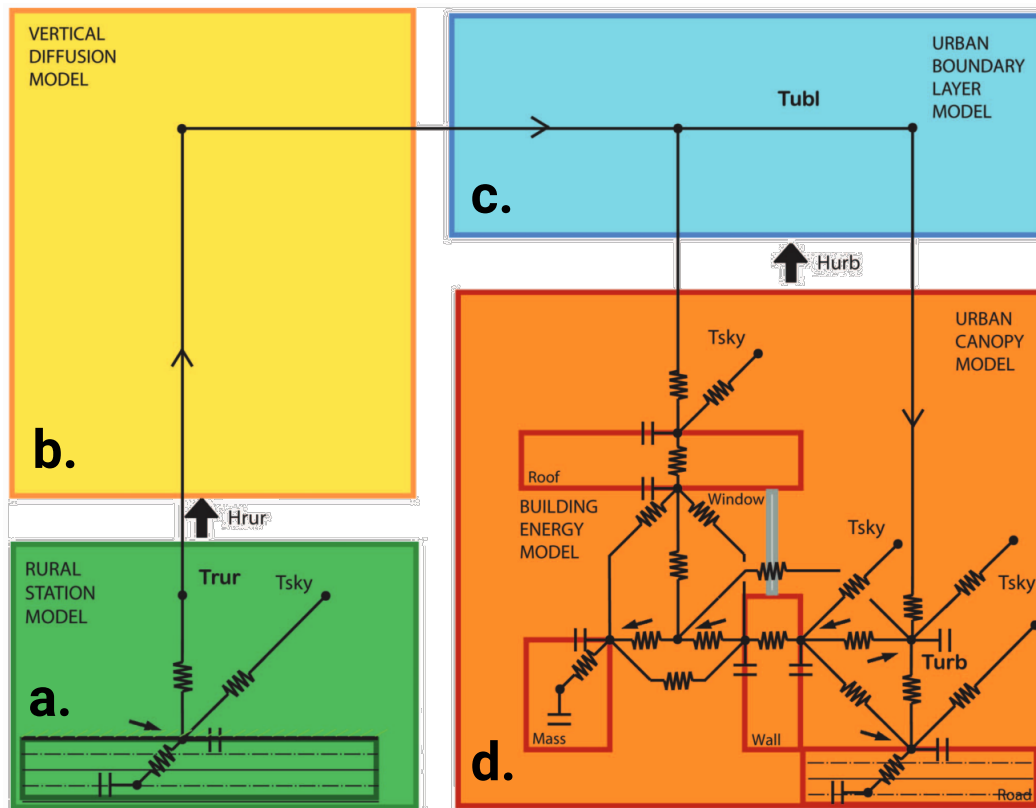


Figure 3. UWG Engine Components : the Rural Station Model (RSM), the Vertical Diffusion Model (VDM), the Urban Boundary-Layer (UBL) model and the Urban Canopy and Building Energy Model (UC-BEM). (Bruno Bueno et al., 2012)

The UWG engine has been tested for several climates, and through evaluations against measured data, the performance is found to be satisfactory; the expected error margin is within the air temperature range observed in different locations of the simulated urban area (Bruno Bueno et al., 2012). The engine's performance is also found to be comparable to counterpart atmospheric weather prediction models that can be computationally expensive; UWG's computational cost is intentionally maintained at the same order of magnitude as annual building energy simulations (Bueno et al., 2012). The economical computational nature of the engine lends itself well to iterative and parametric workflows that require relatively rapid feedback. The output allows for precise microclimate analysis that can lead to informed planning in the design process. The output can also be applied toward accurate predictions of energy performance at building and neighborhood scales.

2.1.1.1. UWG Parameters

The UWG requires more than 50 parameters that describe an urban site's morphological and geometrical parameters and a rural reference site's meteorological statistics that are to be morphed using the given urban site data. These inputs can be categorized into five clusters: building construction, including assembly and glazing; building operations and systems, including internal gains, ventilation and conditioning methods; urban characteristics, including site coverage, anthropogenic heat sources, vegetation properties and boundary layer parameters; and lastly, reference site location, obstacle height, meteorological factors and meteorological factors measurement height.

Various sensitivity analyses conducted over the years via UWG were used to zero in on key factors that contribute the highest impact on the UHI effect in different climates and in different urban configurations (Bueno et al., 2012; Mao et al., 2018; Nakano, 2015; Yang, 2016). The results of these analyses supported the UWG engine calibration - to make it more robust, more physically sound, and more capable of processing detailed building information - and critical for user experience, the sensitivity analyses have led to a reduction in the number of inputs to be entered by the user. UWG parameters are classified as required inputs or as optional parameters. From each of the analyses, parameters classified as required were found to have significant impact on the UHI effect across the climates tested and must therefore be input by users. Parameters found to have minor impact on the UHI effect are considered as optional and have been assigned reasonably estimated values as defaults that can be optionally adjusted by users.

The sensitivity analyses have also concluded that the UHI effect varies locally from place to place, and therefore, parameter sensitivity needs to be considered on a case by case basis (Mao et al., 2017). Bueno et al. (2012) conducted a study for Toulouse and Basel that revealed morphological parameters, specifically horizontal building density and façade-to-site area ratio, to be critical. Additionally, some vegetation parameters were found to be sensitive in the Basel case. Boston and Singapore case studies by Nakano (2015) confirmed the significance of site coverage ratio and façade-to-site ratio, and highlighted sensible anthropogenic heat and building roof material to be relevant, but determined that vegetation impact on the UHI effect in Boston was not captured by the UWG engine. Nakano (2015) also found the reference height of the VDM, which relates to the role of advection in the energy balance of the urban boundary layer, to be significant for Boston

and for cities with high wind velocities, although Bueno et al. (2014) resolved that advective heat flux had insignificant impact on the urban boundary layer energy balance. For an analysis completed in Abu Dhabi (Mao et al., 2017), no vegetation parameter was identified as a strong parameter; the authors attributed this to the fact that there is nearly no vegetation for the studied area. The most critical parameters identified by Mao et al. (2017) included the VDM reference height, the UCM-UBL exchange coefficient, the fraction of waste heat directed into the canyon and the winter-season nighttime boundary layer height; these values also happen to be the most uncertain and the most difficult to obtain.

2.1.1.2. Limitations

A major limitation of the UWG is the number of parameters required to run a simulation. In addition to geometric parameters, urban and reference site morphological parameters are also required and these tend to be difficult to obtain or unknown to many potential users outside of urban climatology field.

The UWG is not engineered to indicate varying UHI intensities within a specified urban site although such a study can be accomplished by parceling a broader urban site into microclimate-scaled pieces. The engine is also not engineered to capture specific building level details that could be captured by conducting a full energy analysis.

Depending on the type of vegetation prevalent on a site, grasses or trees, the method that the UWG engine uses to process vegetation representation may affect the outcome of the simulation. For wind, UWG does not simulate flows, rather it calculates the reduced canyon wind speeds due to obstacles and does not consider wind direction (Yang, 2016). Additionally, absolute humidity in urban area is assumed to be the same as the absolute humidity in the rural area and that is used to calculate the relative humidity in the urban area (Mao, 2018).

The simplifications and assumptions of the model prevent it from capturing very site-specific microclimate effects, particularly for highly heterogeneous urban sites. (Bueno et al., 2014). However, these simplifications contribute considerably to the engine's computational efficiency.

2.1.2. User Interfaces

Since the original development, the UWG has been edited and enhanced by Aiko Nakano (Nakano, 2015), Joseph Yang (Yang, 2016), Jiachen Mao (Mao, 2018) and Ladybug Tools LLC (<https://www.ladybug.tools>).

Currently, three different functional interfaces allow access to the UWG engine: an Microsoft Excel interface (UWG 4.1) maintained by Jiachen Mao (https://github.com/Jiachen-Mao/UWG_Matlab), a Python programming script (<https://github.com/ladybug-tools/uwg>), and a plugin for Rhino's graphical algorithm editor Grasshopper (GH) called Dragonfly (<https://www.ladybug.tools/dragonfly.html>). The two latter versions are developed and maintained by Ladybug Tools LLC (<https://www.ladybug.tools>). The Microsoft Excel interface uses the original MATLAB format. This MATLAB code was translated by Ladybug Tools LLC to create the Python programming script and is implemented in the Dragonfly plugin.

2.1.2.1. Workflows

The UWG requires meteorological parameters in the form of an EPW file and an EnergyPlus Weather Data Statistics (STAT) file, and an input file in the form of Microsoft Excel (XLSM), Extensible Markup Language (XML) or Comma Separated Value (CSV) defining the parameters that describe urban geometry, urban morphology and the reference site. The program outputs modified hourly weather data in the form of an EPW file, an open XML spreadsheet (XLSX), or a MATLAB formatted data (MAT) that can be used to extract urban-scale building and climate information.

The three UWG versions differ chiefly by user interaction and workflow. The Microsoft Excel interface (Figure 4) requires the user to key in a set of required values in cells categorized by urban and building characteristics, and a set of values that the interface derives from user input via simple calculations. The user must then open the UWG MATLAB code, provide an EPW file, reference the parameter XLSM file and define a save location file path before prompting UWG to run. The output options are XLSX, EPW and MAT formatted data. Apart from interface and interaction, UWG 4.1's other obstacle to accessibility is purchased license access to MATLAB, a software not commonly used within design workflows.

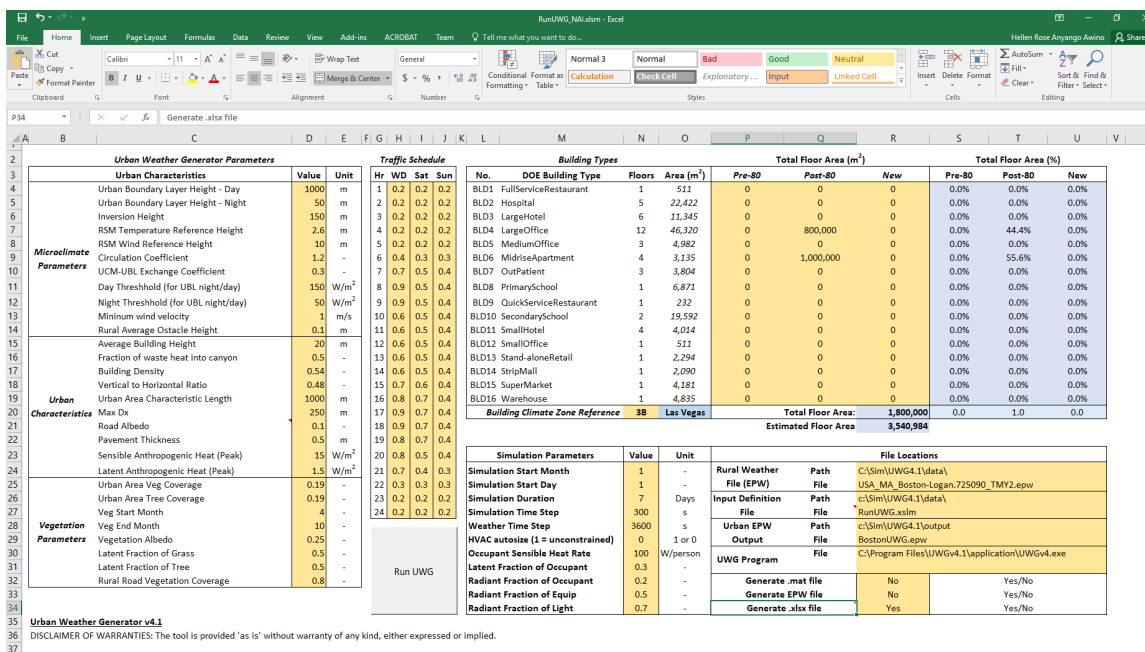


Figure 4. UWG Microsoft Excel Interface

The Python translation by Ladybug Tools LLC requires a parameter CSV file, an EPW file and a save directory. After editing the CSV file, the user must call a generated Python script, which references the required files and directory; via command prompt to execute UWG.

Presently, Dragonfly is the only functional UWG interface with a design-integrated workflow. Aiko Nakano, contributor to UWG 3.0, also recognized the need for the UWG tool within a design platform and developed a standalone interface as well as a plugin coupled with the Urban Modeling Interface (umi) plugin for Rhino, an engine used to simulate urban-scale operational energy, walkability and daylighting (Nakano, 2015). Maintenance, software compatibility issues, and hosting platform updates led to the UWG 4.1 upgrade although Nakano's accomplishment built the foundation for UWG design platform- and workflow-integration. Dragonfly enables the modeling and estimation of large-scale phenomena such as UHI, climate change, and local climate factors, such as topography, and makes climate variables accessible to a network of analysis tools that rely on climate data as a basis for analysis and simulation. The benefit of hosting UWG within the Ladybug Tools toolkit is to use standardized open formats for data transfer, to build interoperability with other Ladybug tools and to coalesce multiple components to accomplish specific tasks (Mackey & Roudsari, 2017).

2.1.2.2. Tool Accessibility

UWG 4.1 and the Python translation are text-based interfaces that predominantly require manual data entry and have workflows disconnected from those of CAD users, a large population of students, researchers and professionals who would benefit from including the UWG into early phases of urban climate prediction and analysis. The gap in the workflow is having to textually describe geometric parameters that can be extracted from the CAD models already created by CAD users. From the authors' experiences, this gap, along with the impression that the process may be less intuitive and less user-friendly for some designers, architects, and urban planners, discourages the implementation of the UWG into design analysis and consequently bypasses the iterative design feedback loop that can be engaged due to the computationally inexpensive nature of UWG calculations.

Moderately advanced visual scripting ability is required to run the UWG using Dragonfly, and Ladybug Tools provides sample workflow (Figure 5) with all necessary components (Mackey, 2017). Dragonfly uses GH to collect CAD objects from Rhino, fed in as boundary representation objects (BREPs) and obtains the geometric properties required for UWG parameters. Non-geometric parameters are input via text panels, drop-down selections or Boolean toggle buttons. The components are prepopulated with default values for parameters determined through UWG case studies and sensitivity analyses to have a small magnitude of impact on simulation results once set to initial reasonable estimates (Mao et al., 2017; Nakano, Bueno, Norford, & Reinhart, 2015). This significantly reduces the number of inputs required from the user but all parameters are visible and available for users to set. Values obtained from the interface populate a CSV file that runs UWG upon user command in GH. Dragonfly is a significant development in the process of incorporating UHI and urban climate analysis into an established network of building science tools within the design workflow.

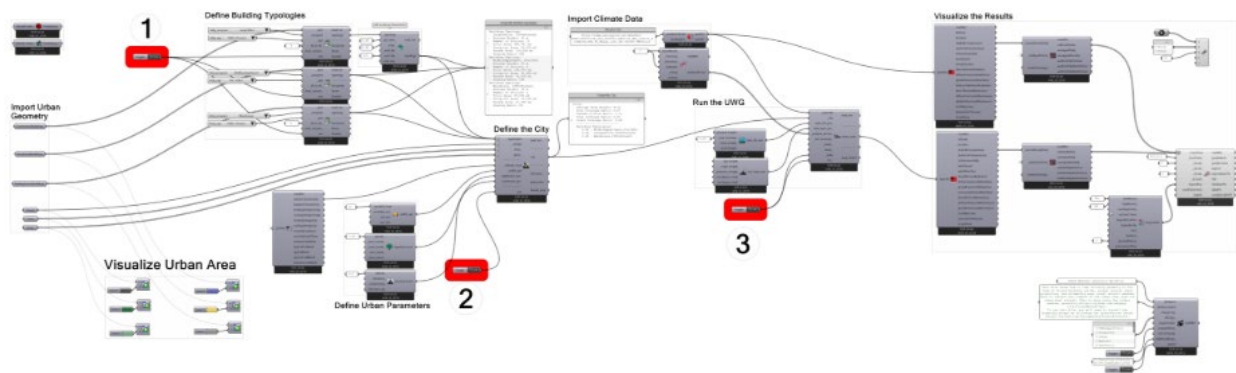


Figure 5. UWG Dragonfly Workflow

2.2. Local Climate Zone Classification System

Taking the temperature difference between what is classified as rural and what is classified as urban has made a simple framework to define and compare UHI intensity (I. D. Stewart & Oke, 2012). However, the clarity of the definitions for “rural” and “urban” make measuring UHI intensity more complex and sometimes problematic, especially for an entire urban space. Rural and urban environments vary greatly in complexity in each of their scopes. Variability in surfaces and surface roughness, material classifications, vegetation properties and the densities of these spaces all affect readings at both rural and the urban meteorological measurement stations. The contextual setting of a rural station, which is the base point for UHI intensity comparison, is just as important as the urban context.

Urban climate experts Iain Stewart and Timothy Oke introduced the Local Climate Zone (LCZ) classification system as a means to standardize the quantitative physical descriptions of cities in a way that is relevant to observing urban climates. They define a local climate zone as an area of uniform surface roughness and surface cover with a characteristic length of hundreds to several thousands of meters (I. D. Stewart & Oke, 2012). The uniformity of roughness element, buildings and vegetation, and surface cover types, permeable and impermeable, causes LCZ classifications to differ from one another in air temperature regime at one to two meters above ground (I. D. Stewart & Oke, 2012).

Other such classification schemes exist; however, the LCZ system is visual and largely based on the standard and quantitative characterizations of urban and rural spaces. The components of the classification have clear definitions for the values and ranges for four categories: the height of roughness features - buildings and vegetation, the density or packing of the roughness features, the permeability and impermeability of surrounding surface cover types, and the thermal admittance of the roughness features' and surface cover types' materials (Figure 6).

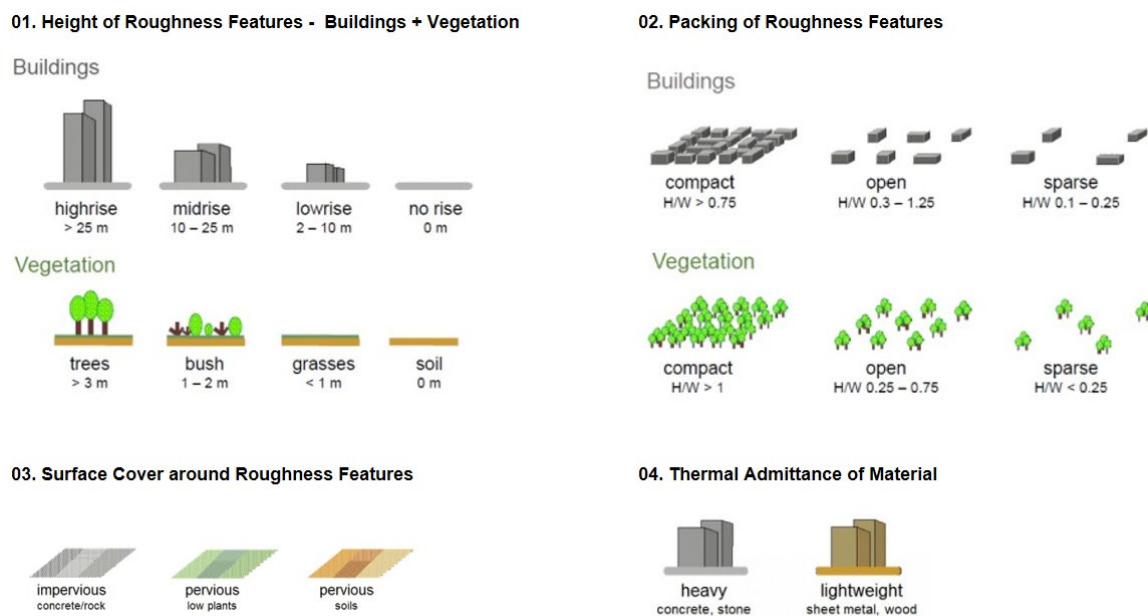


Figure 6. LCZ Classification Components (I.D. Stewart, 2011)

2.2.1. Typologies

The four defining LCZ components shown in Figure 6 result in numerous typological configurations that describe a range of terrains between the two extremes of rural and urban settings. For example, the urban extreme is a high, densely compact, impervious neighborhood constructed by heavy materials, and the rural extreme is a flat, open, pervious and bare landscape. The LCZ authors formulated a set of 17 likely but generic typologies to be used as the starting point for area classifications (Figure 7). These 17 types are divided into a built category comprising of LCZ numbers 1-10 in the classification, and land cover category - LCZ letters A - G in the

classification. The built category is based on predominant constructed features on a single land cover type and the land cover category is based on the parcel's seasonal or ephemeral features (I. D. Stewart & Oke, 2012).

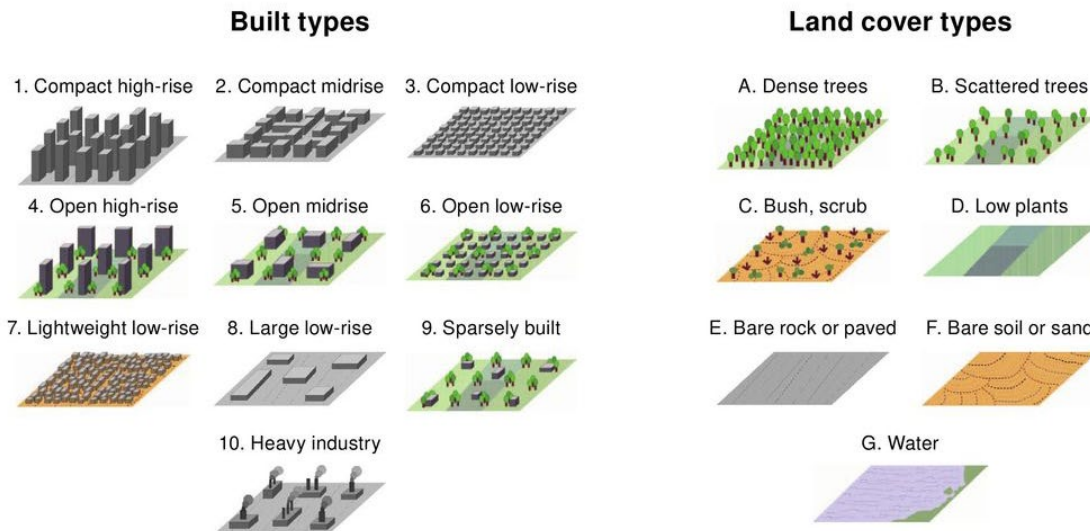


Figure 7. Standard classified LCZs (I.D. Stewart, 2011)

The authors formulated a means to conjoin the standard classes to create new, diversified and varied subclasses that accommodate flexibility. As opposed to the generic and strictly uniform compositions of the 17 standard typologies, the conjoined classes, or subclasses, are able to capture peculiarities and nuanced variations that are common in real rural and urban systems (Figure 8). The subclasses are composed of different mixtures of built types, land cover types and land cover properties of the higher and lower parent classes. The sub-classification system is best for including secondary features that are assumed to affect local climate and improve comparison of a particular site with other studies. For example, sub-classification allows temporal flexibility for studies focused on monthly, weekly or daily scales, or for studies that have features that change significantly with weather pattern i.e. snow covered ground, agricultural practices i.e. barren ground or seasonal changes i.e. wet, water-logged ground (I. D. Stewart & Oke, 2012). The authors advise against too many or too complex sub-classifications for the purpose of enhancing the physical site description because these undermine the principal function and may not result in observations significant difference from any parent class involved (I. D. Stewart & Oke, 2012).

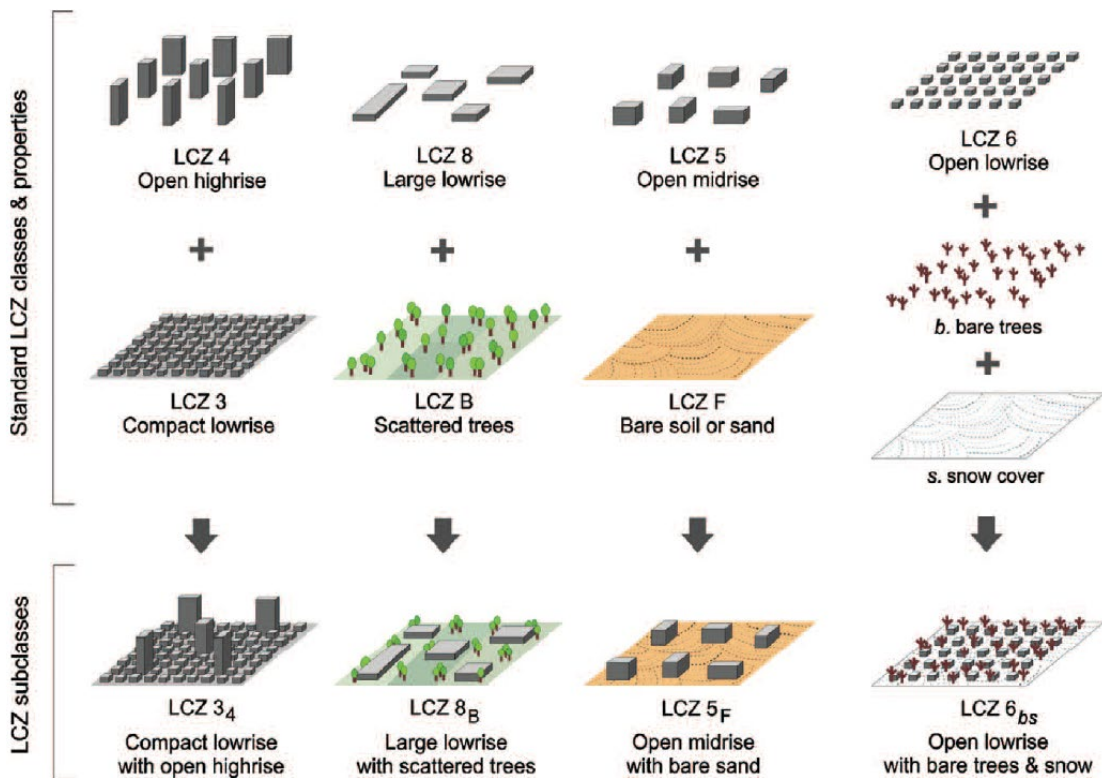


Figure 8. LCZ Subclasses with combined built and land cover types
(I. D. Stewart & Oke, 2012) ©American Meteorological Society. Used with permission.

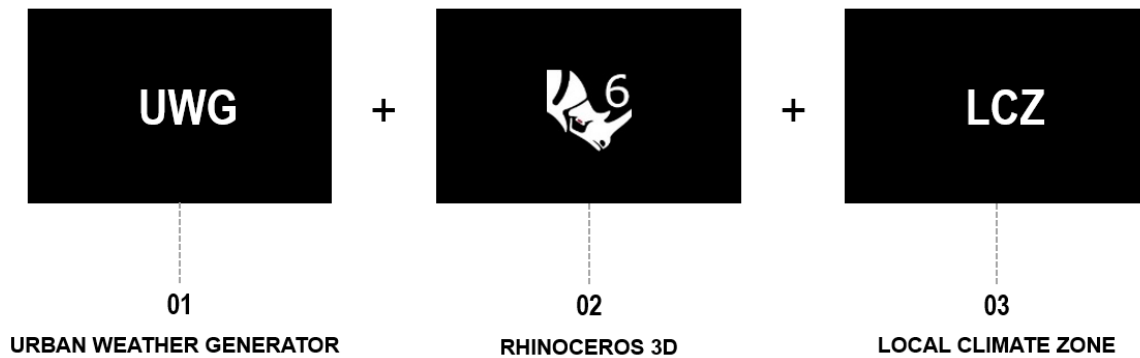
The key advantage of the LCZ classification system for UHI studies is that it clarifies the definitions of the terms “urban” and “rural” as typically used in UHI analyses thereby creating a framework for the standardization of urban temperature observations (I. D. Stewart & Oke, 2012). Because the system is based heavily on standard and defined geometric characterizations, urban spaces and rural areas are straightforwardly organized by where they fall on the spectrum.

2.3. UWG and LCZ

The LCZ framework is suitable for coupling with UWG because the difficult-to-obtain urban morphological parameters necessary for UWG simulation can be extracted through this classification system. From the observations made for each LCZ, a range of values is observed for sky view factor, aspect ratio, mean building or tree height, terrain roughness class, building surface fraction, pervious and impervious cover, surface admittance, albedo and anthropogenic heat flux. A combination of the first seven properties can be used to categorize a given site's LCZ class. Thereafter, the last three properties, which are relevant for UWG inputs, can be extracted and used to complete simulations.

This classification scheme was proposed as a more accurate framework for UHI effect studies. The property ranges defined by the authors are determined from urban climate studies and observations and are a better and more reliable means of estimating unknown urban morphological parameters. Additionally, there is an ongoing effort by World Urban Database and Access Portal Tools (WUDAPT) to map cities according to the LCZ scheme (www.wudapt.org/). Through a mapping tool published on their website, one can access LCZ maps available for various regions worldwide as they progressively become mapped. This means that LCZ parameters will increasingly become readily available and accessible information for microclimate studies.

A full definition and description of these parameter values can be found in the appendix of Local Climate Zones for Urban Temperature Studies (I. D. Stewart & Oke, 2012). Table 3 in the appendix C of this document displays LCZ properties.



3. Urban Weather Generator for Rhino

The UHI effect presents an urban design challenge, but only recently has there been a platform for design workflow integration. Despite existing engines that accurately evaluate UHI intensity in urban environments, architects, designers, and urban planners have often not incorporated such simulation into microclimate studies due to prohibitively expensive computational costs, disconnected workflows within unintuitive or unfamiliar platforms, and uncertainty of difficult-to-obtain urban climatology parameters. These hindrances cause impactful delay within the design feedback loop and often generate a lack of confidence in the simulation process and output.

The proposed tool, UWG for Rhino, is a CAD integrated GUI for the UWG. The goal is to make the powerful and computationally cheap engine accessible to design workflows by incorporating it as a plugin within the conventional design software Rhino 3D, and by coupling it with the LCZ classification scheme. The proposed update automates geometric parameter extraction through Rhino 3D and implements a reliable means of urban morphological parameter estimation through the LCZ scheme.

3.1. Integration into Rhino and Use Interaction

UWG for Rhino runs the Python translation of the original UWG MATLAB code completed by Ladybug Tools LLC (<https://github.com/ladybug-tools/uwg>). The Python programming application is more accessible than the MATLAB version because it does not require a license purchase. The plugin is programmed within Rhino version 6, which hosts a built-in developer

platform, Rhino.Python, used for cross-platform scripting (McNeel, 2019b). Rhino.Python applications operate on both Windows and Mac systems. The platform allows access to exclusive functions used within Rhino software that are otherwise inaccessible. It also offers Eto controls (McNeel, 2019a), an open source cross-platform dialog box framework unavailable to older Rhino versions, that is used to achieve a GUI consistent with the Rhino interface design.

UWG for Rhino handles geometric parameters the same way that Dragonfly does. It extracts geometric building properties such as height, footprint, floor area, and façade area, and geometric urban properties, such as land area, characteristic length and average obstacle height. From these properties, it is able to calculate building density, site coverage ratio, and façade-to-site ratio as well as generate weighted averages for building program and age so that users must not manually calculate and record these parameters.

3.1.1. Graphical User Interface

The GUI is clustered into three parts: (01) preliminary input, (02) parameter input and (03) simulation input as shown in Figure 9.

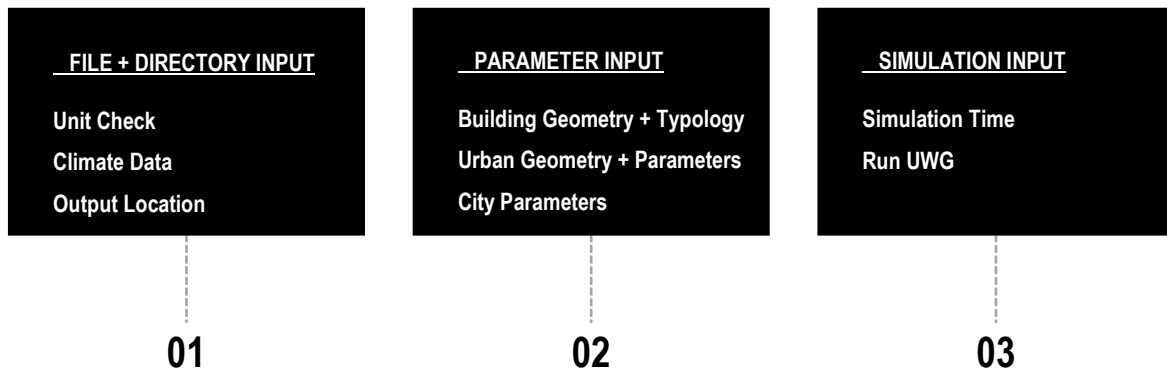


Figure 9. UWG for Rhino Input Framework

The preliminary inputs include import of climate data and the selection of an output directory for the resulting EPW file (01 in Figure 9). In this stage, there is a unit check, and conversion is possible, to assure the user is in metric units. The parameter input part is subdivided into three parts: selection of urban geometry and definition of building typology, definition of urban parameters and

definition of city parameters (02 in Figure 9). The simulation input is where the user can execute UWG after entering simulation run time (03 in Figure 9).

3.1.1.1. File and Directory Input

The first step is to prompt the user to input the necessary climate files: an EPW file as well as a STAT file. These can be downloaded directly from the U.S.DOE EnergyPlus website (<https://energyplus.net/weather>) via the provided “Download files” (Figure 10) or input from a local directory with the “Files on computer” (Figure 11) option. Next, the Rhino 3d file unit setting is checked. The user is warned in the case which a unit conversion must be completed.

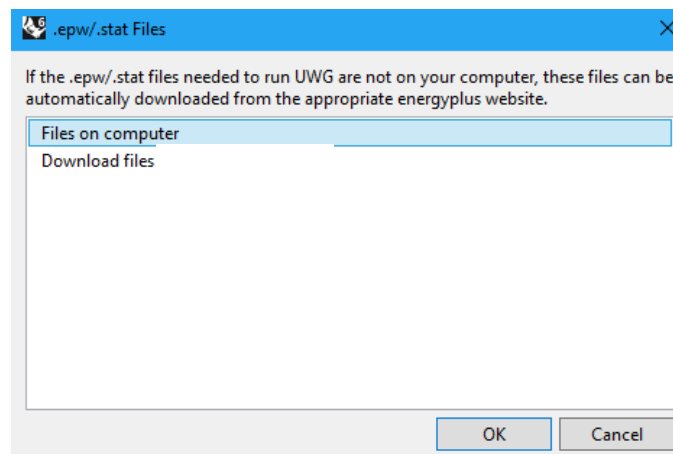


Figure 10. EPW + STAT File Input

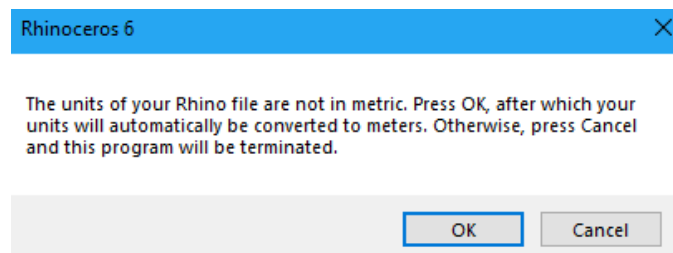


Figure 11. Unit Check

3.1.1.2. Building and Urban Parameter Input

The second step of the process is to input simulation parameters. Under the typology parameters tab (Figure 12), users can select 3D geometry to define the building typologies. Users can define buildings by selecting the geometry on the Rhino 3D work plane and clicking on “Add Typology” (01 in Figure 12). The selections can then be tagged as one of the U.S.DOE reference building types (<https://www.energy.gov/eere/buildings/commercial-reference-buildings>) and according to age (02 in Figure 12). All non-key parameters can be edited under the “Default Parameters” button (03 in Figure 12). Selected buildings are itemized under the “Select Building Typology” window (01 in Figure 12), and are displayed to the user via color scheme by reference type and color fade for age on the Rhino work plane (Figure 13).

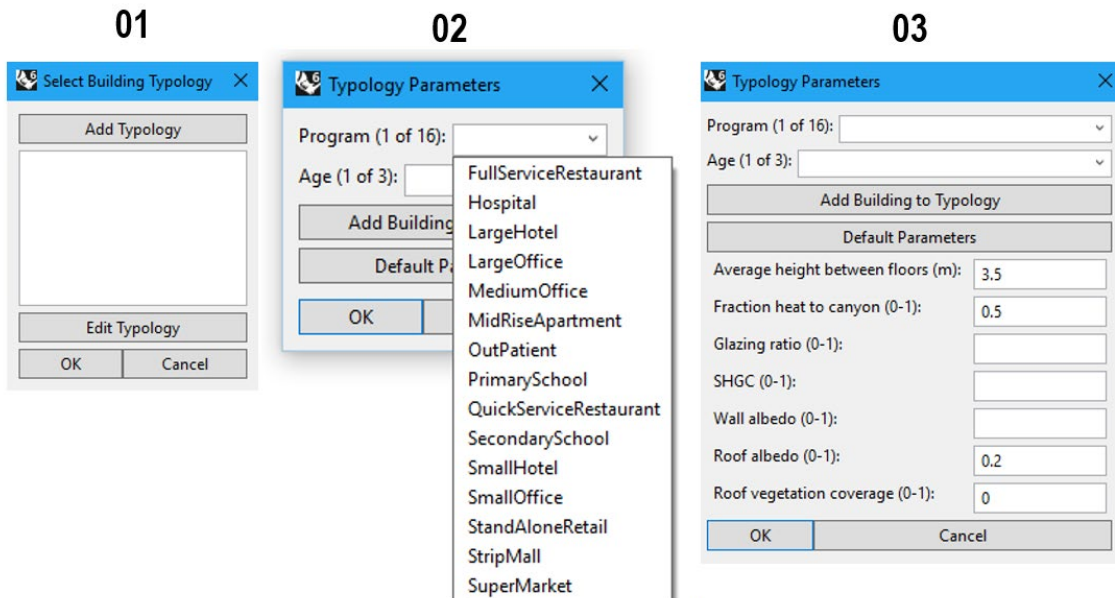


Figure 12. Building Typology Parameters

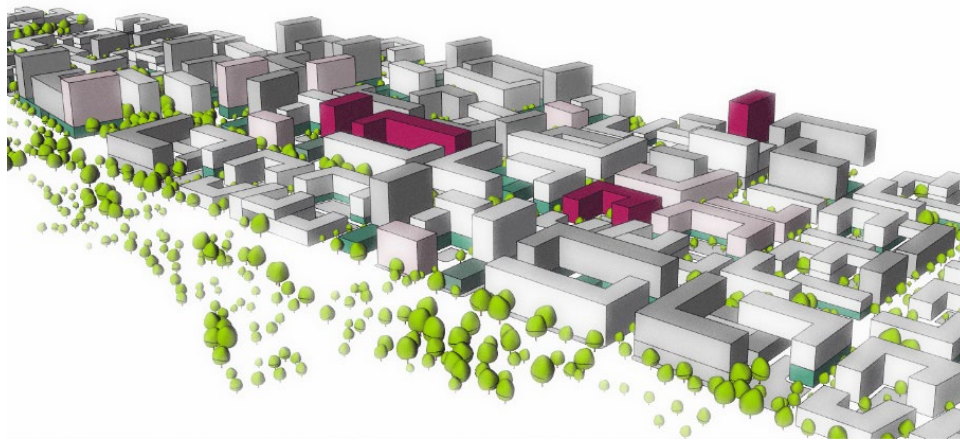


Figure 13. Rhino 3D Canvas Building Selection

Under the urban parameters tab, users select geometry and adjust parameters relating to vegetation (01 and 02 in Figure 14), and traffic parameters (03 in Figure 14). This input tab includes anthropogenic sensible heat flux and has a slider input to adjust traffic schedules.

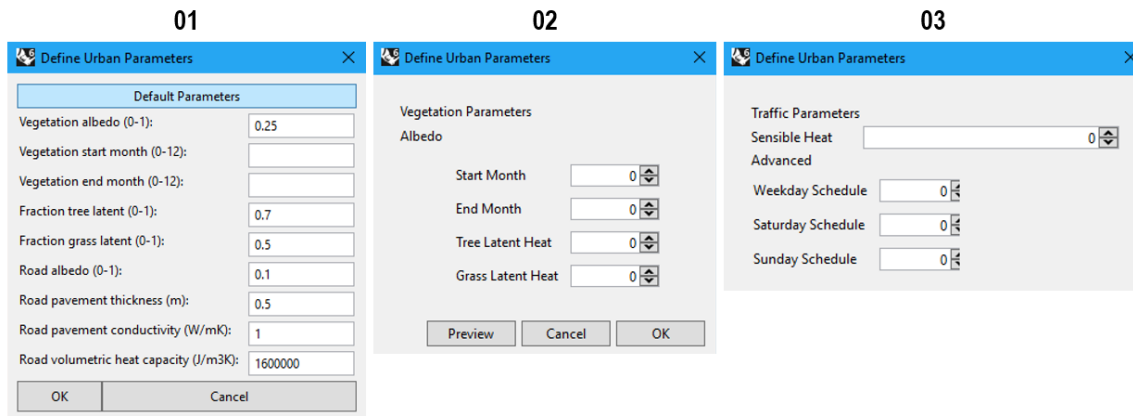


Figure 14. Urban Parameters

3.1.1.3. Simulation Parameter Input

The “Run UWG” tab is where the user can execute UWG (Figure 15). Here, simulation dates and time are defined to execute UWG. Additionally, one can enter advanced parameters regarding the boundary layer and the reference rural site.

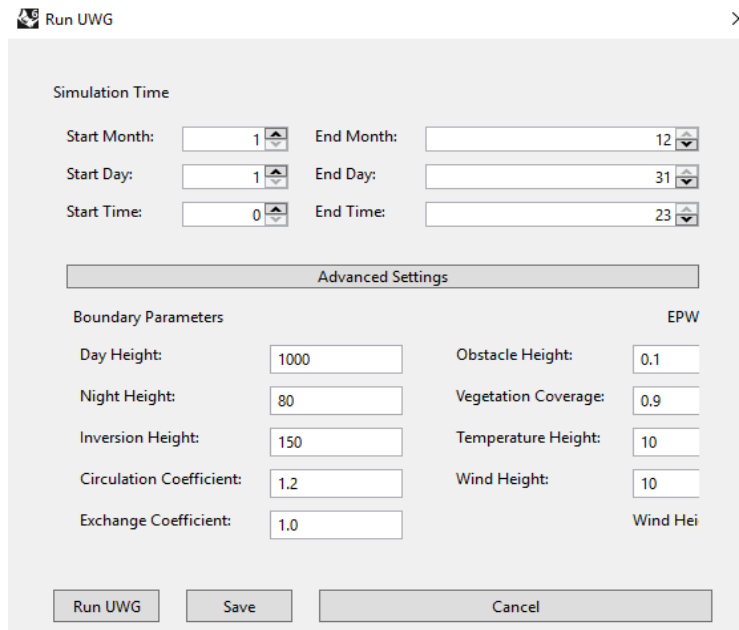


Figure 15. Run UWG Window

3.2. Workflow

In order to produce a morphed EPW weather data file, UWG requires climate data, informs of EPW and STAT files, a description of the reference site where the rural meteorological measurements are taken, and descriptions of the urban site and the urban morphology (Figure 16).

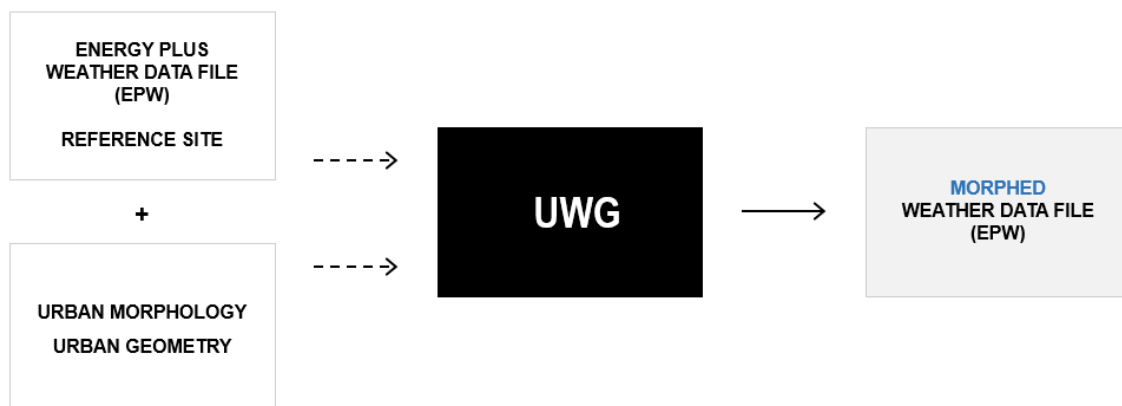


Figure 16. UWG Simulation Process

3.2.1. Current Workflows

The current Microsoft Excel and Python versions are text-based interfaces that predominantly require manual data entry and have workflows disconnected from those of CAD users, a large population of students, researchers and professionals who would benefit from including UWG into early phases of urban climate prediction and analysis. The user starts with an urban site to be analyzed and must textually describe urban geometry and urban morphological parameters in order to input that information into the UWG (Figure 17). Once UWG produces a morphed weather file, if the user changes the urban site based on findings from other studies, such as microclimate analysis, the user must again textually describe urban geometry and urban morphological parameters in order to reprocess the simulation (Figure 17).

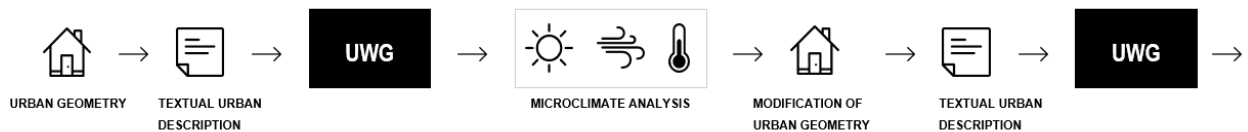


Figure 17. Current Design Workflow of Text-based UIs

The gap in the workflow is having to textually describe geometric parameters that can be extracted from the CAD models already created by CAD users. From the authors' experiences, this gap, along with the impression that the process may be less intuitive and less user-friendly for some designers, architects, and urban planners, discourages the implementation of UWG into design analysis. Consequently, the iterative design feedback loop that can be engaged due to the computationally inexpensive nature of UWG calculations is bypassed.

3.2.2. Proposed Workflow

UWG for Rhino is a design-integrated workflow alternative complementary to Dragonfly, the other functional UWG GUI. Whereas Dragonfly has a customizable workflow with modularized and interoperable components within the GH interface, UWG for Rhino is conceived for a simple and standard workflow. The goal is to further broaden the user base by eliminating, GH, an additional platform which is integral to the principles of Dragonfly as a part of the Ladybug Tools toolkit but not necessary for this purpose. The goal is to make UWG an intuitive, user-friendly and straightforward process for Rhino users, especially those who are not acquainted with visual scripting in GH. The workflow is narrowed to examining UHI and other microclimate aspects as an iterative optimization process rather than an exploratory process that allows users to craft the modular components and address multiple issues. Such dual interface functionality can be seen in other building science tools, such as DIVA for Rhino and DIVA for GH developed by Solemma to run the same background engine and produce the same results through different workflows and interfaces for users with different capabilities within the Rhino platform (“Solemma LLC,” 2019).

3.2.2.1. Geometric Parameter Extraction

By adding Rhino 3D to UWG, the textual description component of the existing workflow can be eliminated (Figure 18). The workflow can therefore, not only be significantly reduced (Figure 19) but transformed into a cyclical and iterative process (Figure 20) that is more compatible with a design feedback loop.

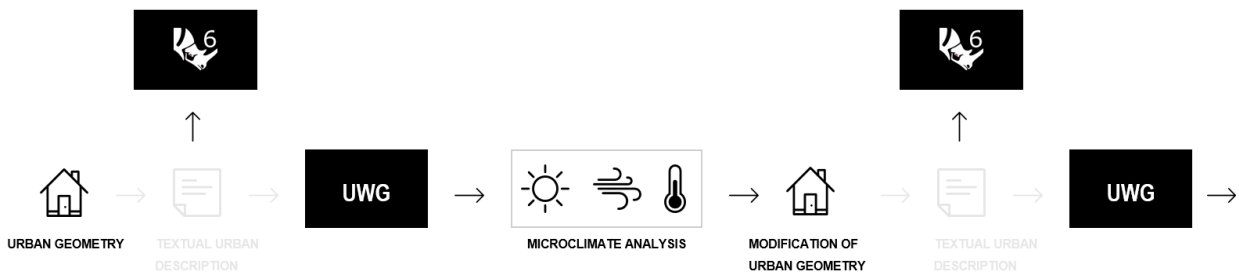


Figure 18. Rhino 3d replaces textual description of urban sites

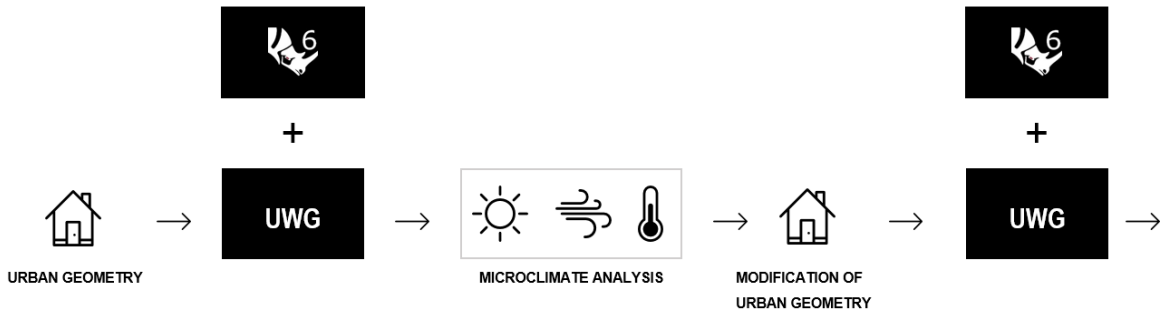


Figure 19. Rhino 3d reduced workflow

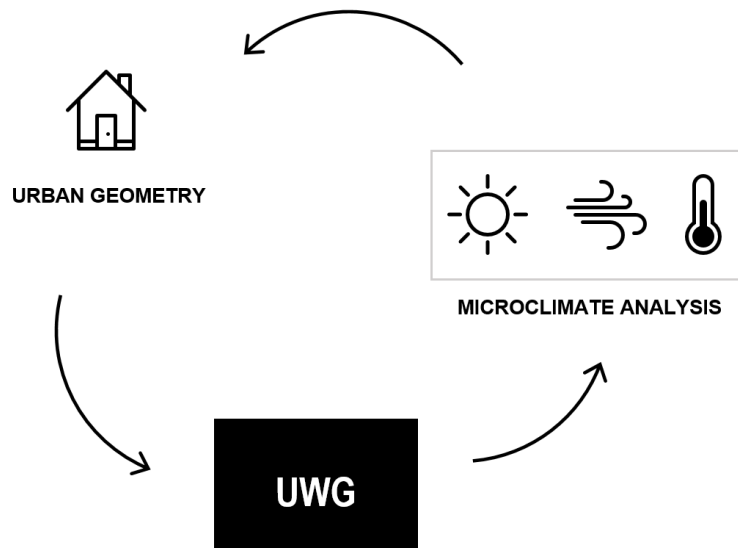


Figure 20. UWG for Rhino Workflow

3.2.2.2. Morphological Parameter Extraction

By coupling UWG for Rhino, the workflow can reduce the error margins associated with morphological parameter input uncertainty. This involves a three-step method (Figure 21):

1. Read the average site building height, site-coverage ratio and façade-coverage ratio from UWG for Rhino (01 in Figure 21).
2. Classify the LCZ class based on the above site properties (02 in Figure 21).
3. Extract surface admittance, surface albedo and anthropogenic heat flux for UWG for Rhino simulation (03 in Figure 21).

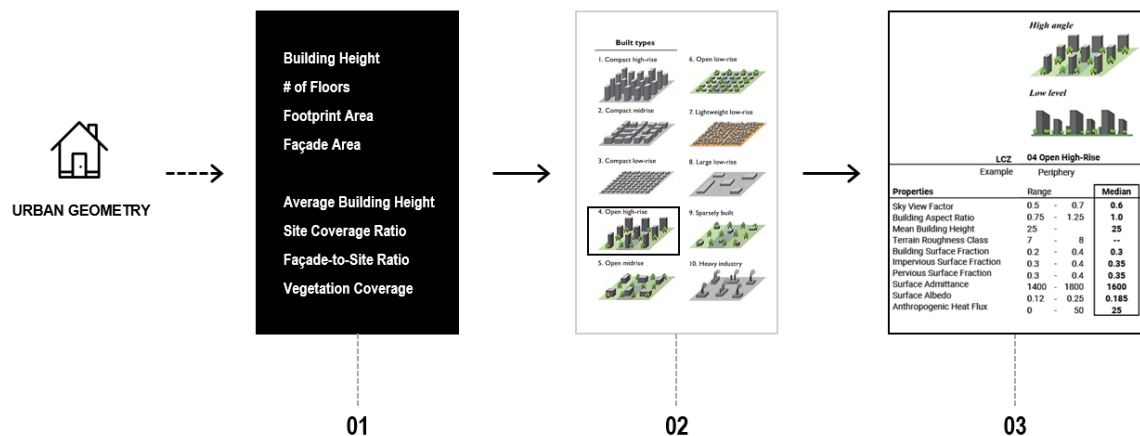
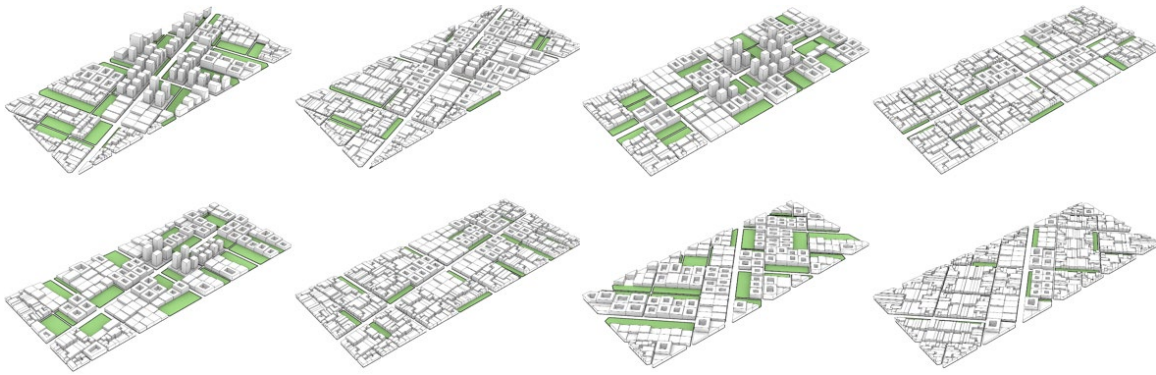


Figure 21. LCZ Parameter Extraction



4. Design-Integrated Urban Analysis

The purpose of this analysis is to identify the impact of UHI effect on cooling and heating energy intensity for a set of proposed urban design iterations by comparing the carbon intensity and cost of electricity of each proposal. The urban design iterations were generated in collaboration with the architectural firm Kohn Pedersen Fox's (KPF) Urban Interface and Environmental Performance groups. The idea is to provide UHI intensity as a useful metric for multi-dimensional urban performance analysis.

4.1. Overview

Out of a pool of 1,000 models, eight are selected as candidates for simulation and are tested in the five cities in different ASHRAE climate zones indicated on Figure 22. The models have the same floor-area-ratio ((FAR) of 3.6) distributed over an area that is 1.75 by 0.72 kilometers. The mixed-use building typology ratio is consistent (60% commercial, 30% residential and 10% retail). The vegetation coverage ratio is varied (10% or 30%), therefore dividing the eight models into four sets. Each set (numbered 1 through 4) contains one iteration with 10% vegetation coverage (Group A) and a second with 30% vegetation coverage (Group B); the horizontal and vertical density distribution changes accordingly.

The methodology, tested model set and simulation parameters are described in Chapter 4.2. The results and findings are presented in Chapter 4.3.

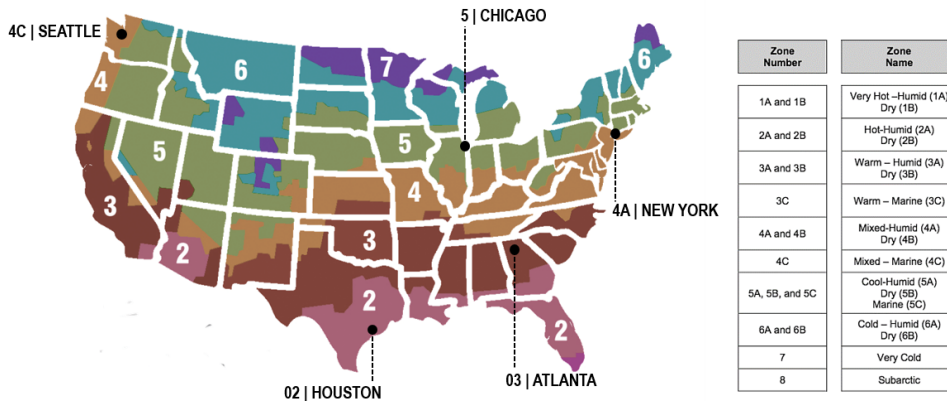


Figure 22. ASHRAE Climate Zones

4.2. Methodology

To generate the modified EPW for each of the eight models, the three-step UWG for Rhino and LCZ workflow described in Chapter 3.2.2 is implemented (Figure 23). To determine neighborhood-wide cooling and heating energy use intensity (EUI), the original, rural EPW and the modified, urban EPW is applied to each of the eight models in the Urban Modeling Interface (umi) software. To determine carbon intensity, the grid emissions for each city is retrieved from the Emissions and Generation Resource Integrated database (US EPA, 2018). To determine cost, the average price of electricity to customers is retrieved from EIA (US EIA, 2019).

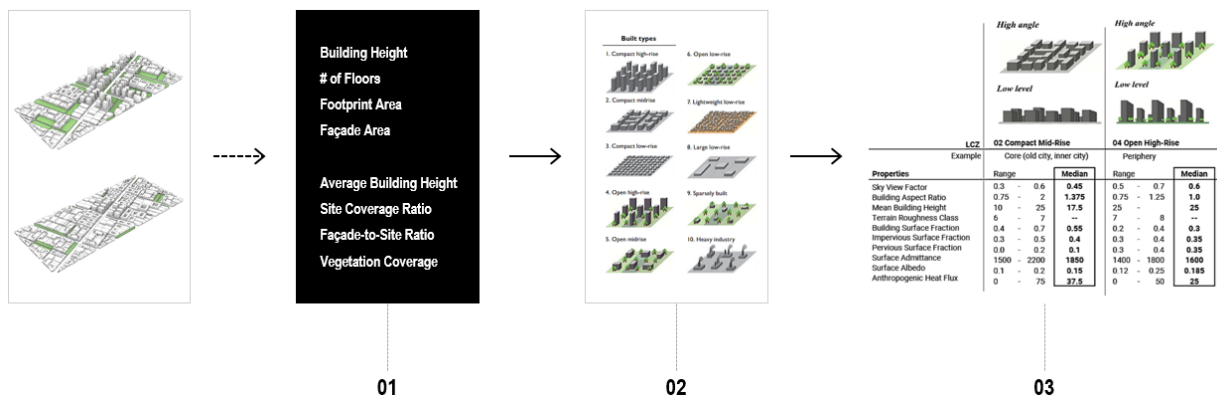


Figure 23. LCZ Parameter Extraction

4.2.1. Tested Model Sets

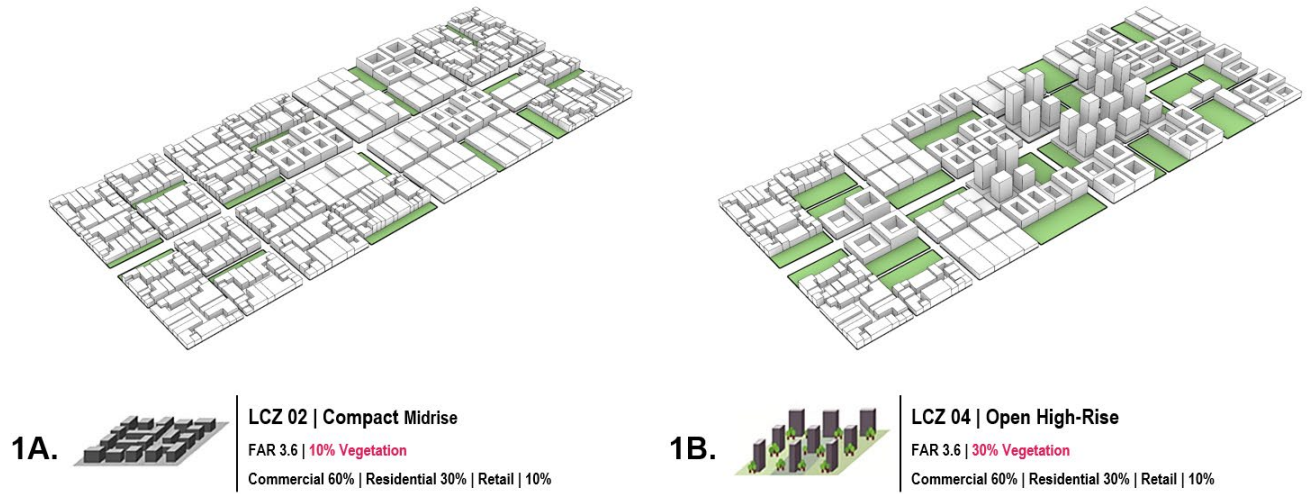


Figure 24. Iteration 1

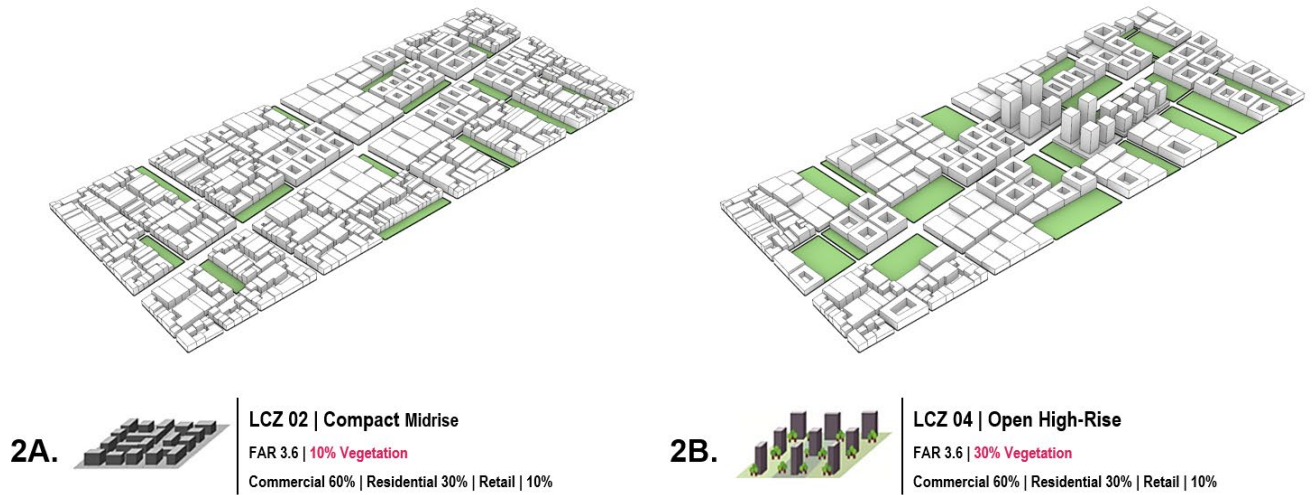


Figure 25. Iteration 2

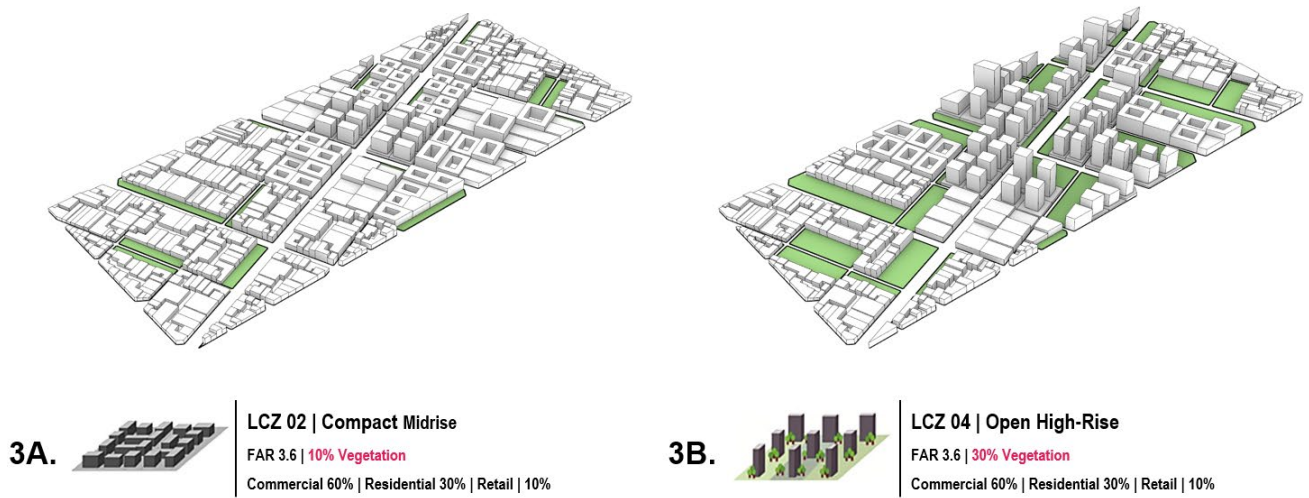


Figure 26. Iteration 3

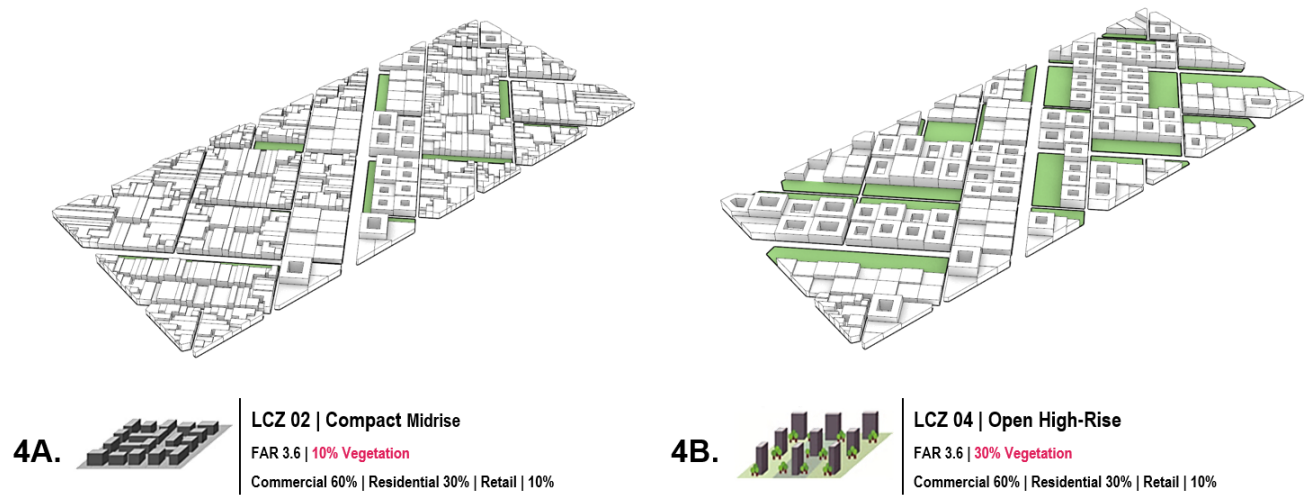


Figure 27. Iteration 4

Expanded model information is attached in Appendix A, Tested Model Sets Expanded Information.

4.2.2. Simulation Parameters

Table 1. UWG Simulation Parameters

| Parameter | Unit | Value |
|---|--------------------|----------------------------|
| <i>Urban Parameters</i> | | |
| Vegetation Albedo | - | LCZ Input ¹ |
| Vegetation Start Month | - | Climate Input ² |
| Vegetation End Month | - | Climate Input ² |
| Tree Latent Fraction | - | 0.7 |
| Grass Latent Fraction | - | 0.5 |
| Road Albedo | - | LCZ Input ¹ |
| Road Pavement Conductivity | W/mK | 1 |
| Road Volumetric Heat capacity | J/m ³ K | 1600000 |
| Road Thickness | m | 0.2 ¹ |
| <i>Traffic Parameters</i> | | |
| Non-building Sensible Heat | W/m ² | LCZ Input ³ |
| Weekday Schedule | - | See Figure 28 |
| Saturday Schedule | - | See Figure 28 |
| Sunday Schedule | - | See Figure 28 |
| <i>Boundary Layer Parameters⁴</i> | | |
| Daytime Boundary Layer Height | m | 1000 |
| Nighttime Boundary Layer Height | m | 80 |
| Vertical Profile Inversion Height | m | 150 |
| Circulation Coefficient | - | 1.2 |
| Exchange Coefficient | - | 1 |
| <i>Reference Site Parameters</i> | | |
| Obstacle Height | m | 0.1 |
| Vegetation Coverage | - | Climate Input ⁵ |
| Temperature Height | m | 10 |
| Wind Height | m | 10 |
| <i>Simulation Parameters</i> | | |
| Start Month | - | 1 |
| End Month | - | 12 |
| Start Day | - | 1 |
| End Day | - | 31 |

1. Table 3. LCZ Properties for used typologies (I. D. Stewart & Oke, 2012)

2. Calculated by estimating 1st month which outdoor temperature is greater than 10°C

3. 45.2% of Anthropogenic heat from Table 3. LCZ Properties for used typologies (I. D. Stewart & Oke, 2012) according to (Sailor, 2011).

4. (Mao, 2018)

5. Based on weather station surroundings observation

Table 2. UWG Building Typology Parameters

| Parameter | Unit | Value | | |
|-----------------------------------|------|-----------------------|------------------------|-------------------|
| | | <i>Commercial 60%</i> | <i>Residential 30%</i> | <i>Retail 10%</i> |
| Age | - | New Construction | New Construction | New Construction |
| Floor Height ¹ | m | 4 | 3 | 6 |
| Glazing Ratio ¹ | - | 0.36 | 0.15 | 0.1 |
| SHGC ¹ | - | Climate Input | Climate Input | Climate Input |
| Wall Albedo ² | - | LCZ Input | LCZ Input | LCZ Input |
| Roof Albedo ² | - | LCZ Input | LCZ Input | LCZ Input |
| Roof Vegetation | - | 0 | 0 | 0 |
| Canyon Heat Fraction ⁴ | - | 0.5 | 0.5 | 0.5 |

¹ Deru et al., 2011

² Table 3. LCZ Properties for used typologies (I. D. Stewart & Oke, 2012)

³ U.S.DOE, 2012

⁴ Dragonfly

Table 3. LCZ Properties for used typologies (I. D. Stewart & Oke, 2012)

| Parameter | Unit | Value | | | |
|-----------------------------|------|-------------------------------|--------|------------------------------|--------|
| | | <i>LCZ 02 Compact Midrise</i> | | <i>LCZ 04 Open High-Rise</i> | |
| | | Range | Median | Range | Median |
| Sky View Factor | % | 0.2 – 0.6 | 0.45 | 0.5 – 0.7 | 0.6 |
| Canyon Aspect Ratio | - | 0.75 – 1.5 | 1.375 | 0.75 – 1.25 | 1.0 |
| Average Building Height | m | 3 – 10 | 17.5 | 25+ | 25+ |
| Terrain Roughness Class | - | 6 | - | 7/8 | - |
| Building Surface Fraction | - | 0.4 – 0.7 | 0.55 | 0.2 – 0.4 | 0.3 |
| Impervious Surface Fraction | - | 0.2 – 0.5 | 0.4 | 0.3 – 0.4 | 0.35 |
| Pervious Surface Fraction | - | 0.0 – 0.3 | 0.1 | 0.3 – 0.4 | 0.35 |
| Surface Admittance | - | 1500 – 2200 | 1850 | 1400 – 1800 | 1600 |
| Albedo | - | 0.1 – 0.2 | 0.15 | 0.12 – 0.25 | 0.185 |
| Anthropogenic Heat Flux | - | 0 - 75 | 37.5 | 0 - 50 | 25 |

A complete list of LCZ class properties used is attached in Appendix C: Local Climate Zone Parameters.

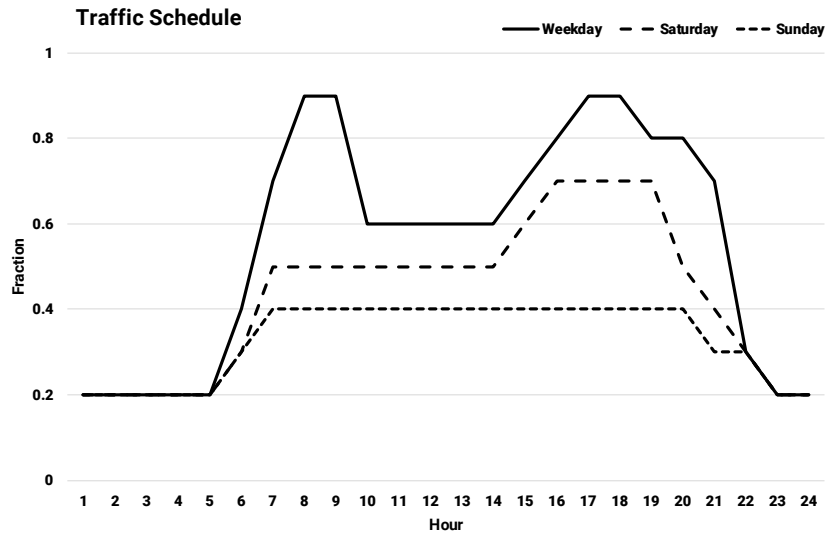


Figure 28. Traffic Schedule

4.3. Results and Findings

An analysis of the UHI effect has been conducted for the eight models listed in Chapter 4.2.1 using UWG for Rhino and the workflow described in Chapter 3.2.2. The original rural EPW file and the modified urban EPW file generated from the simulation are used to determine the UHI effect's impact on temperature observations and cooling and heating EUI. The impact of vegetation is assessed through a comparison of the cooling and heating EUIs generated from the urban EPW files. In a concluding comparative analysis, the performance of each model in each climate is evaluated by comparing calculated carbon intensity and electricity cost.

4.3.1. Model Results

For each iteration, a result sheet is produced containing:

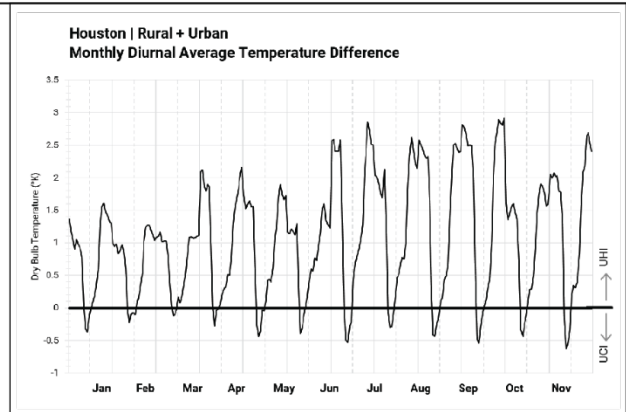
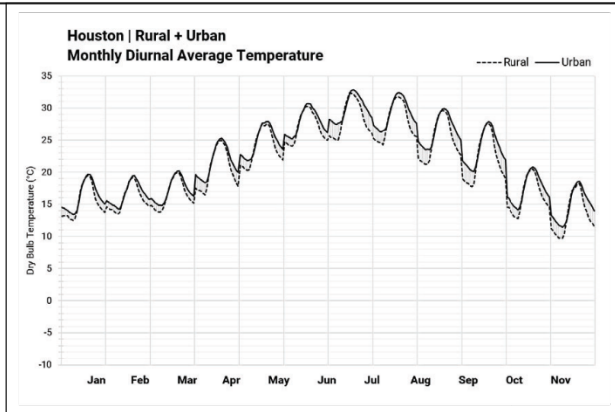
1. UHI intensity displayed by a plot of monthly average diurnal temperature and a plot of monthly average diurnal temperature difference between rural and urban locations.
2. Plots of monthly cooling and heating EUI and monthly cooling and heating EUI difference between rural and urban locations displays EUI.

The plots are displayed below.

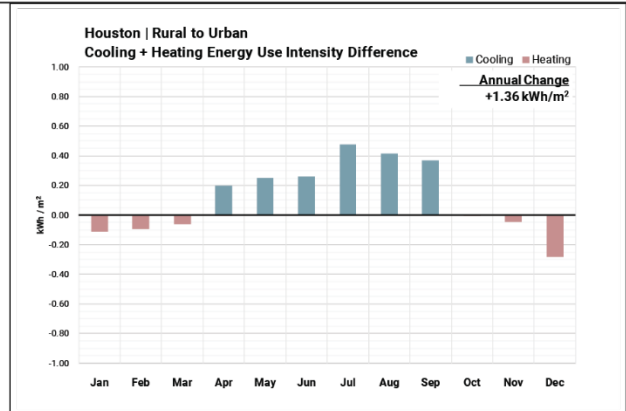
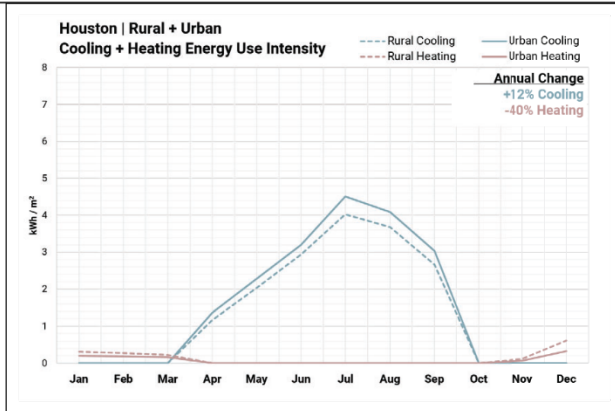
ITERATION #1A | HOUSTON LCZ 02 | Compact Midrise ASHRAE Climate Zone 2



1. UHI INTENSITY



2. COOLING + HEATING ENERGY USE INTENSITY

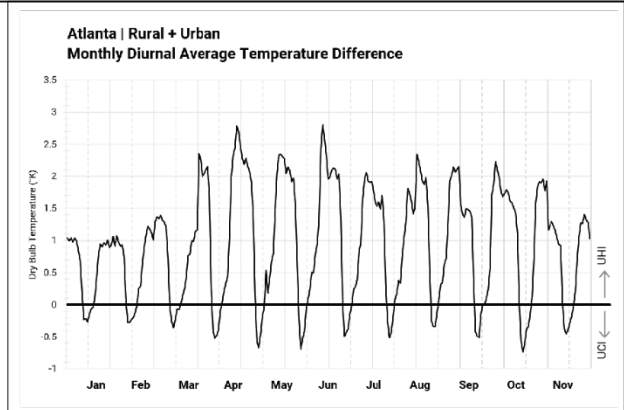
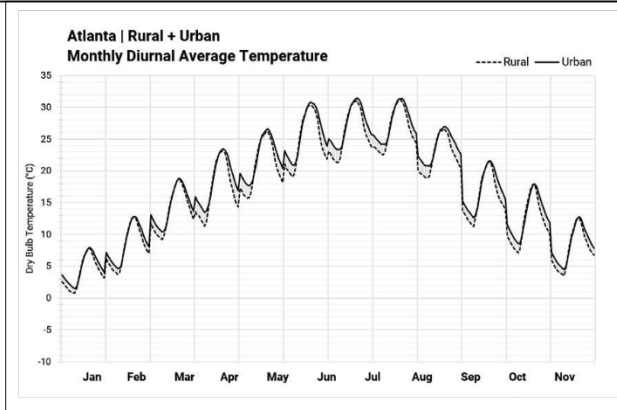


ITERATION #1A | ATLANTA

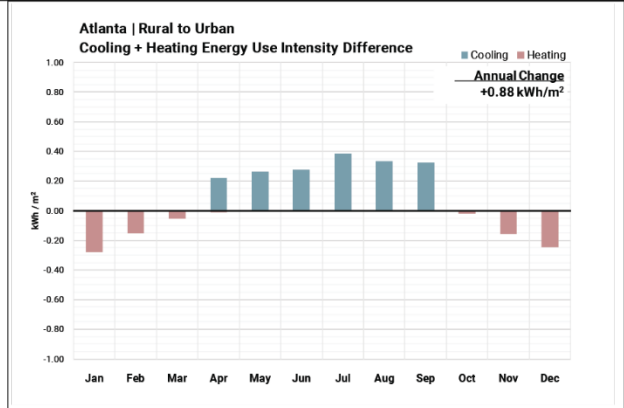
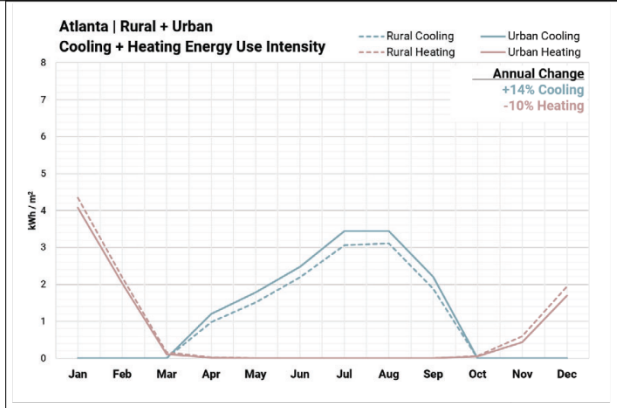
LCZ 02 | Compact Midrise
ASHRAE Climate Zone 3



1. UHI INTENSITY



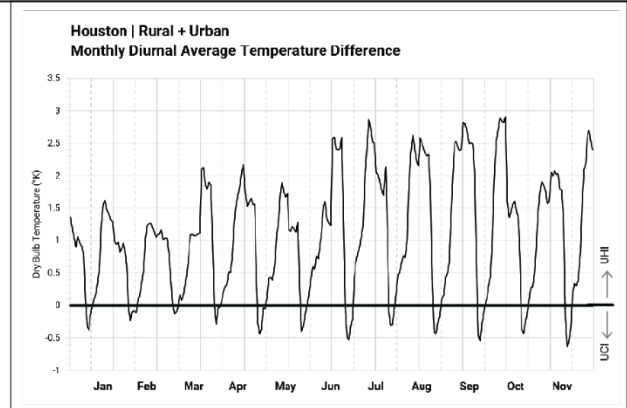
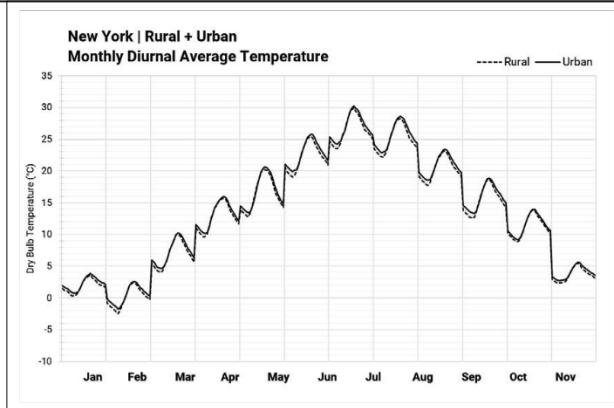
2. COOLING + HEATING ENERGY USE INTENSITY



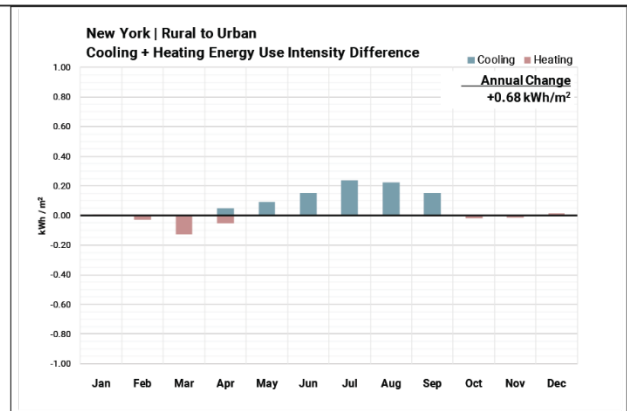
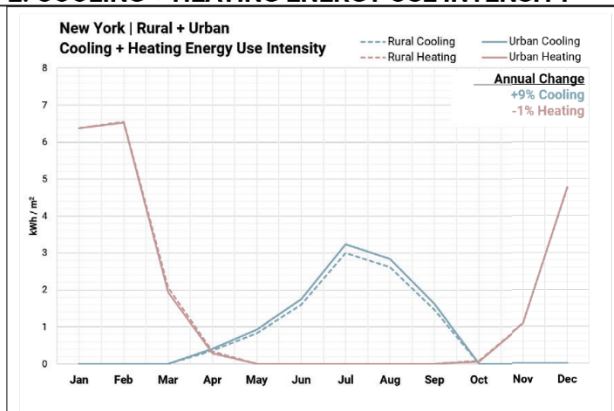
ITERATION #1A | NEW YORK LCZ 02 | Compact Midrise ASHRAE Climate Zone 4A



1. UHI INTENSITY



2. COOLING + HEATING ENERGY USE INTENSITY

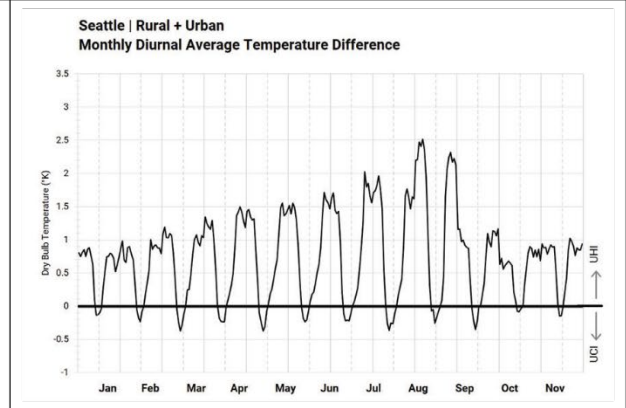
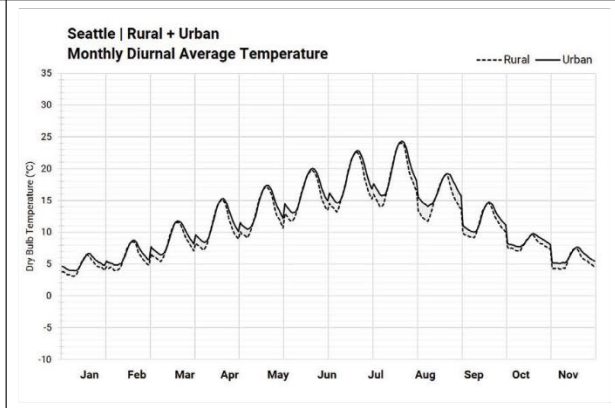


ITERATION #1A | SEATTLE

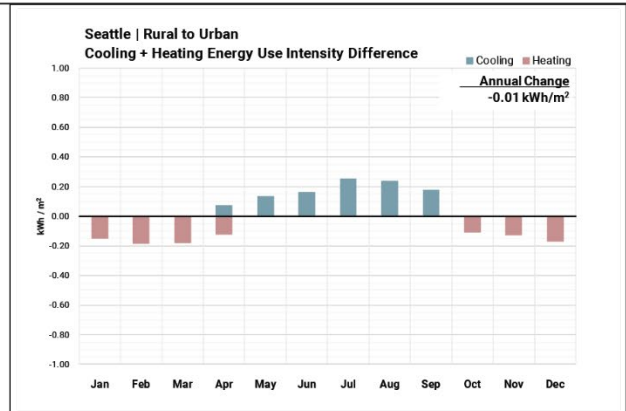
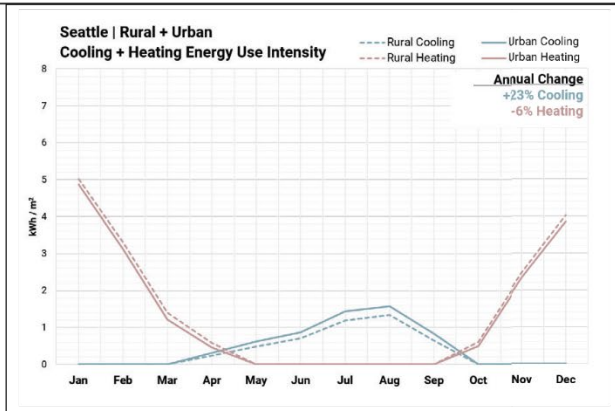
LCZ 02 | Compact Midrise
ASHRAE Climate Zone 4C



1. UHI INTENSITY



2. COOLING + HEATING ENERGY USE INTENSITY

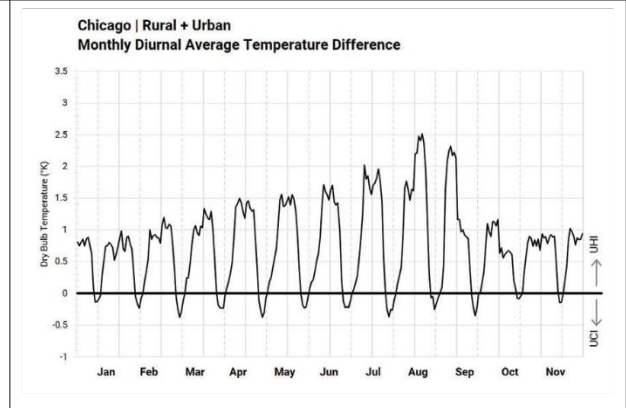
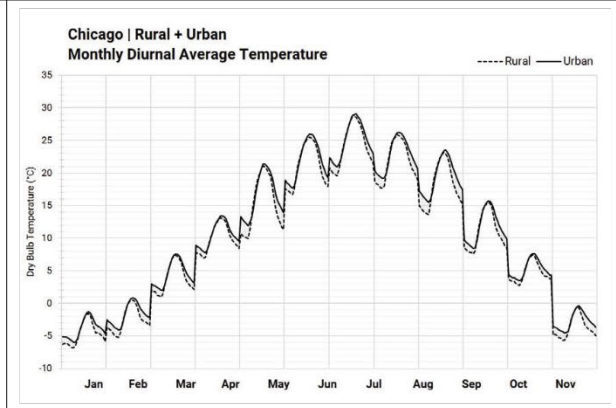


ITERATION #1A | CHICAGO

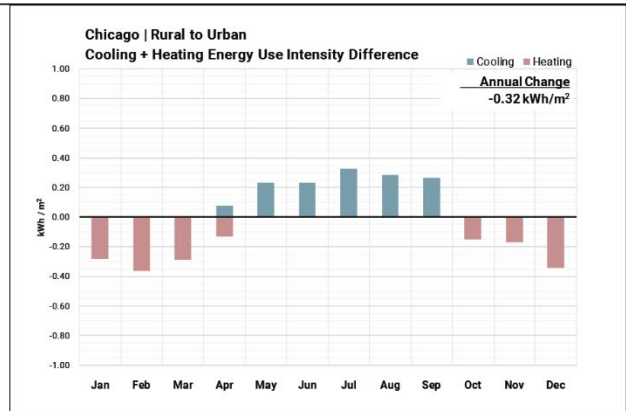
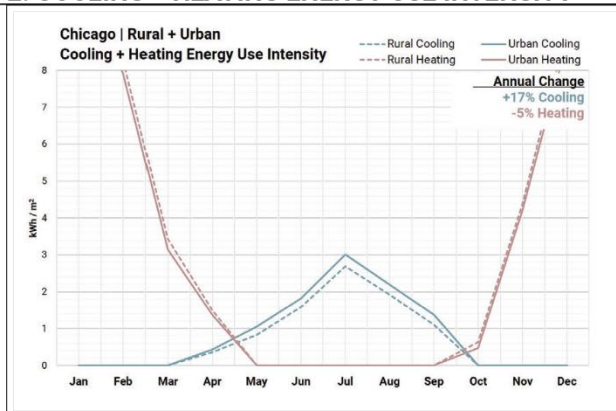
LCZ 02 | Compact Midrise
ASHRAE Climate Zone 5



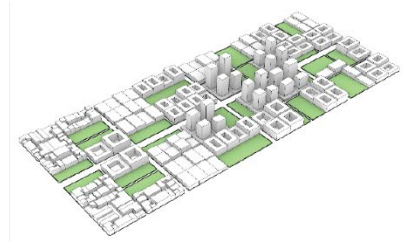
1. UHI INTENSITY



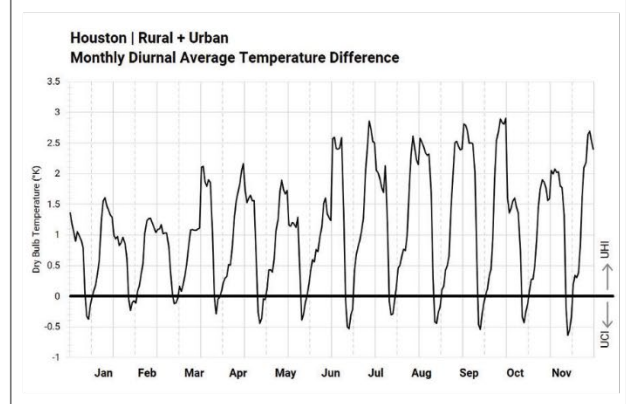
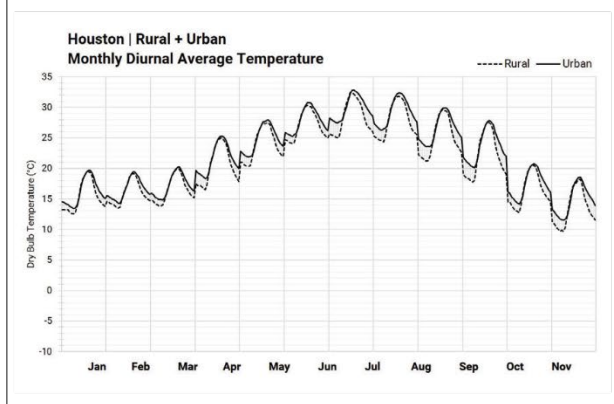
2. COOLING + HEATING ENERGY USE INTENSITY



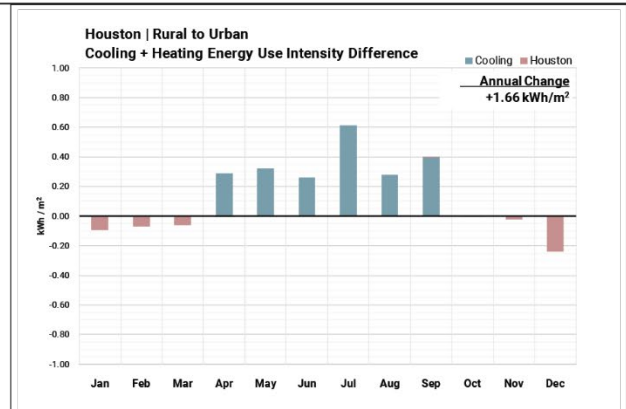
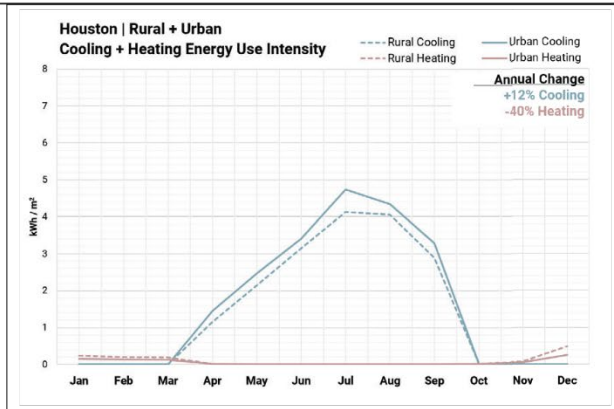
ITERATION #1B | HOUSTON LCZ 04 | Open High-Rise ASHRAE Climate Zone 2



1. UHI INTENSITY

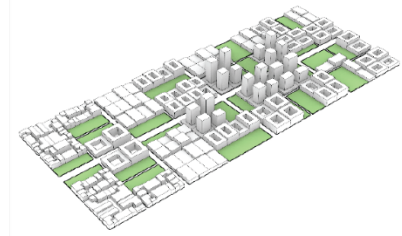


2. COOLING + HEATING ENERGY USE INTENSITY

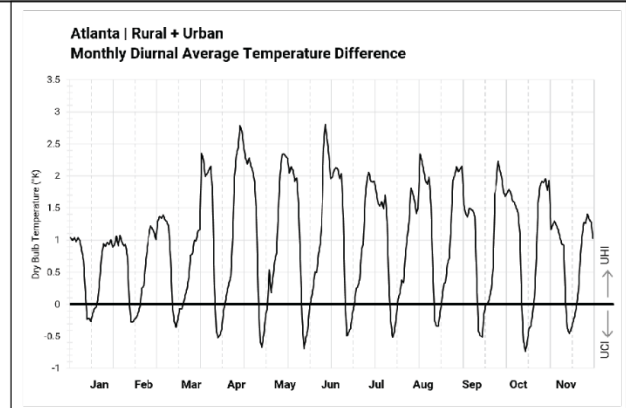
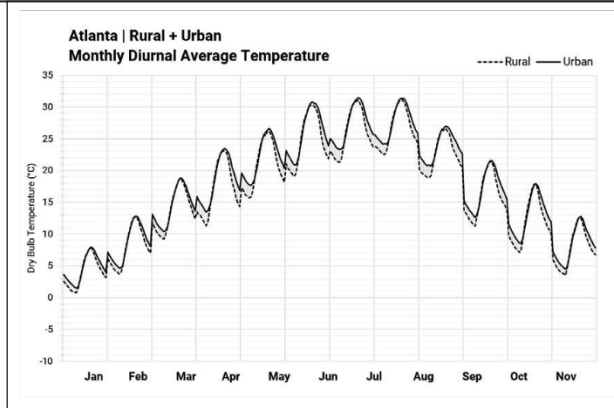


ITERATION #1B | ATLANTA

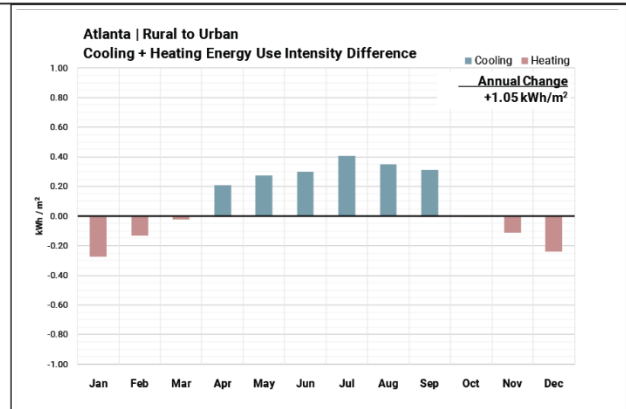
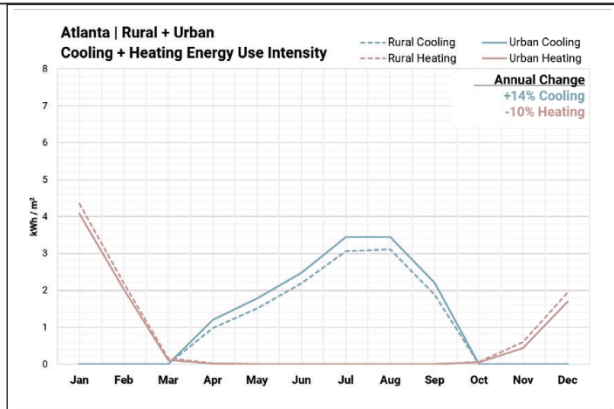
LCZ 04 | Open High-Rise
ASHRAE Climate Zone 3



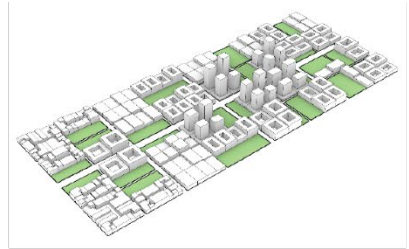
1. UHI INTENSITY



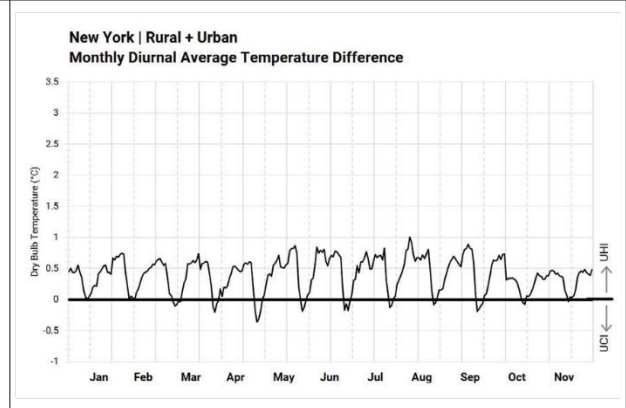
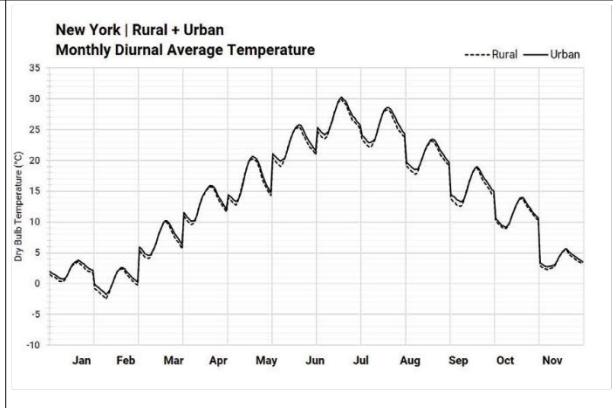
2. COOLING + HEATING ENERGY USE INTENSITY



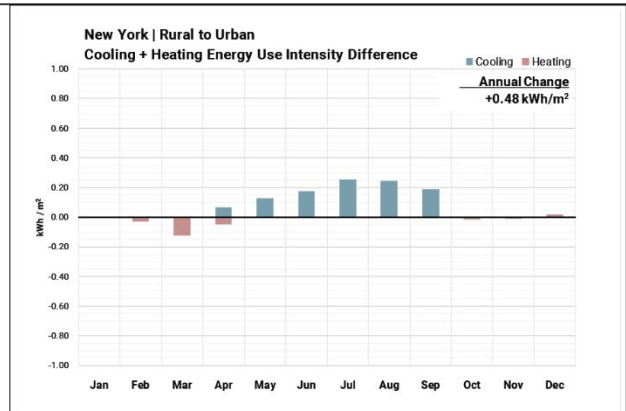
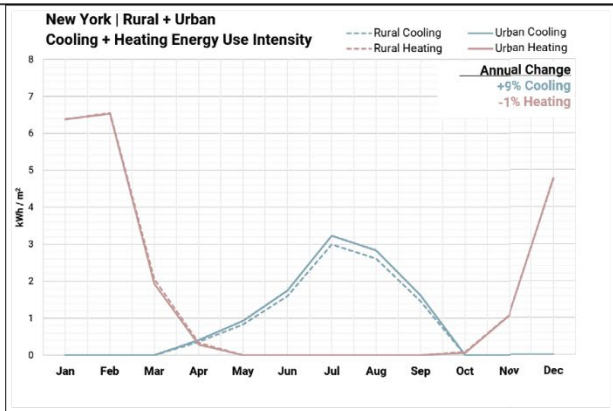
ITERATION #1B | NEW YORK LCZ 04 | Open High-Rise ASHRAE Climate Zone 4A



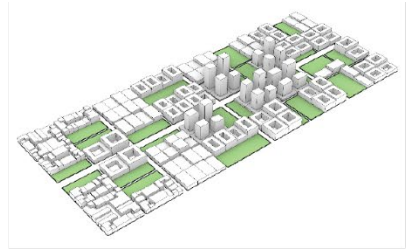
1. UHI INTENSITY



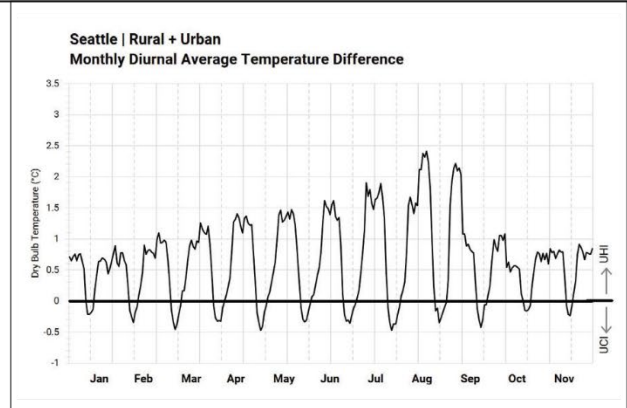
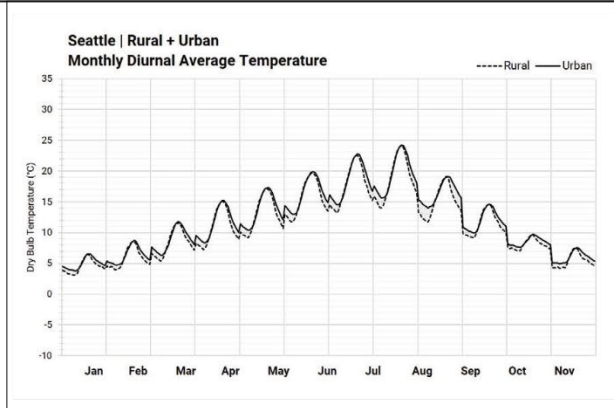
2. COOLING + HEATING ENERGY USE INTENSITY



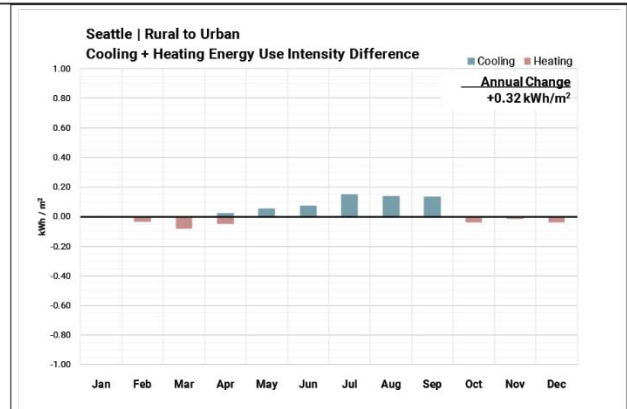
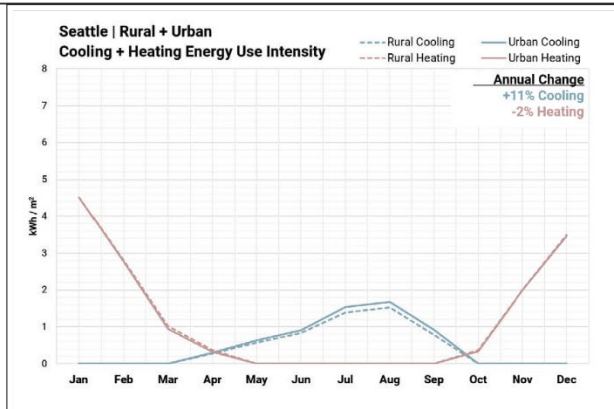
ITERATION #1B | SEATTLE LCZ 04 | Open High-Rise ASHRAE Climate Zone 4C



1. UHI INTENSITY

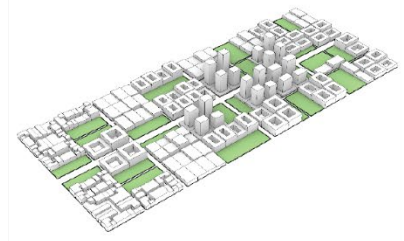


2. COOLING + HEATING ENERGY USE INTENSITY

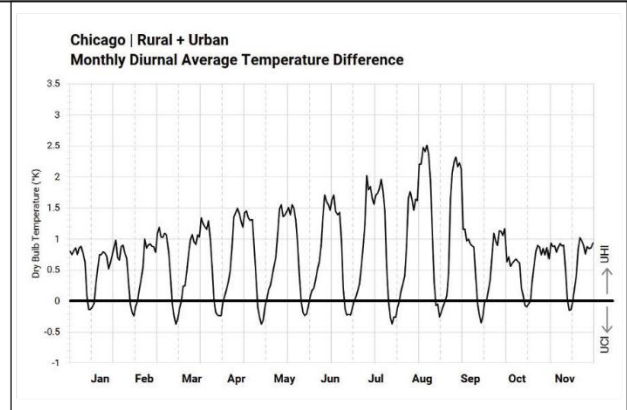
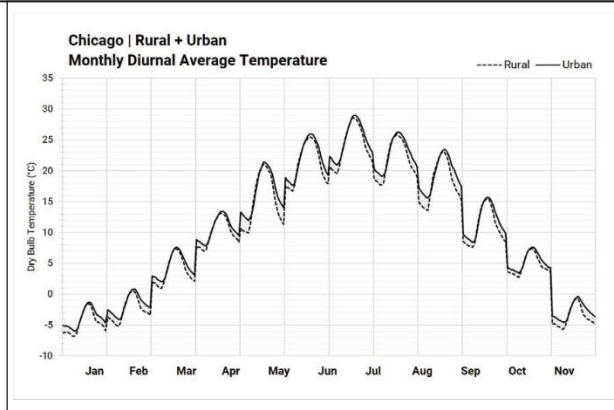


ITERATION #1B | CHICAGO

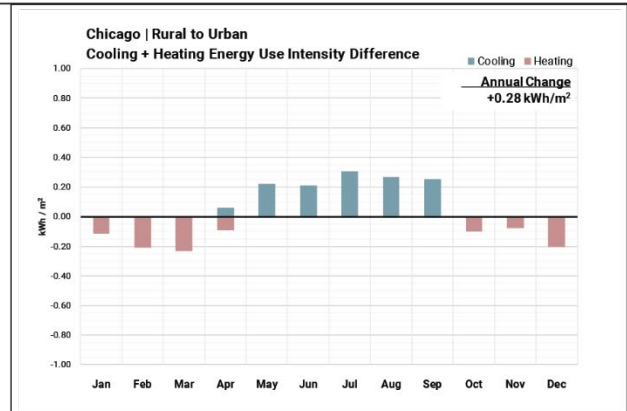
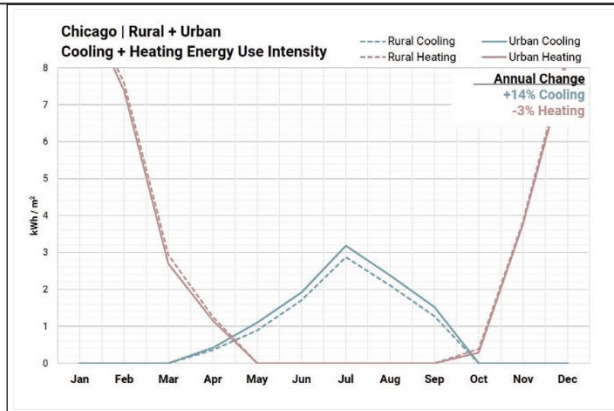
LCZ 04 | Open High-Rise
ASHRAE Climate Zone 5



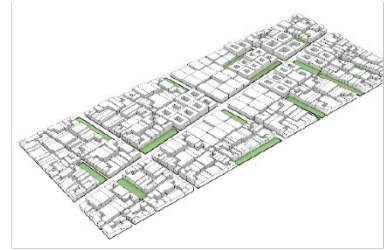
1. UHI INTENSITY



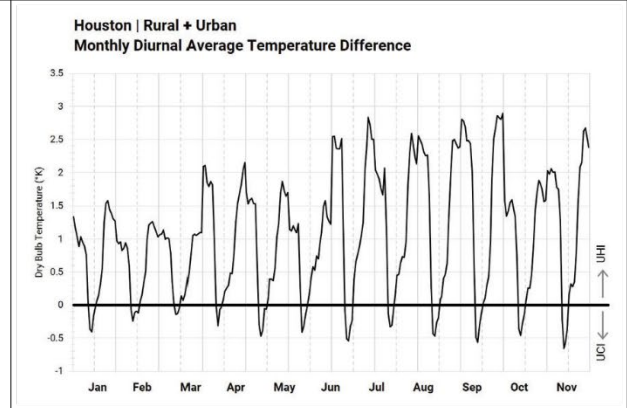
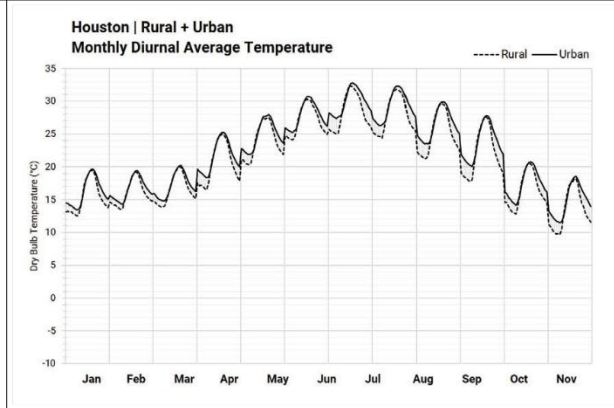
2. COOLING + HEATING ENERGY USE INTENSITY



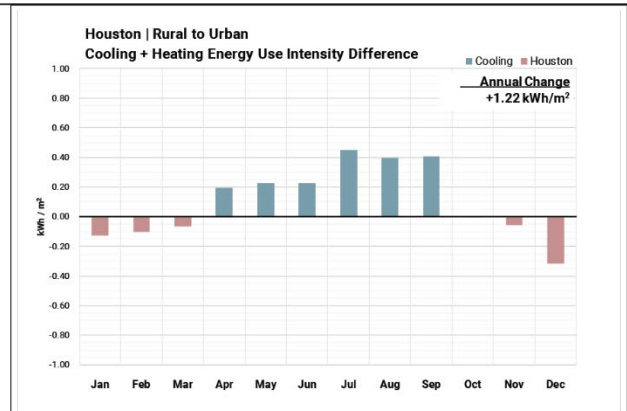
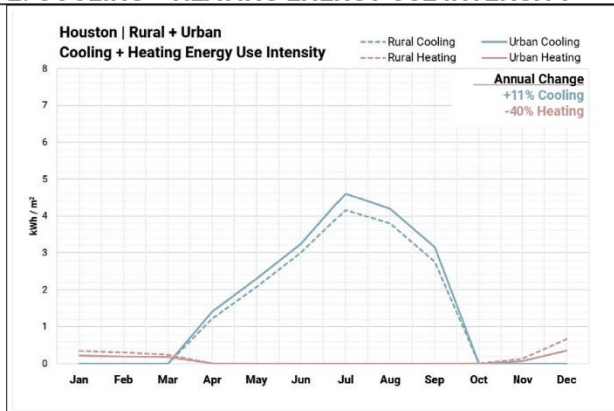
ITERATION #2A | HOUSTON LCZ 02 | Compact Midrise ASHRAE Climate Zone 2



1. UHI INTENSITY

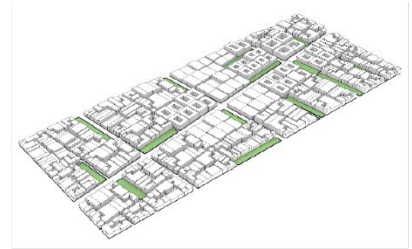


2. COOLING + HEATING ENERGY USE INTENSITY

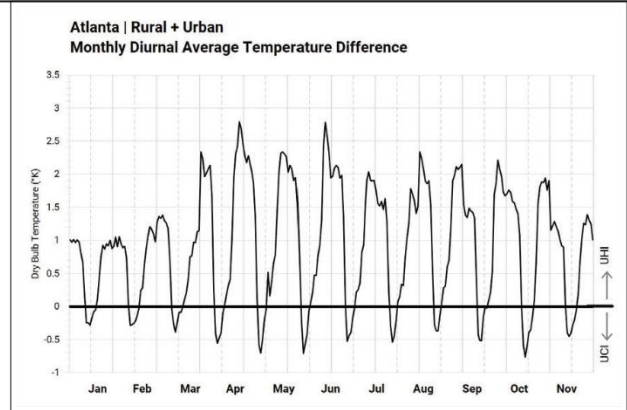
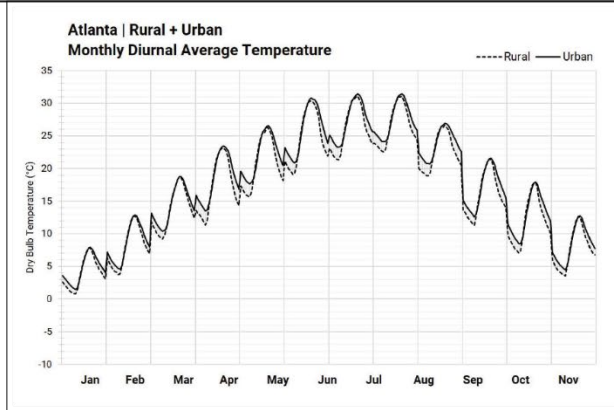


ITERATION #2A | ATLANTA

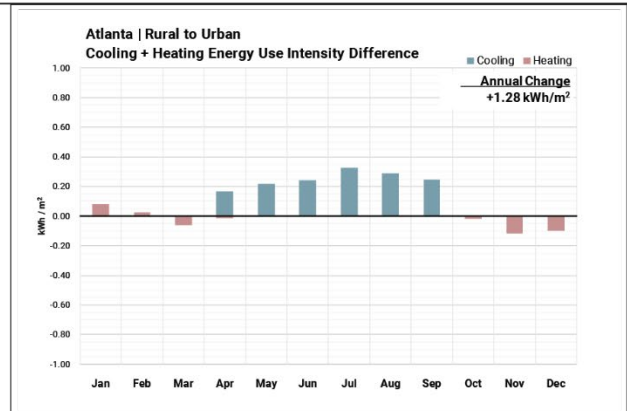
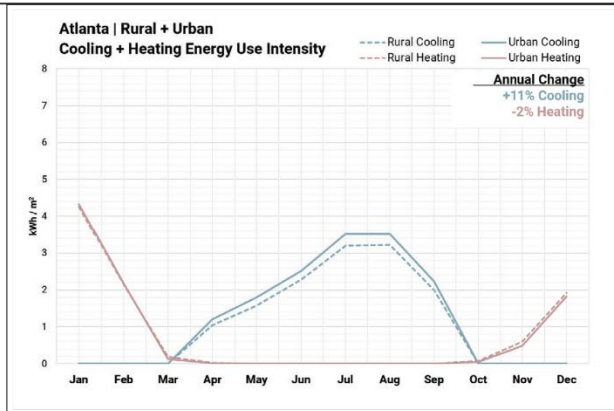
LCZ 02 | Compact Midrise
ASHRAE Climate Zone 3



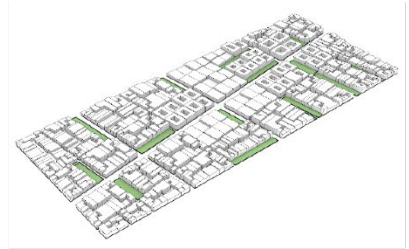
1. UHI INTENSITY



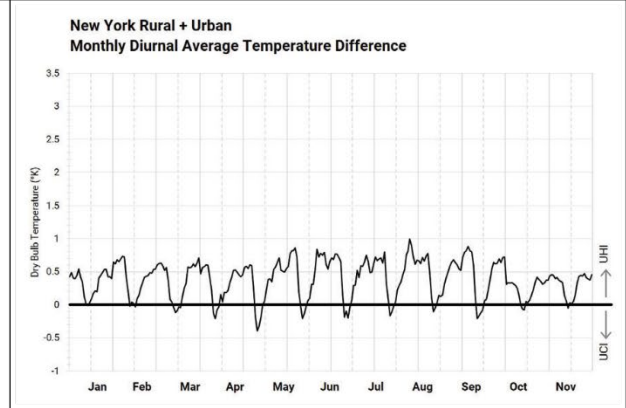
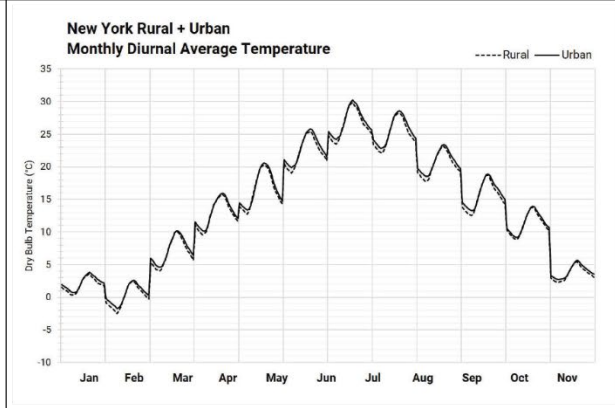
2. COOLING + HEATING ENERGY USE INTENSITY



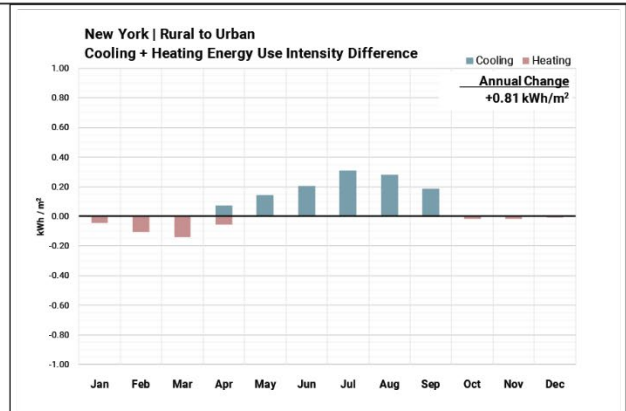
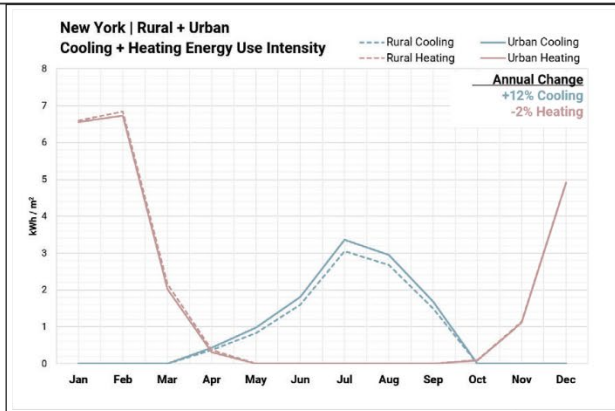
ITERATION #2A | NEW YORK LCZ 02 | Compact Midrise ASHRAE Climate Zone 4A



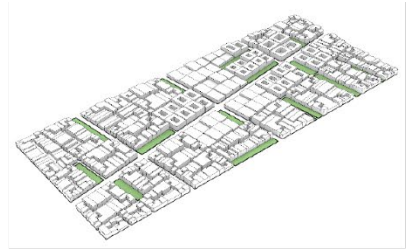
1. UHI INTENSITY



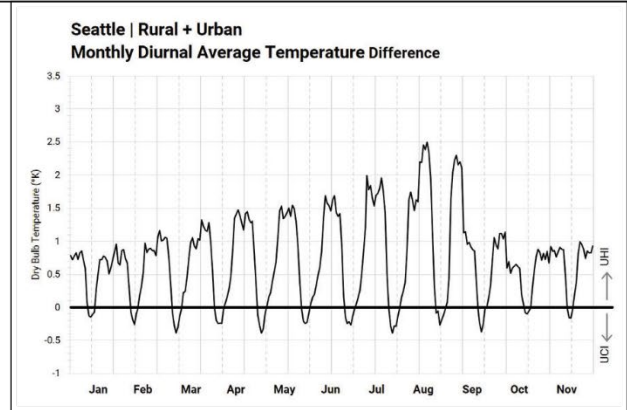
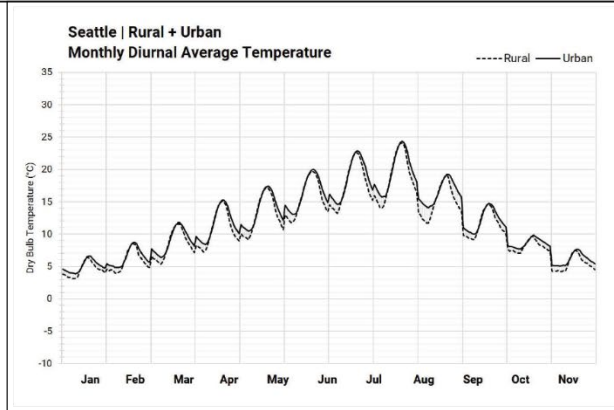
2. COOLING + HEATING ENERGY USE INTENSITY



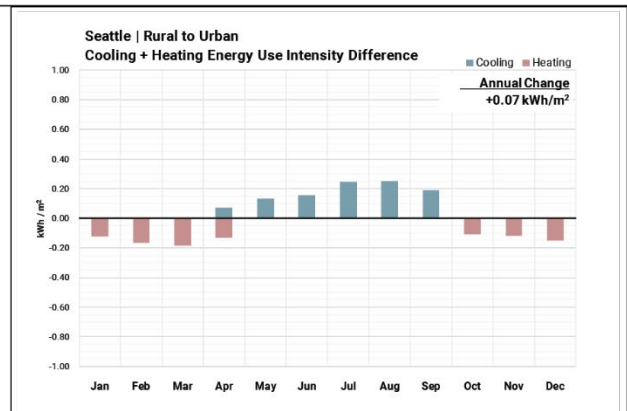
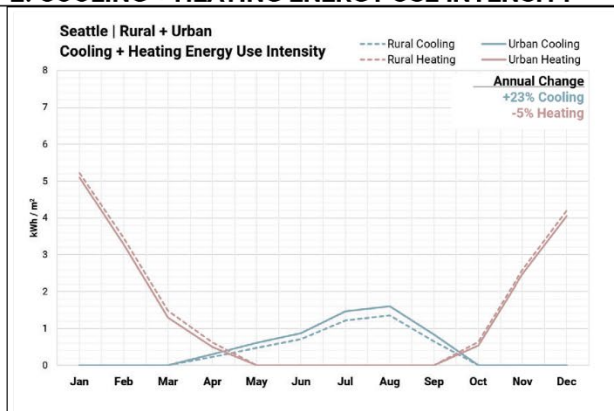
ITERATION #2A | SEATTLE LCZ 02 | Compact Midrise ASHRAE Climate Zone 4C



1. UHI INTENSITY



2. COOLING + HEATING ENERGY USE INTENSITY

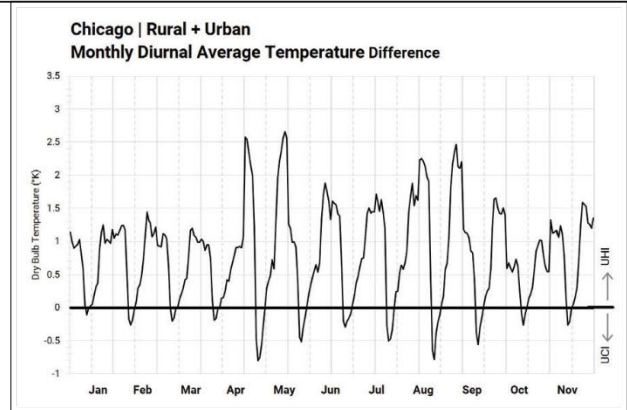
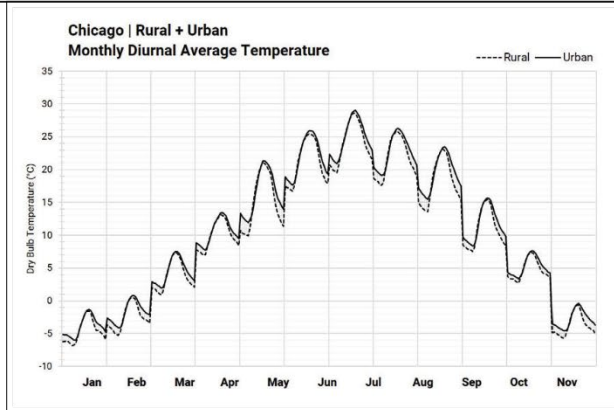


ITERATION #2A | CHICAGO

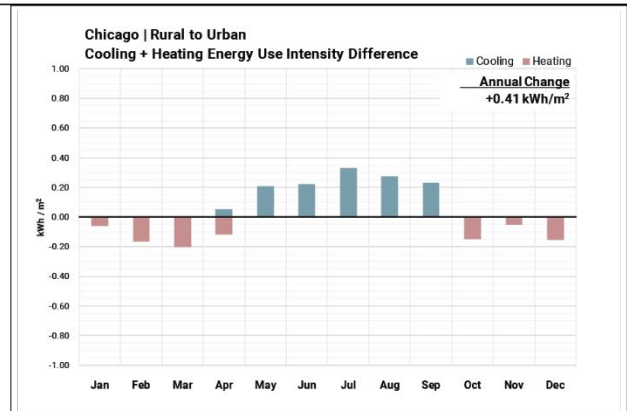
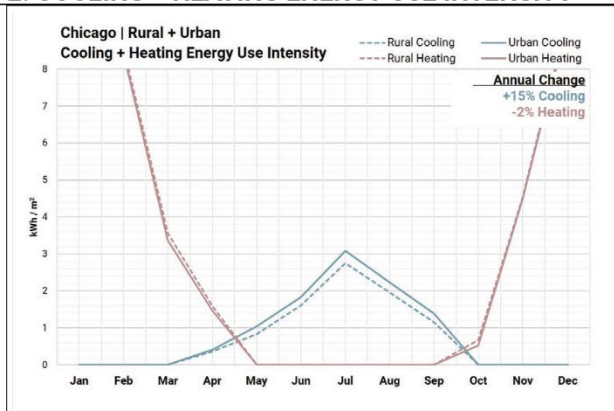
LCZ 02 | Compact Midrise
ASHRAE Climate Zone 5



1. UHI INTENSITY



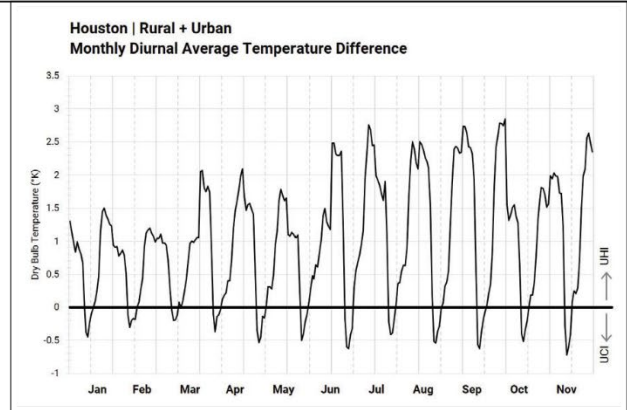
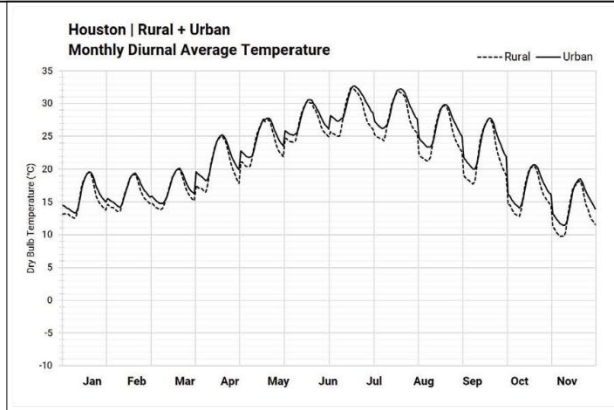
2. COOLING + HEATING ENERGY USE INTENSITY



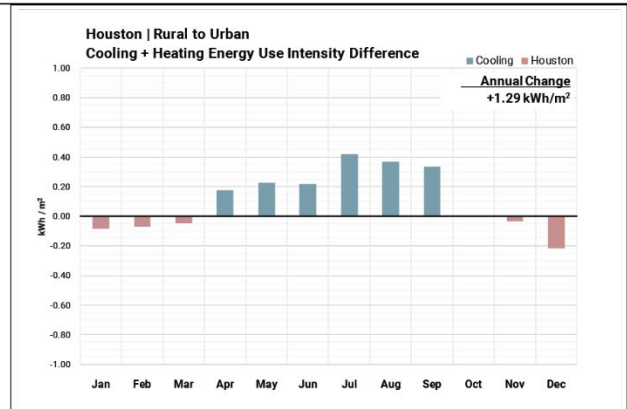
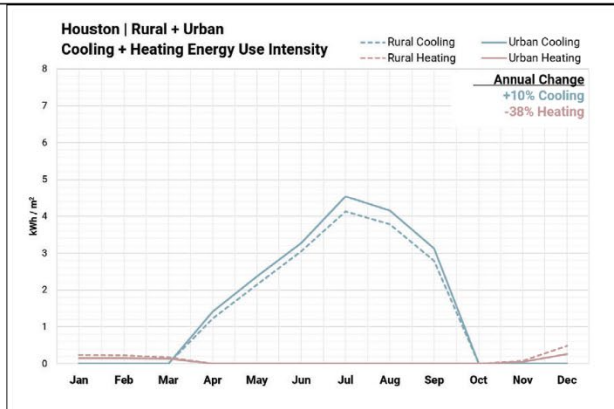
ITERATION #2B | HOUSTON LCZ 04 | Open High-Rise ASHRAE Climate Zone 2



1. UHI INTENSITY



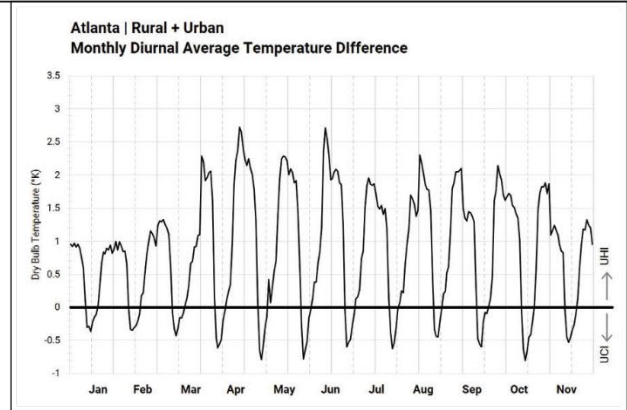
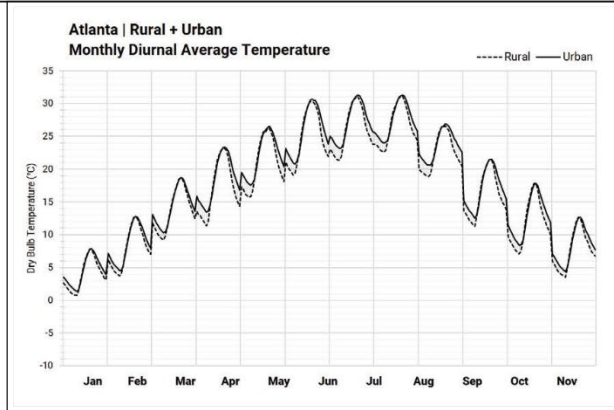
2. COOLING + HEATING ENERGY USE INTENSITY



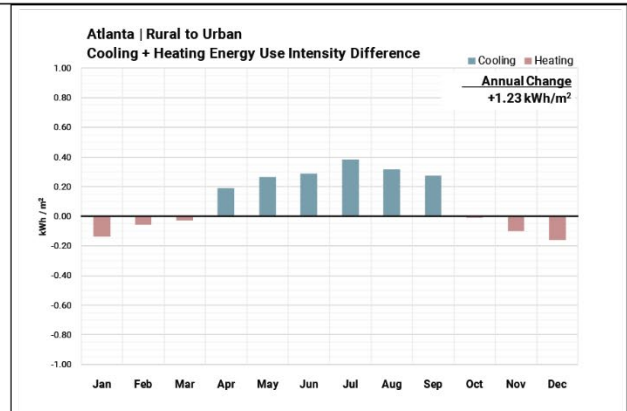
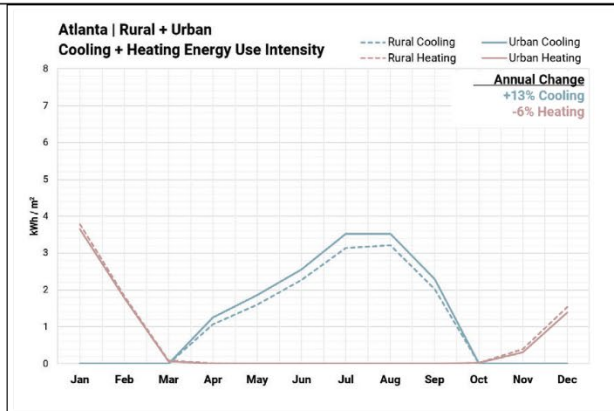
ITERATION #2B | ATLANTA LCZ 04 | Open High-Rise ASHRAE Climate Zone 3



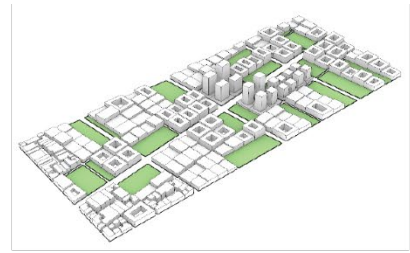
1. UHI INTENSITY



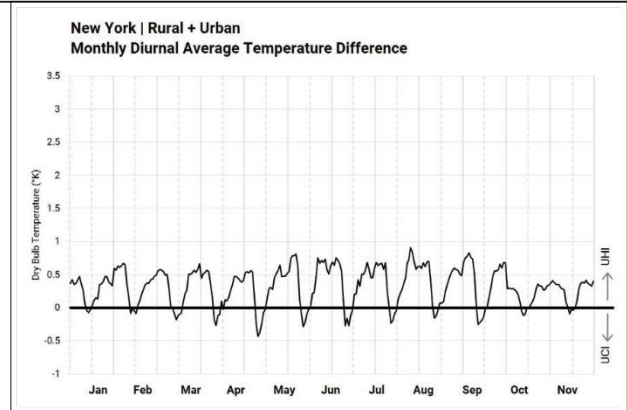
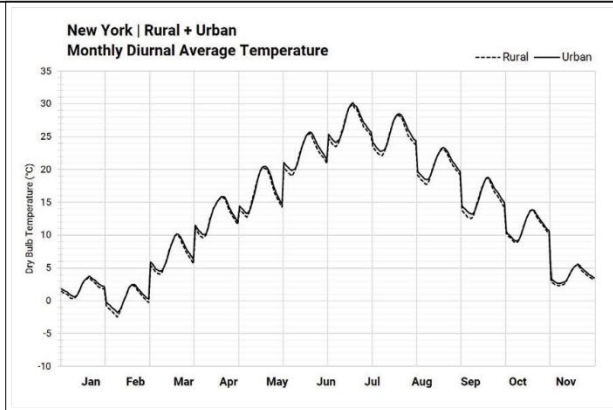
2. COOLING + HEATING ENERGY USE INTENSITY



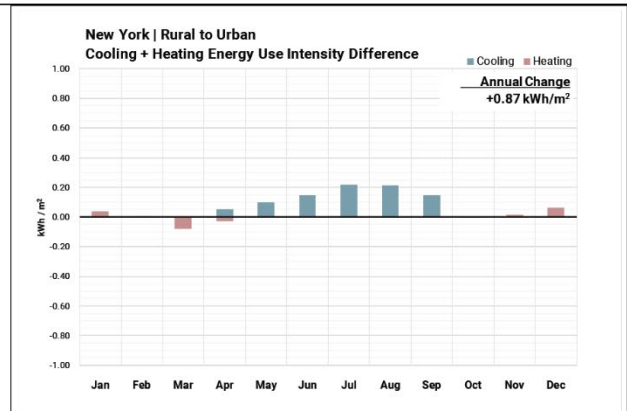
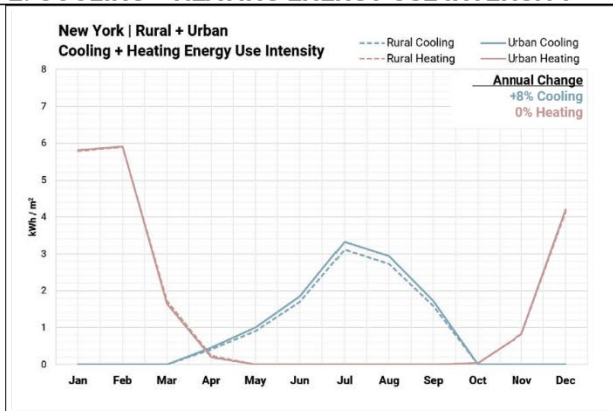
ITERATION #2B | NEW YORK LCZ 04 | Open High-Rise ASHRAE Climate Zone 4A



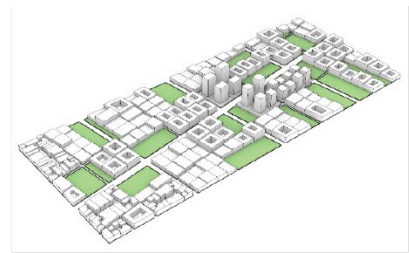
1. UHI INTENSITY



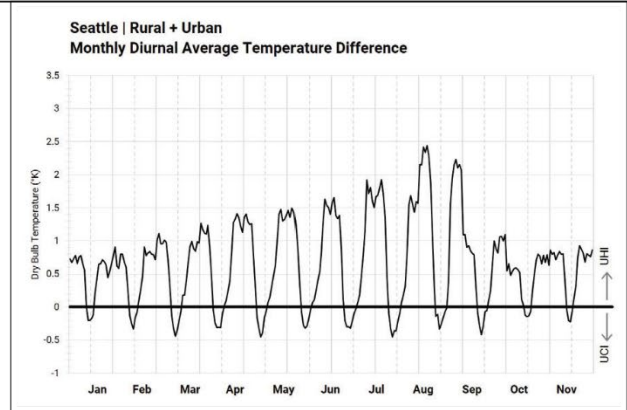
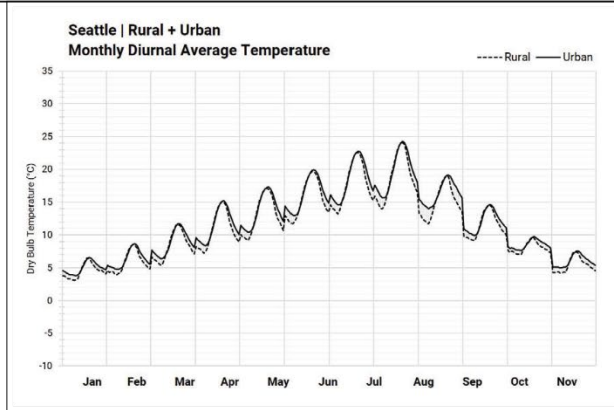
2. COOLING + HEATING ENERGY USE INTENSITY



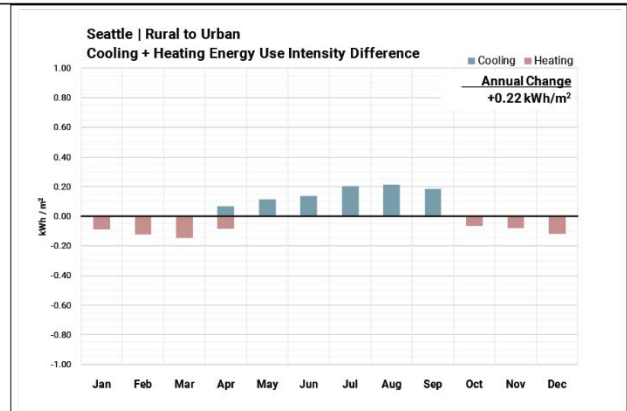
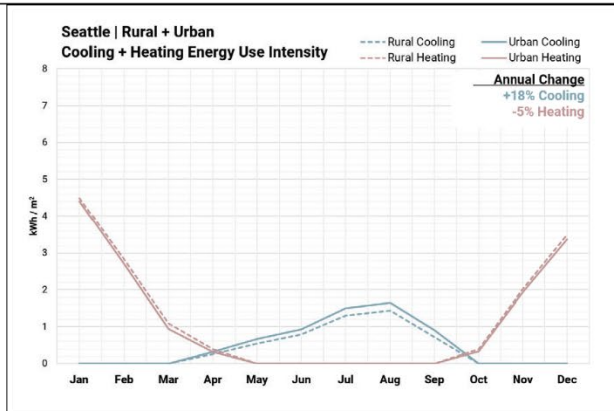
ITERATION #2B | SEATTLE LCZ 04 | Open High-Rise ASHRAE Climate Zone 4C



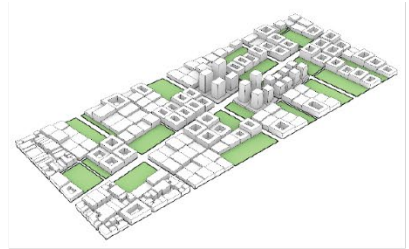
1. UHI INTENSITY



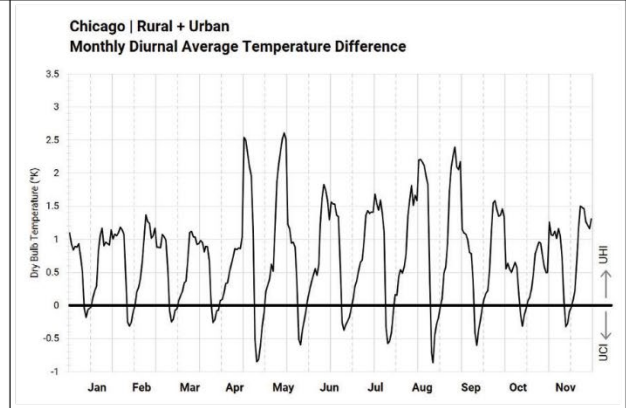
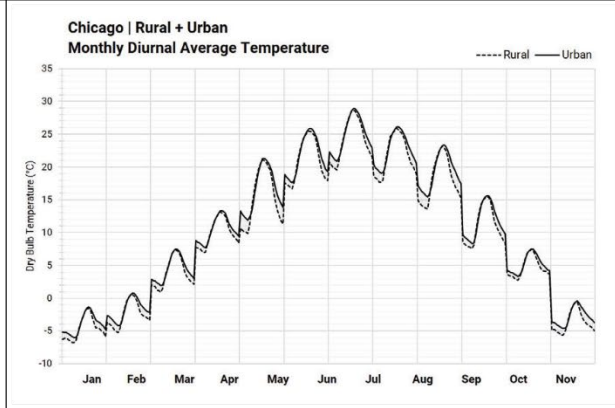
2. COOLING + HEATING ENERGY USE INTENSITY



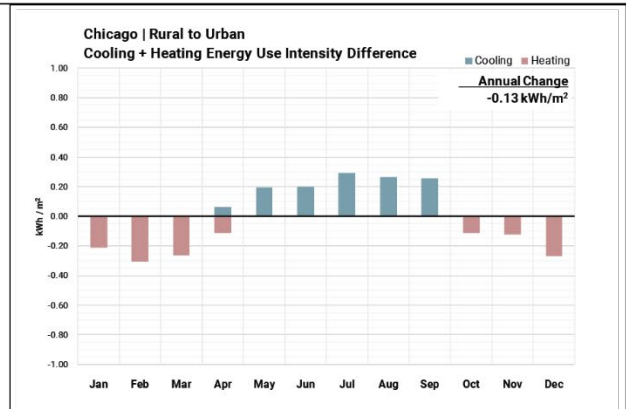
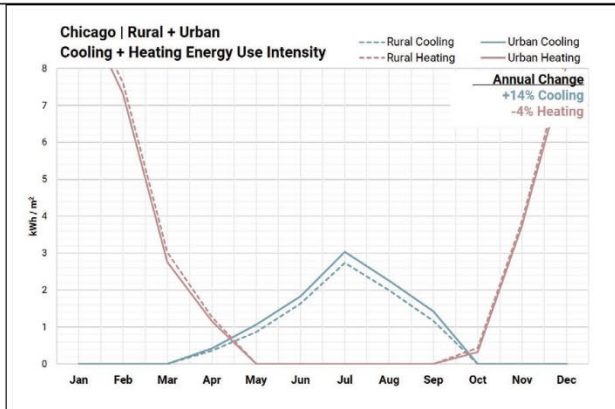
ITERATION #2B | CHICAGO LCZ 04 | Open High-Rise ASHRAE Climate Zone 5



1. UHI INTENSITY

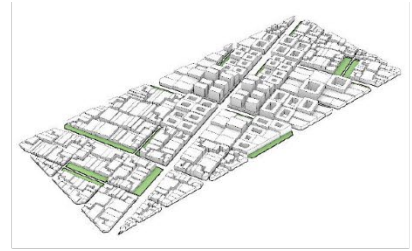


2. COOLING + HEATING ENERGY USE INTENSITY

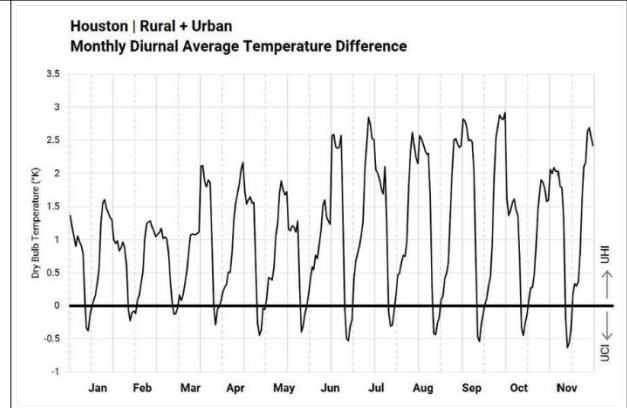
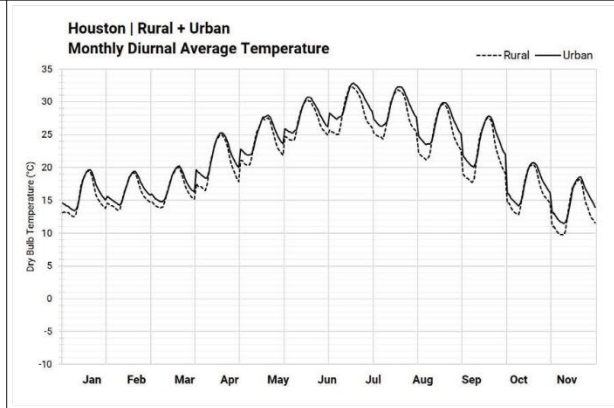


ITERATION #3A | HOUSTON

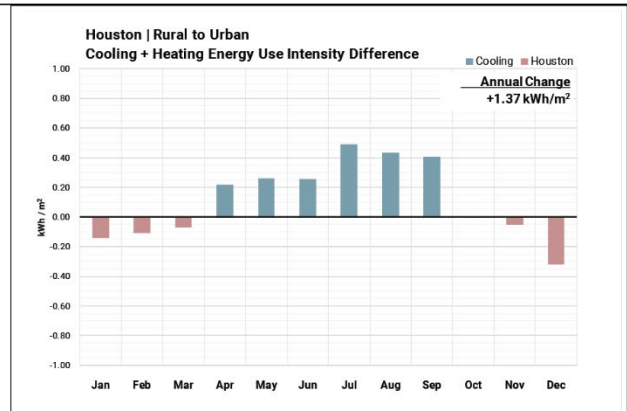
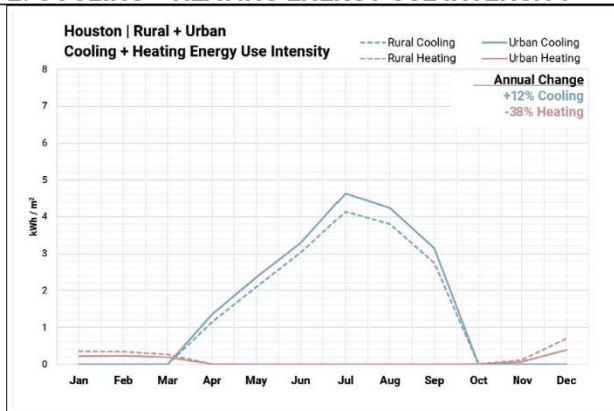
LCZ 02 | Compact Midrise
ASHRAE Climate Zone 2



1. UHI INTENSITY

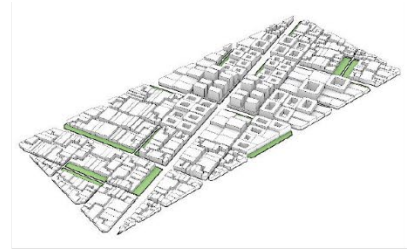


2. COOLING + HEATING ENERGY USE INTENSITY

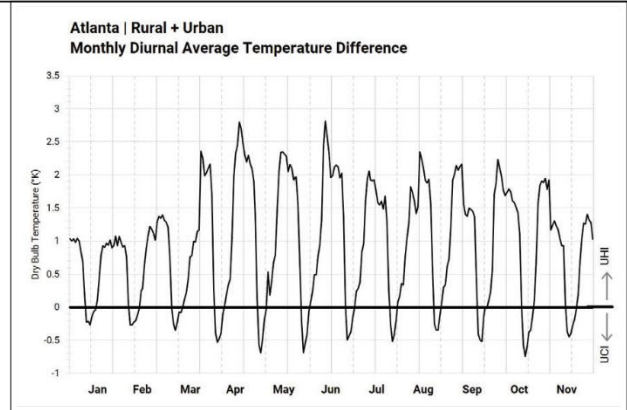
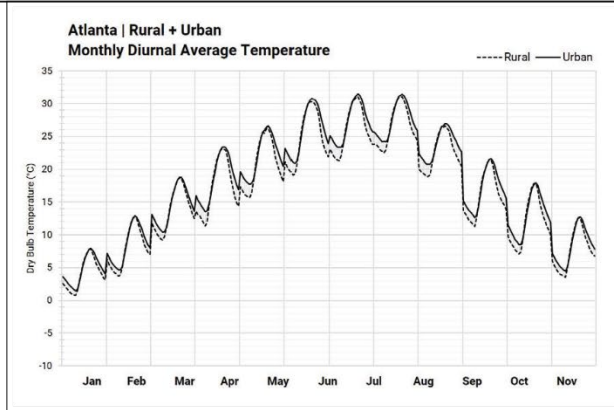


ITERATION #3A | ATLANTA

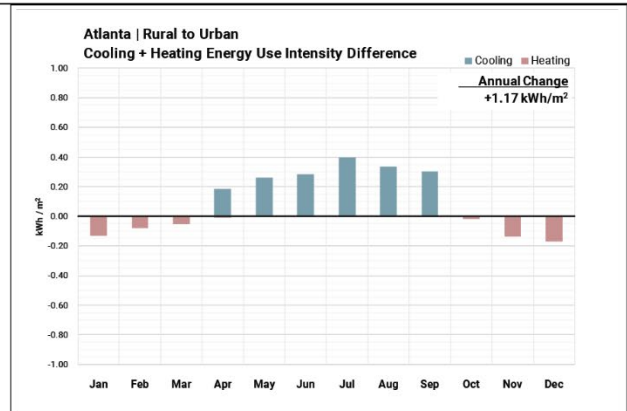
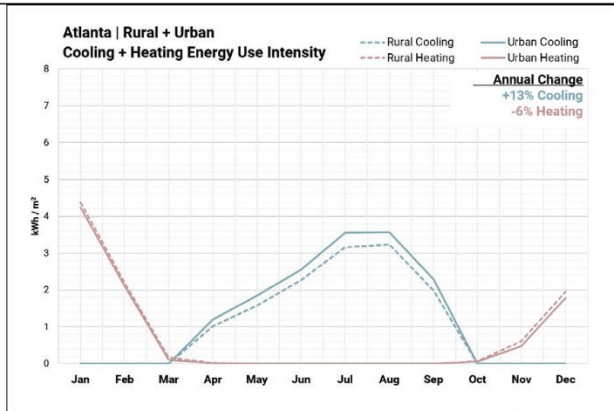
LCZ 02 | Compact Midrise
ASHRAE Climate Zone 3



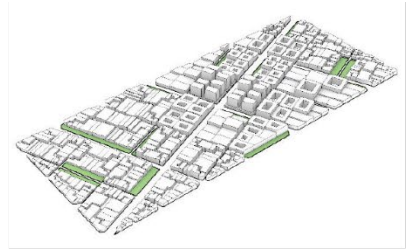
1. UHI INTENSITY



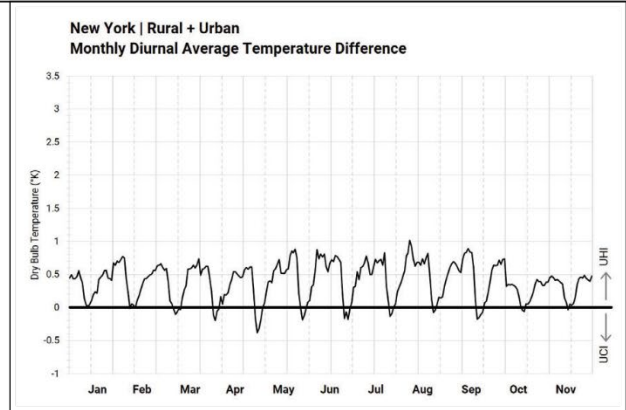
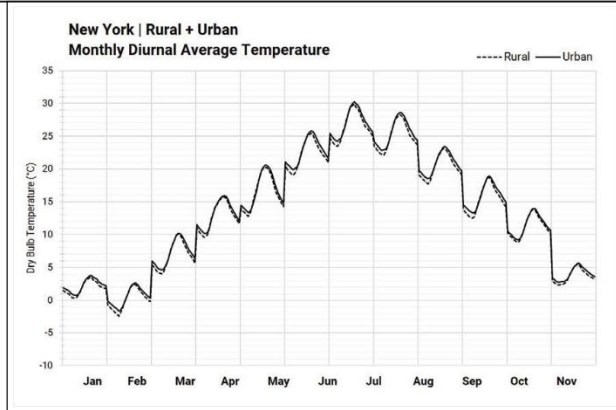
2. COOLING + HEATING ENERGY USE INTENSITY



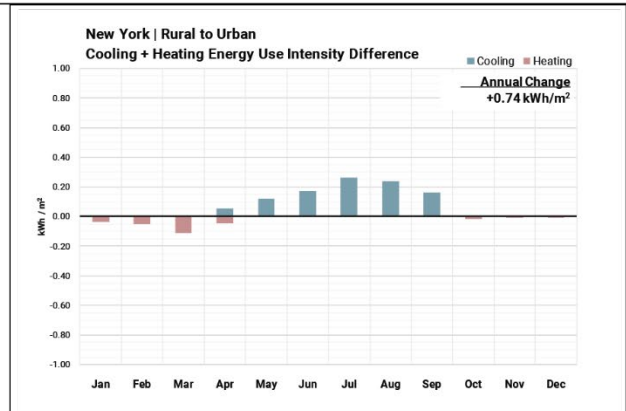
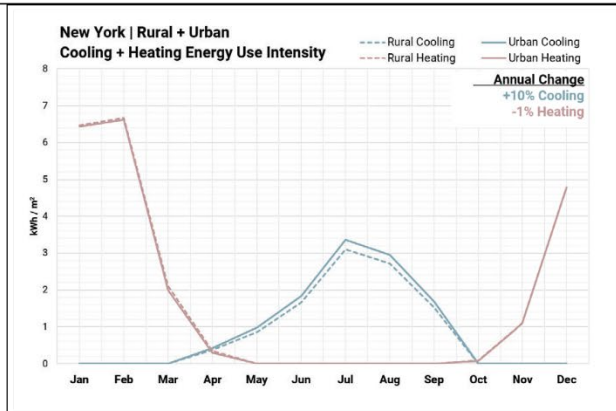
ITERATION #3A | NEW YORK LCZ 02 | Compact Midrise ASHRAE Climate Zone 4A



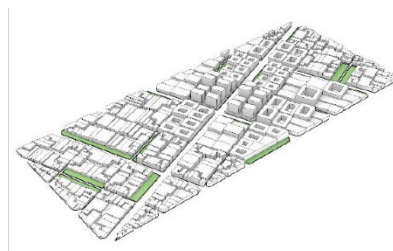
1. UHI INTENSITY



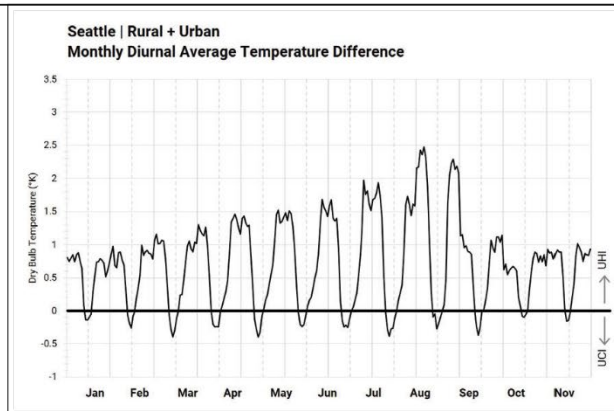
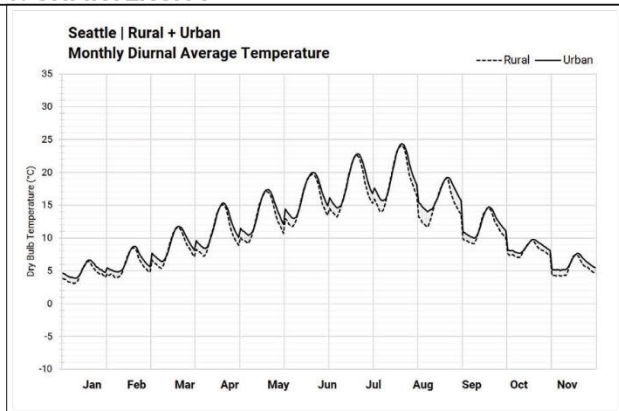
2. COOLING + HEATING ENERGY USE INTENSITY



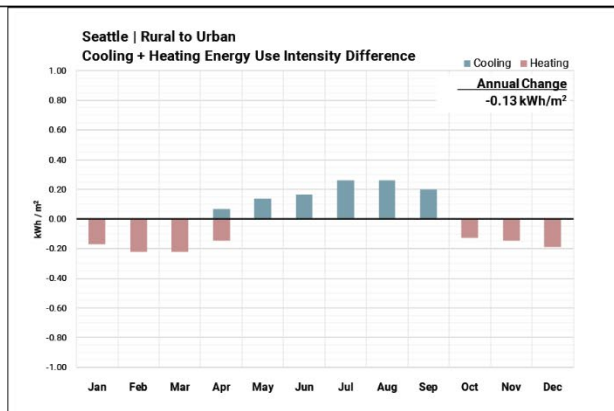
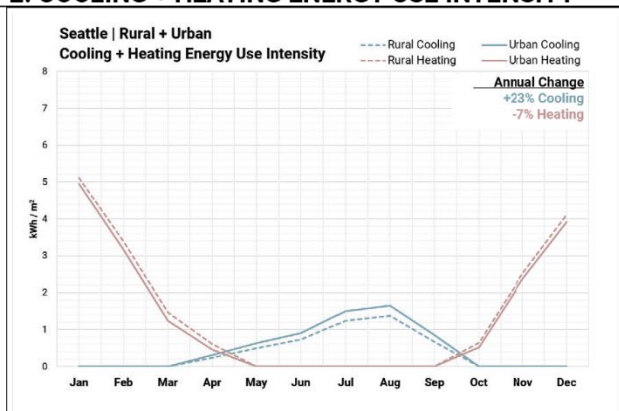
ITERATION #3A | SEATTLE LCZ 02 | Compact Midrise ASHRAE Climate Zone 4C



1. UHI INTENSITY

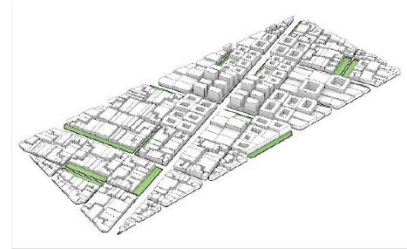


2. COOLING + HEATING ENERGY USE INTENSITY

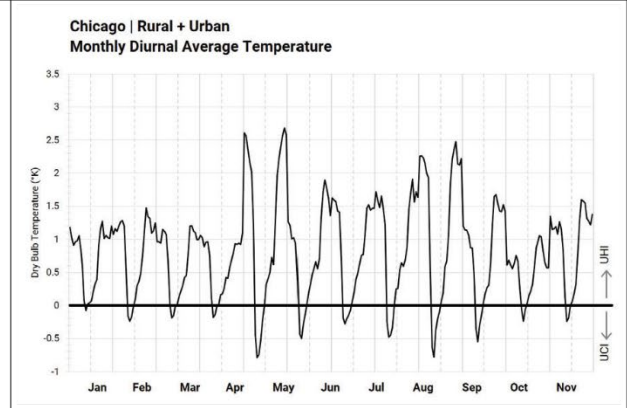
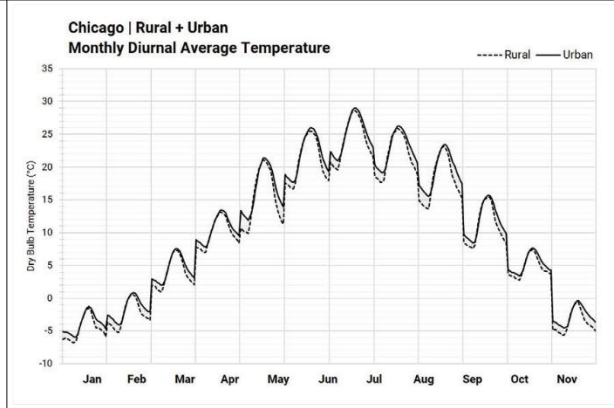


ITERATION #3A | CHICAGO

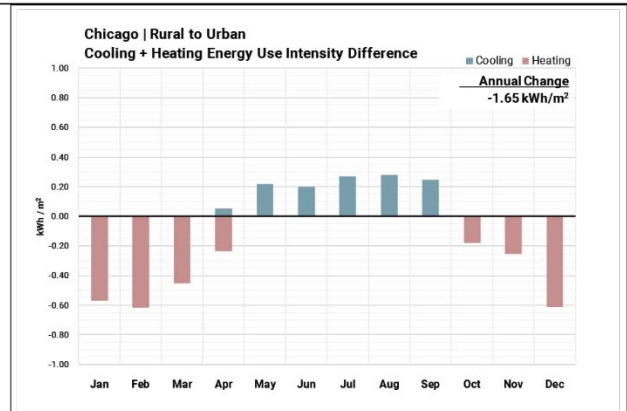
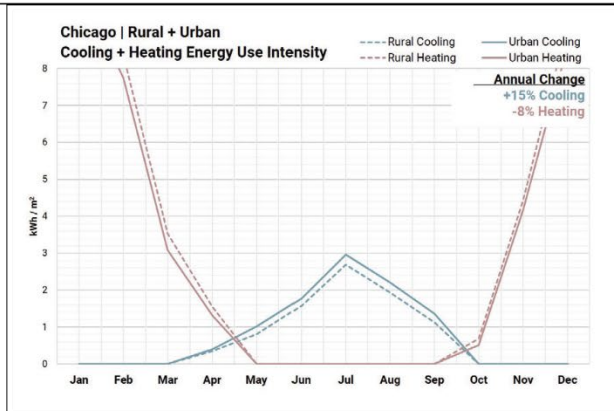
LCZ 02 | Compact Midrise
ASHRAE Climate Zone 5



1. UHI INTENSITY



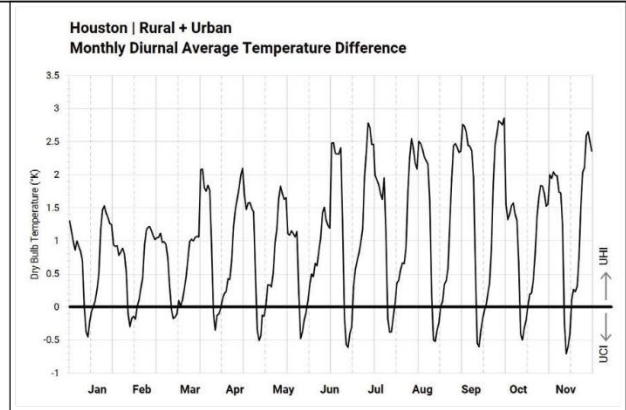
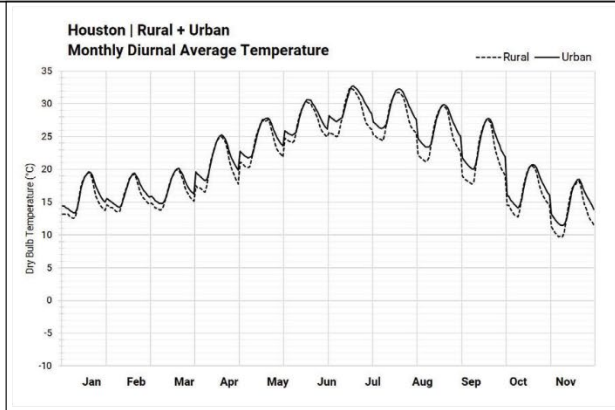
2. COOLING + HEATING ENERGY USE INTENSITY



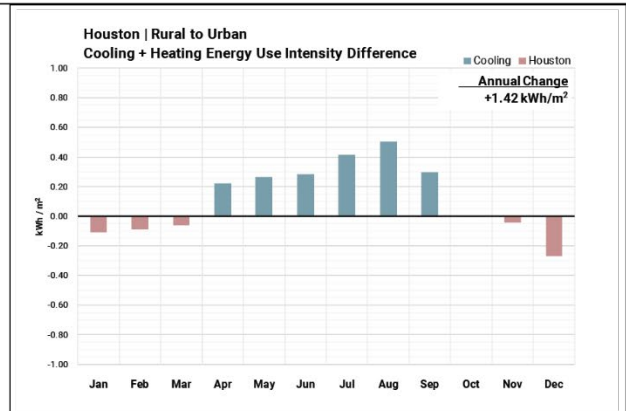
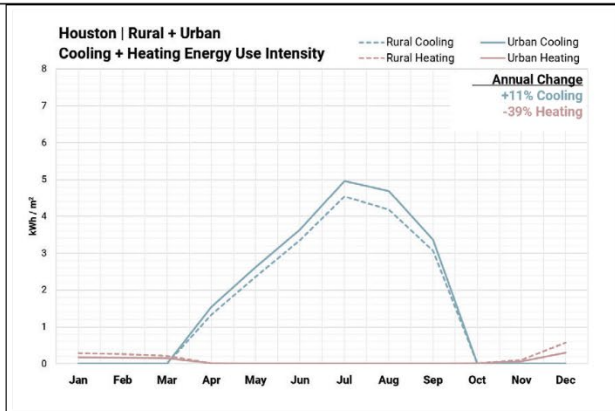
ITERATION #3B | HOUSTON LCZ 04 | Open High-Rise
ASHRAE Climate Zone 2



1. UHI INTENSITY



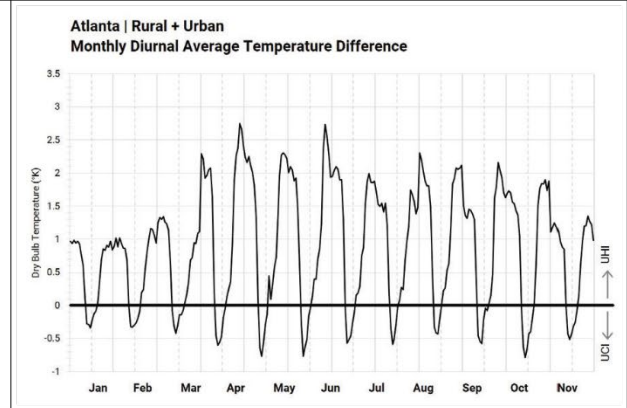
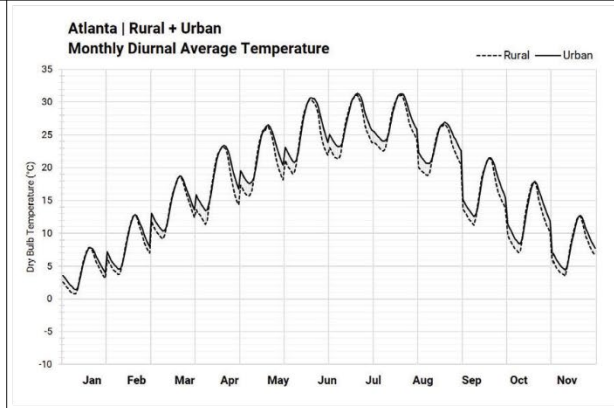
2. COOLING + HEATING ENERGY USE INTENSITY



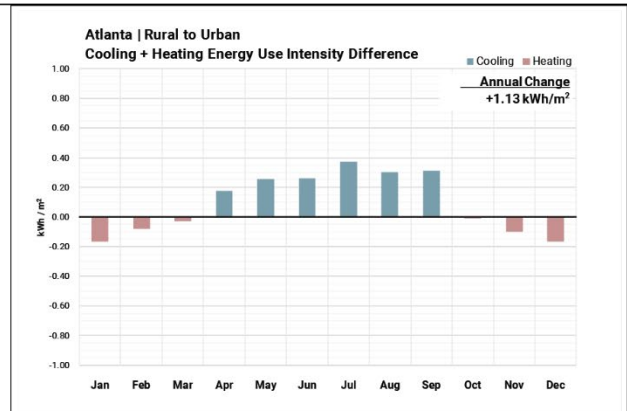
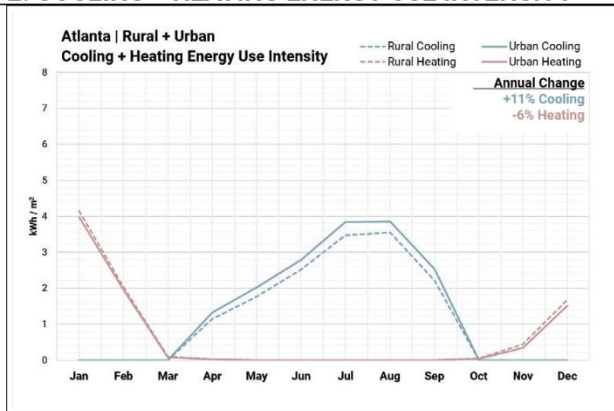
ITERATION #3B | ATLANTA LCZ 04 | Open High-Rise ASHRAE Climate Zone 3



1. UHI INTENSITY



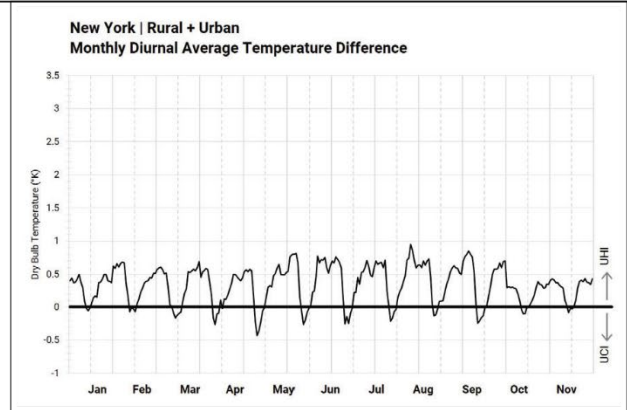
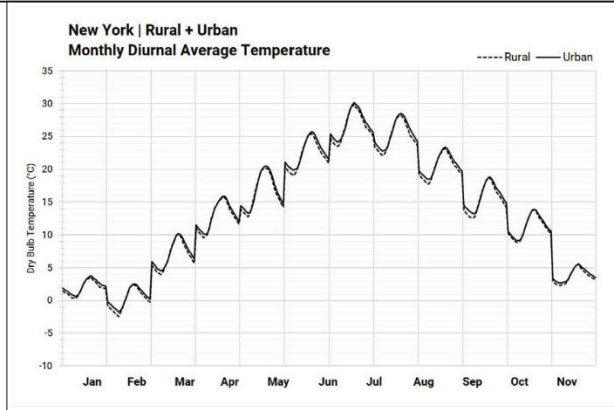
2. COOLING + HEATING ENERGY USE INTENSITY



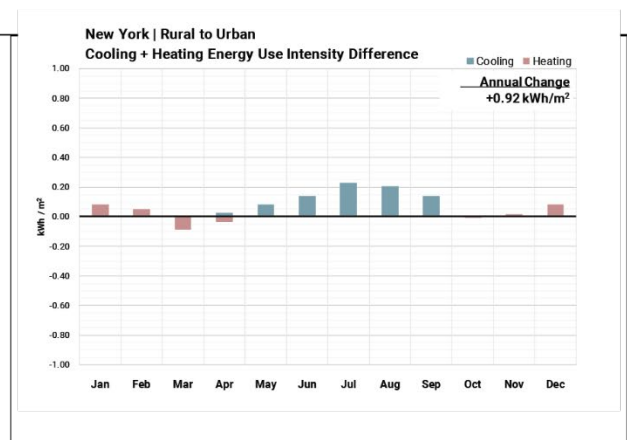
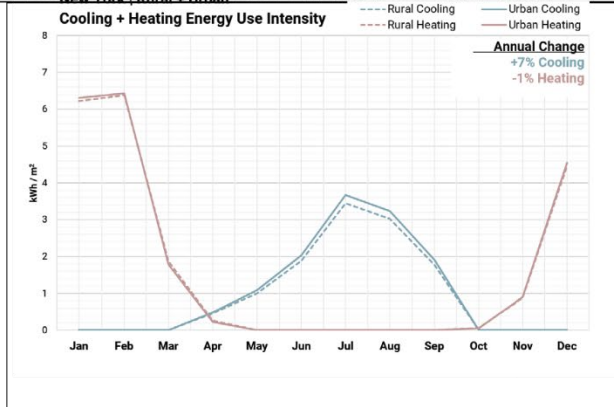
ITERATION #3B | NEW YORK LCZ 04 | Open High-Rise ASHRAE Climate Zone 4A



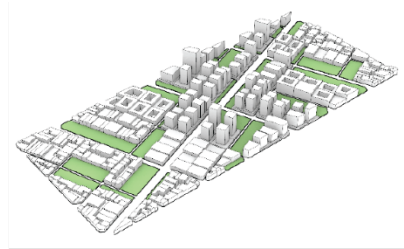
1. UHI INTENSITY



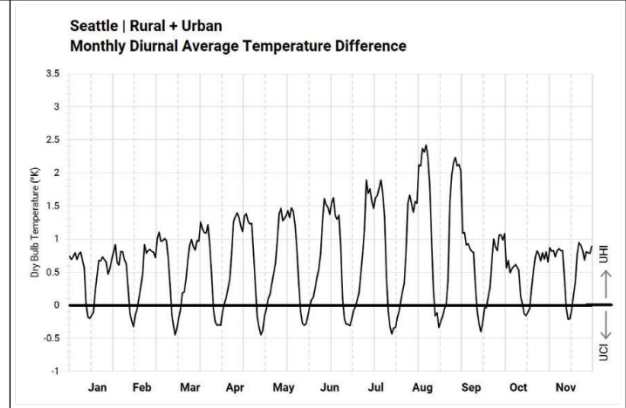
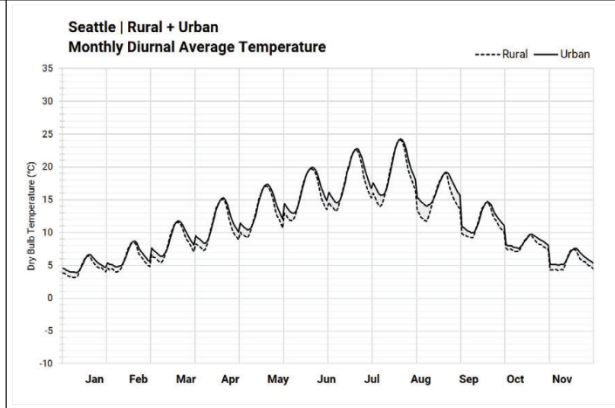
2. COOLING + HEATING ENERGY USE INTENSITY



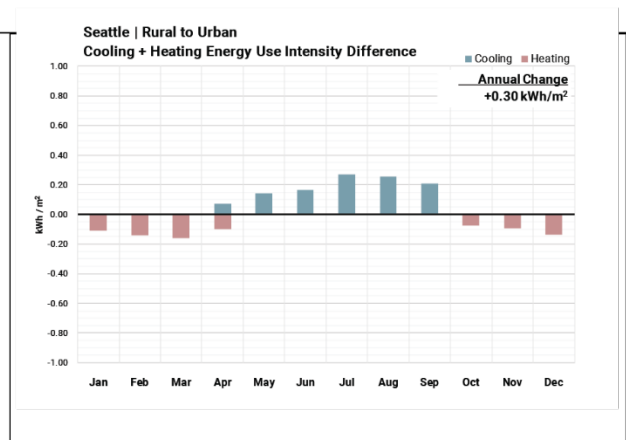
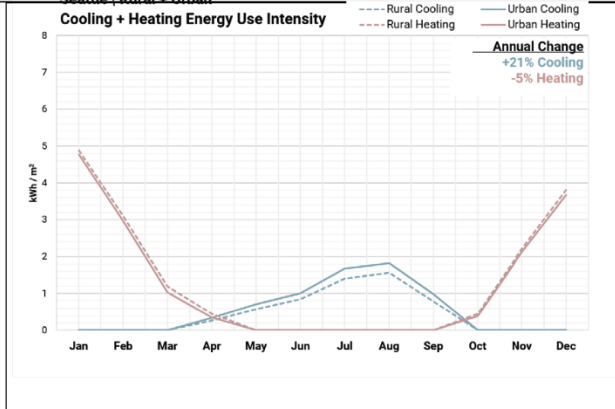
ITERATION #3B | SEATTLE LCZ 04 | Open High-Rise
ASHRAE Climate Zone 4C



1. UHI INTENSITY



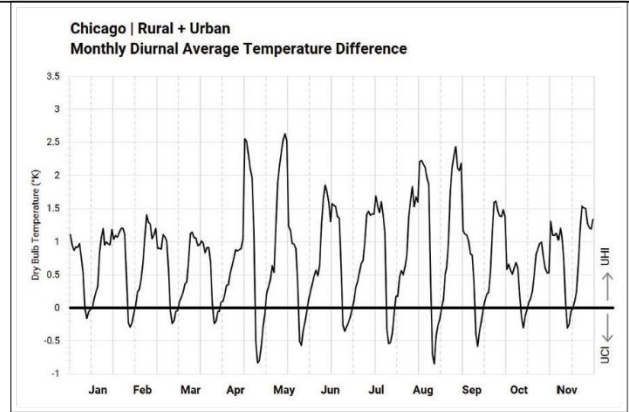
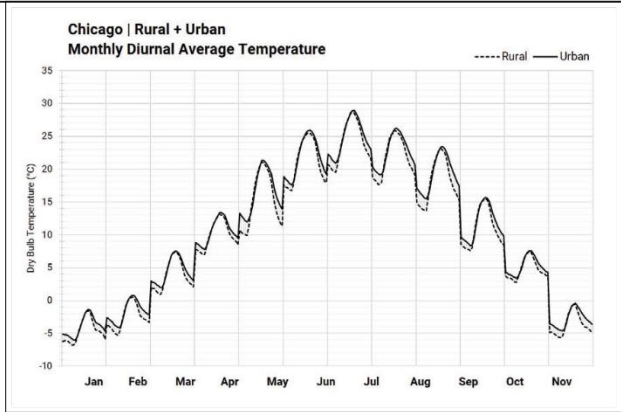
2. COOLING + HEATING ENERGY USE INTENSITY



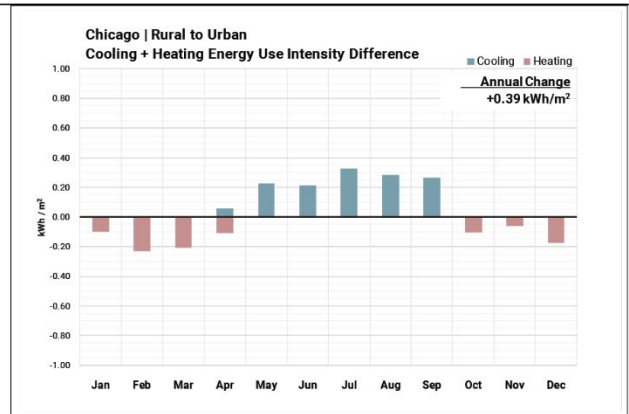
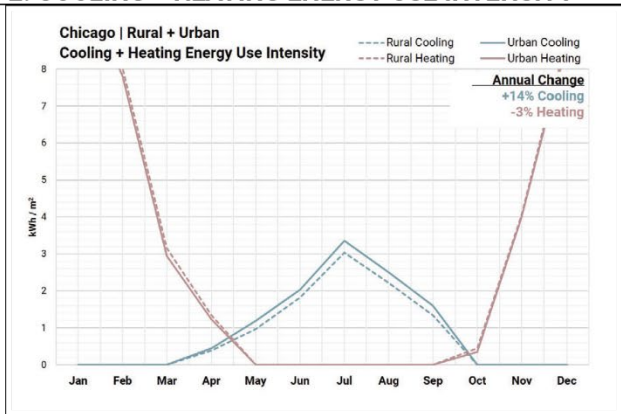
ITERATION #3B | CHICAGO LCZ 04 | Open High-Rise ASHRAE Climate Zone 5



1. UHI INTENSITY



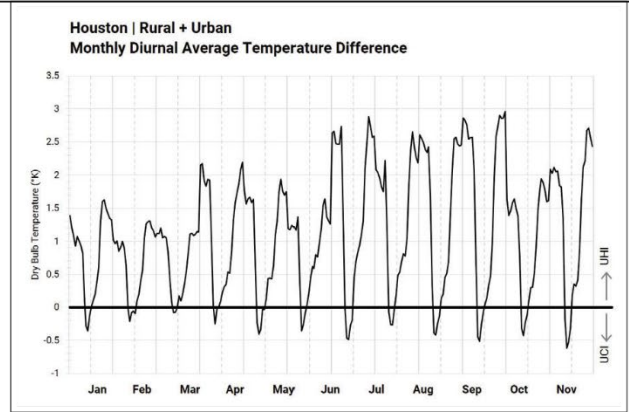
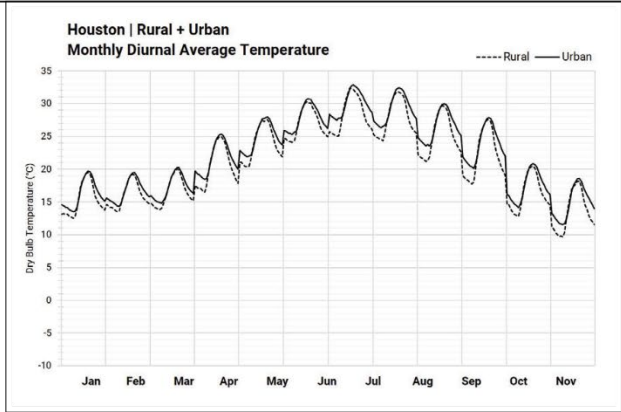
2. COOLING + HEATING ENERGY USE INTENSITY



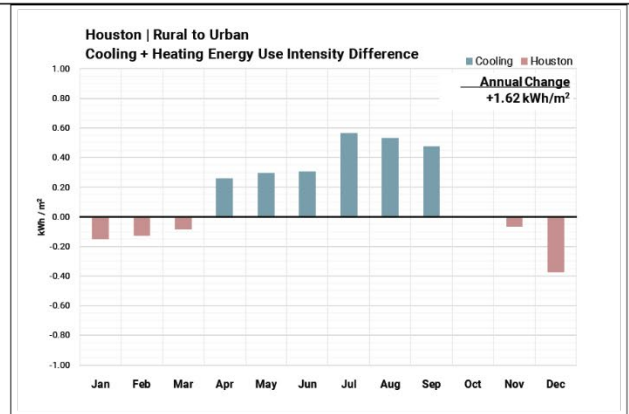
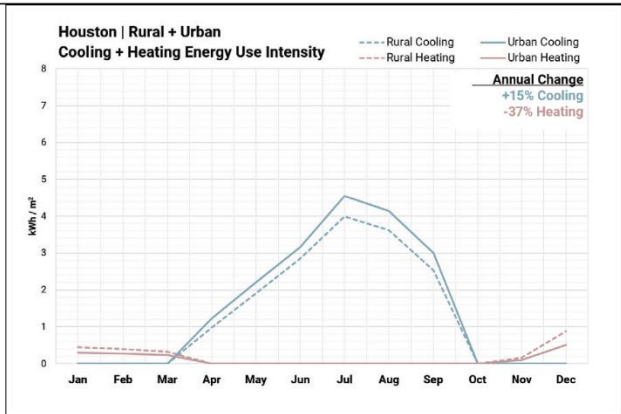
ITERATION #4A | HOUSTON LCZ 02 | Compact Midrise ASHRAE Climate Zone 2



1. UHI INTENSITY

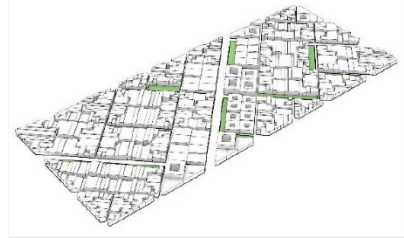


2. COOLING + HEATING ENERGY USE INTENSITY

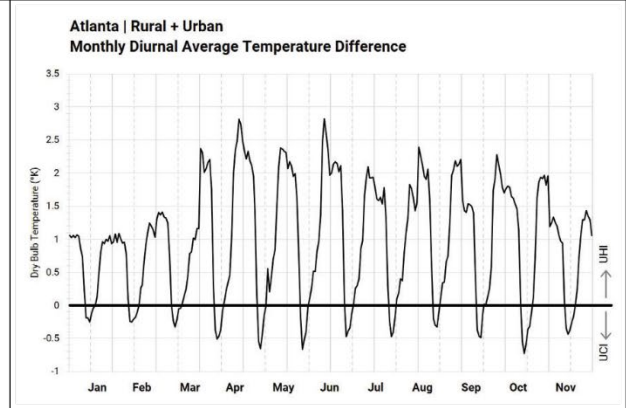
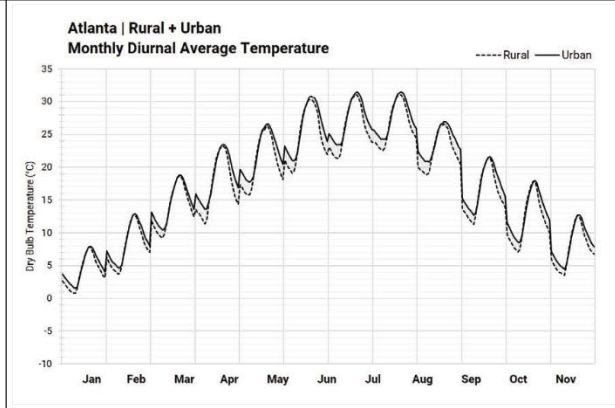


ITERATION #4A | ATLANTA

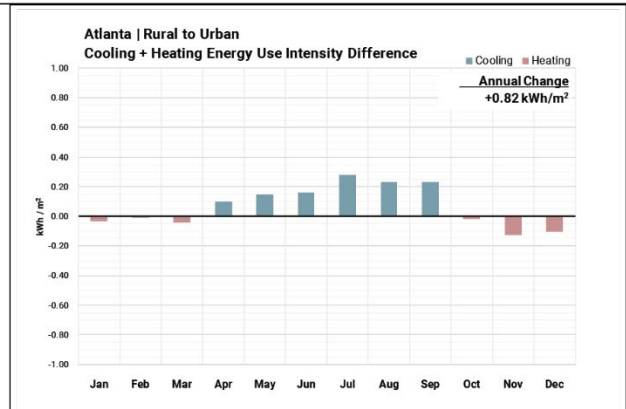
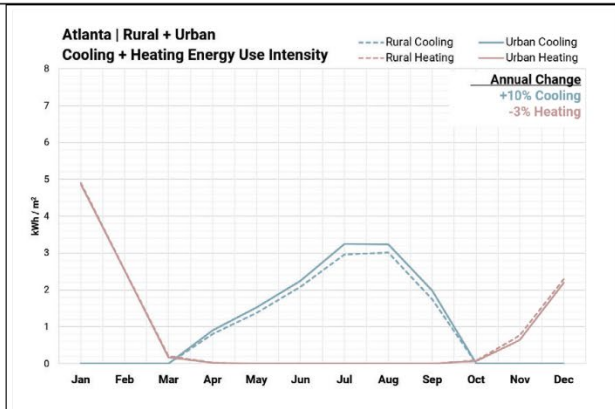
LCZ 02 | Compact Midrise
ASHRAE Climate Zone 3



1. UHI INTENSITY



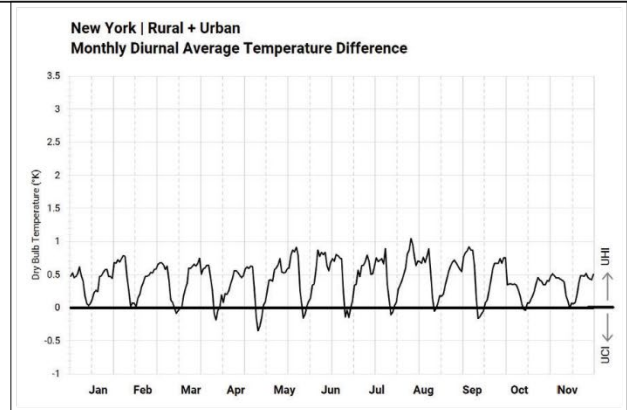
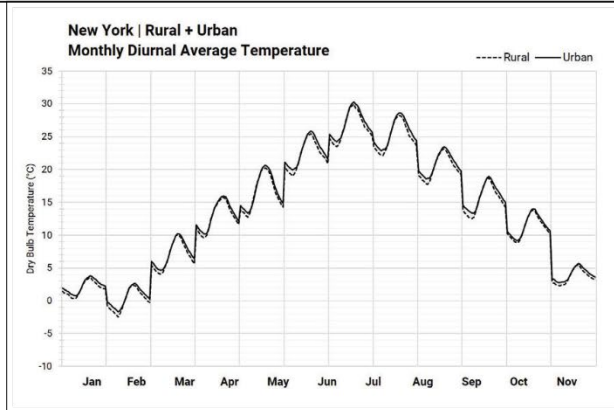
2. COOLING + HEATING ENERGY USE INTENSITY



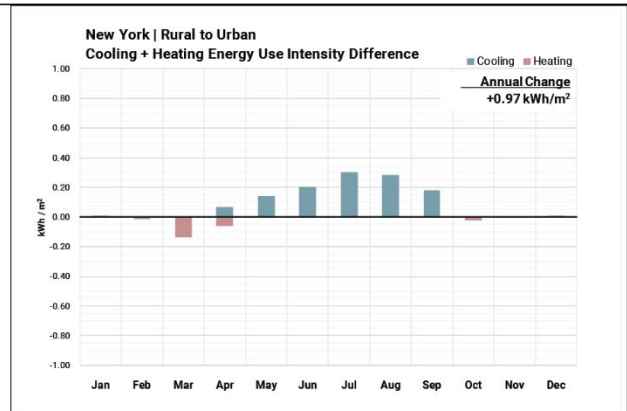
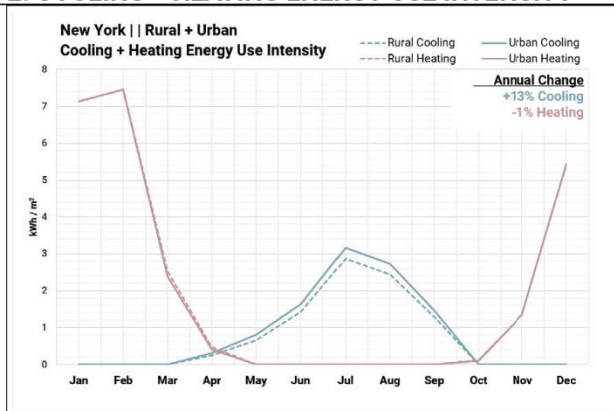
ITERATION #4A | NEW YORK LCZ 02 | Compact Midrise ASHRAE Climate Zone 4A



1. UHI INTENSITY



2. COOLING + HEATING ENERGY USE INTENSITY

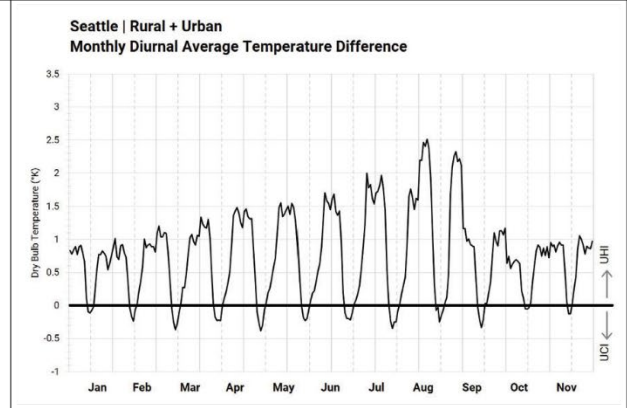
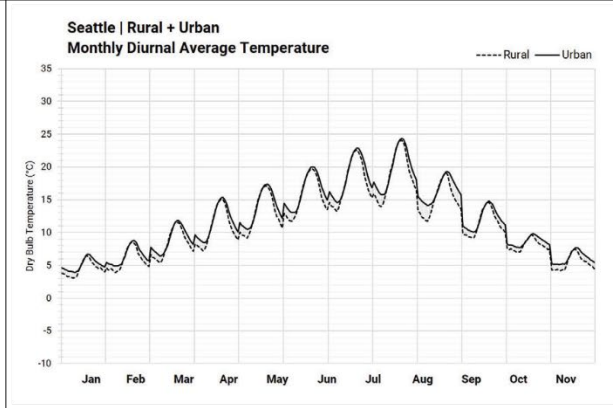


ITERATION #4A | SEATTLE

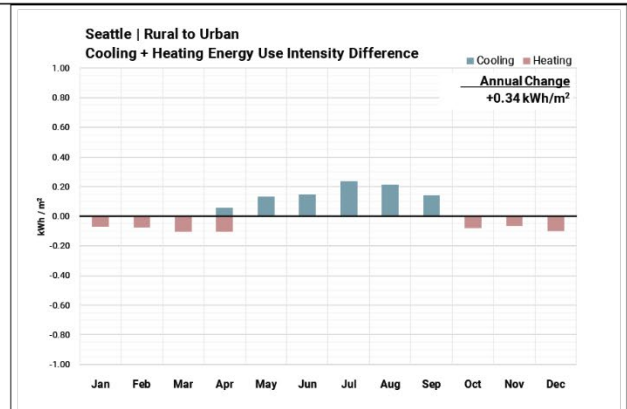
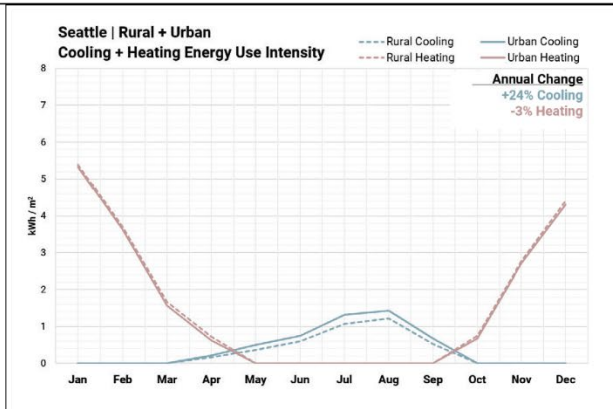
LCZ 02 | Compact Midrise
ASHRAE Climate Zone 4C



1. UHI INTENSITY

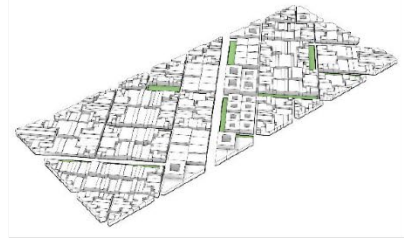


2. COOLING + HEATING ENERGY USE INTENSITY

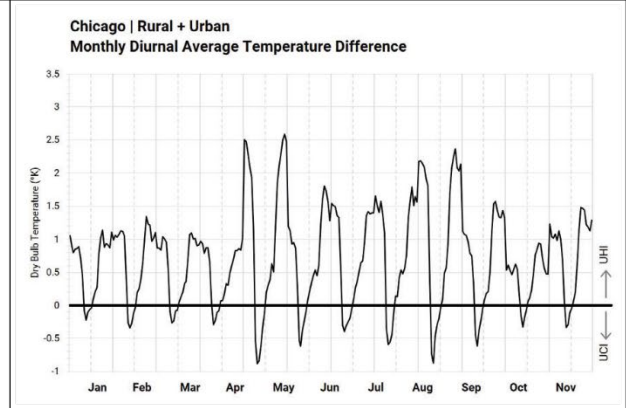
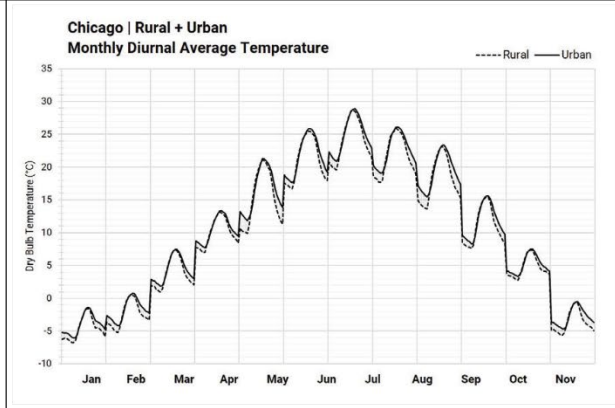


ITERATION #4A | CHICAGO

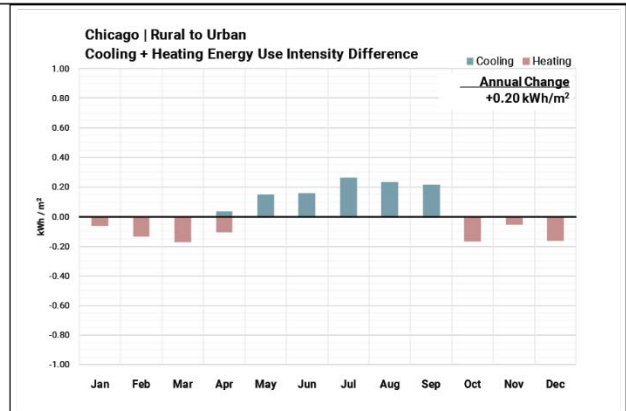
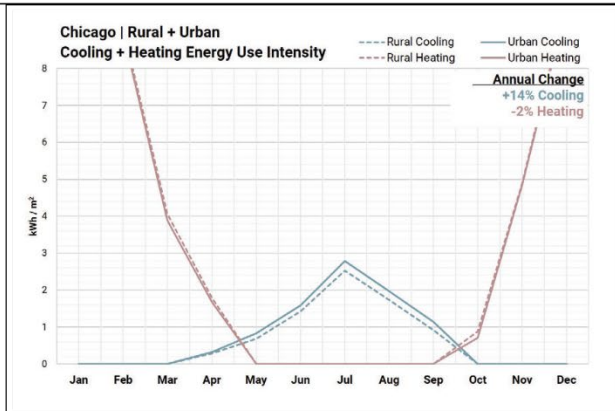
LCZ 02 | Compact Midrise
ASHRAE Climate Zone 5



1. UHI INTENSITY



2. COOLING + HEATING ENERGY USE INTENSITY

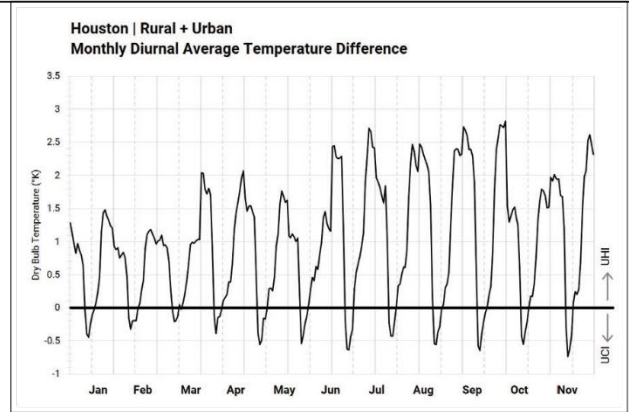
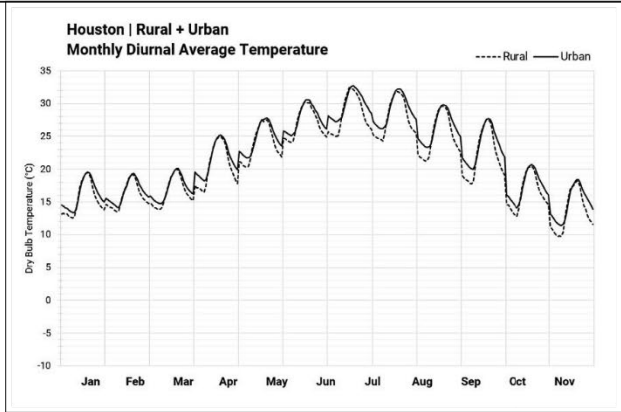


ITERATION #4B | HOUSTON

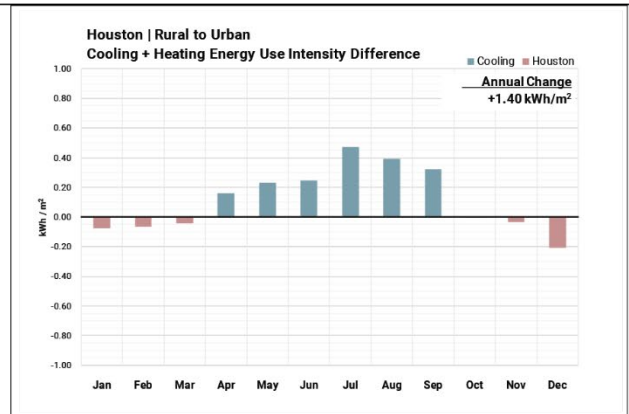
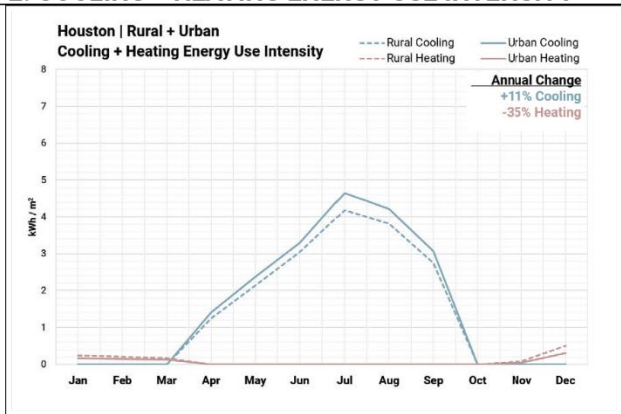
LCZ 04 | Open High-Rise
ASHRAE Climate Zone 2



1. UHI INTENSITY



2. COOLING + HEATING ENERGY USE INTENSITY

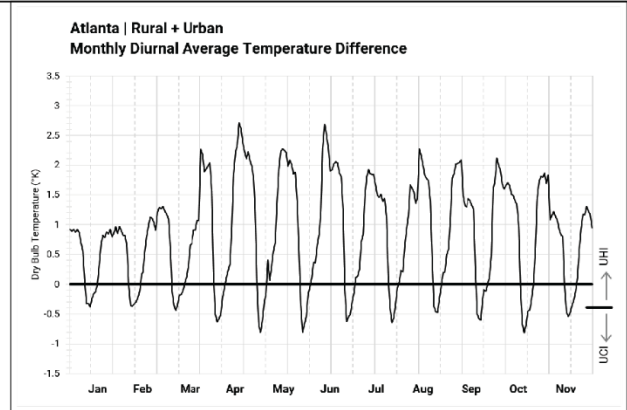
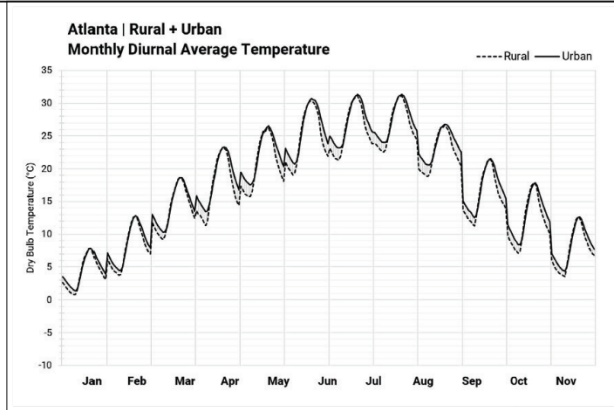


ITERATION #4B | ATLANTA

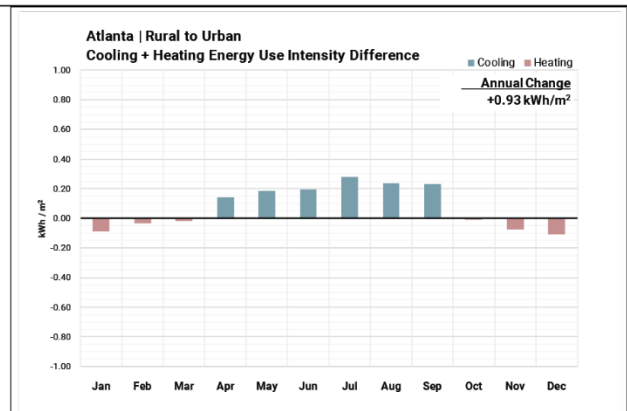
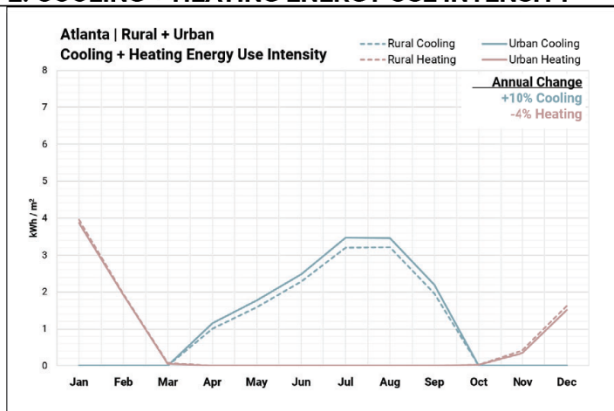
LCZ 04 | Open High-Rise
ASHRAE Climate Zone 3



1. UHI INTENSITY



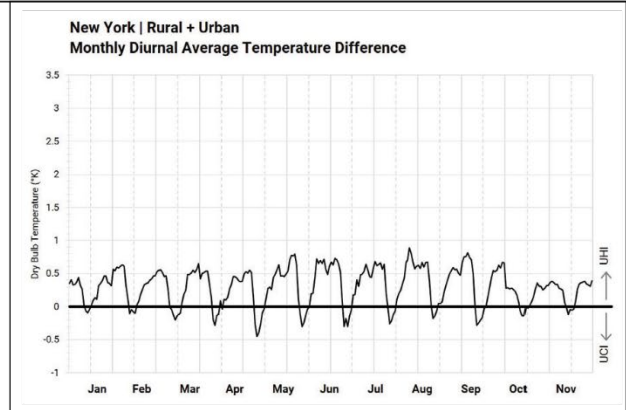
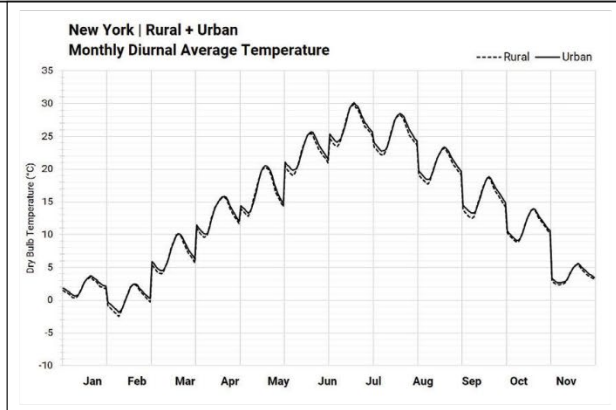
2. COOLING + HEATING ENERGY USE INTENSITY



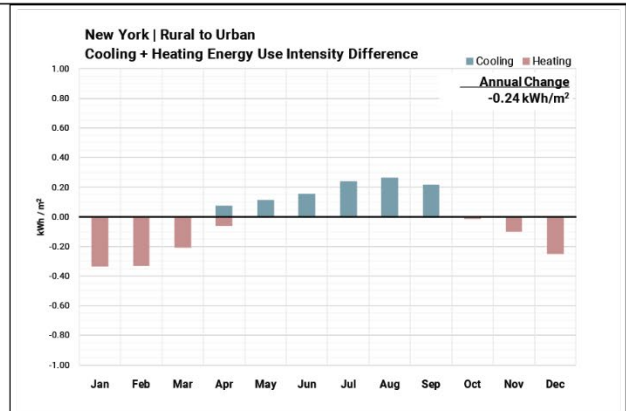
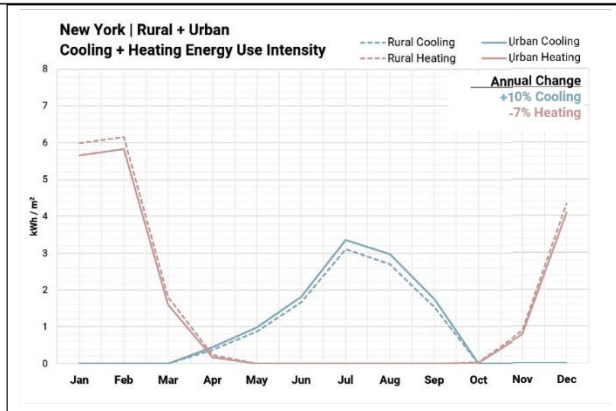
ITERATION #4B | NEW YORK LCZ 04 | Open High-Rise ASHRAE Climate Zone 4A



1. UHI INTENSITY



2. COOLING + HEATING ENERGY USE INTENSITY

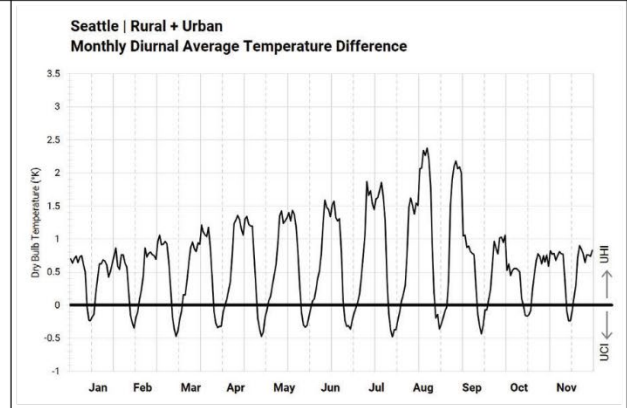
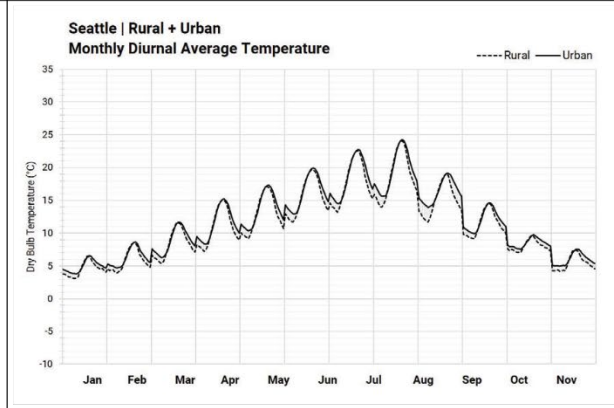


ITERATION #4B | SEATTLE

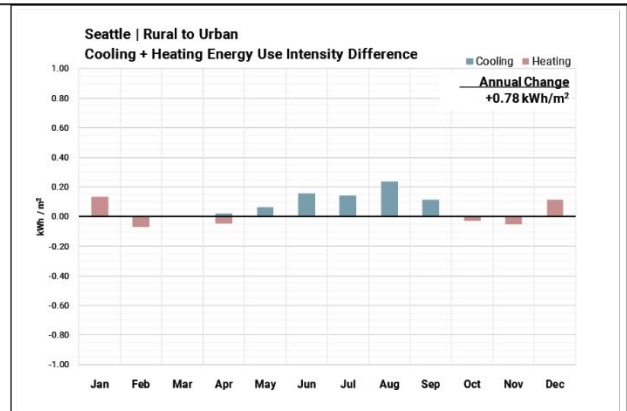
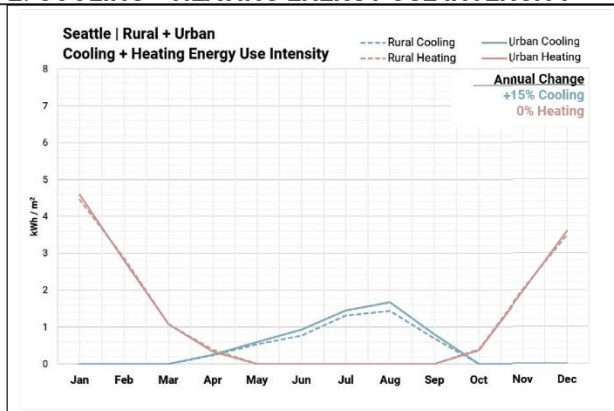
LCZ 04 | Open High-Rise
ASHRAE Climate Zone 4C



1. UHI INTENSITY



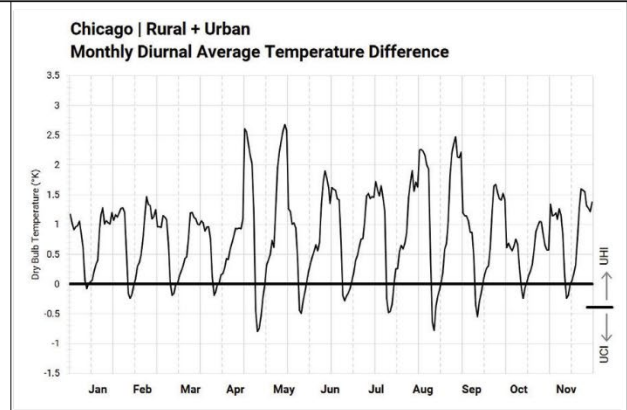
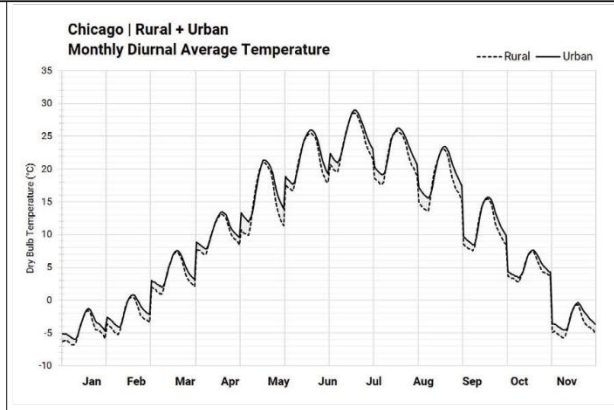
2. COOLING + HEATING ENERGY USE INTENSITY



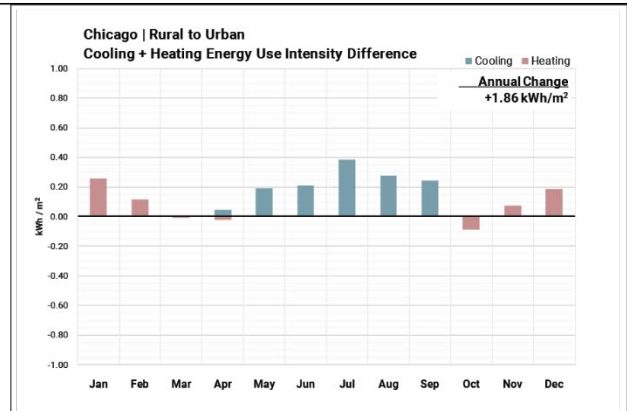
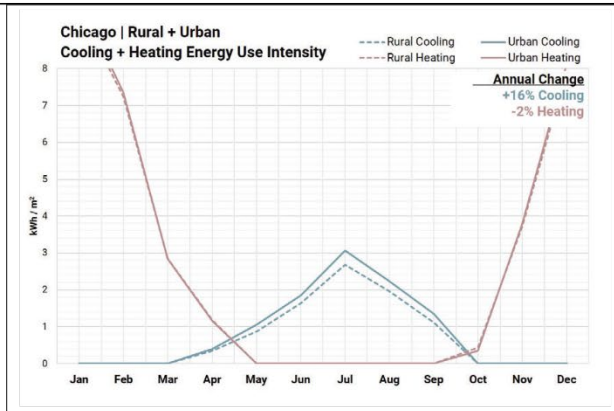
ITERATION #4B | CHICAGO LCZ 04 | Open High-Rise ASHRAE Climate Zone 5



1. UHI INTENSITY



2. COOLING + HEATING ENERGY USE INTENSITY



4.3.2. Climate Impact

The impact UHI intensity has on temperatures can be observed in section 1. UHI Intensity on the result sheets produced for each graph in Chapter 4.3.1.

4.3.2.1. Temperature

For warm climates, like Houston and Atlanta, the impact that UHI intensity has on temperatures is straightforward, resulting in consistently increased temperatures year-round. For the tested models, the highest intensities reach near 3°K. The reverse UCI effect in these warm climates is observed to reduce temperatures less than 0.5°K year-round. For Seattle and Chicago, the warmest months, experience near 2.5°K increase while cooler months experience less than 1°K increase. For Seattle, an UCI effect is observed at less than 0.5°K year-round, while in Chicago, the UCI intensity can be observed to near 1°K for some on the tested models. For New York, UHI intensity measures at an unexpectedly lower intensity than for the other climates considered in this study. On average, the year-round temperature increase remains less than 1°K, and the UCI intensity is observed at less than 0.5°K for only a few months of the year.

4.3.2.1. Rural Reference Location

For Houston, Atlanta, Seattle and Chicago, the temperature differences observed from the tested models are not surprising. For New York however, the anomaly of lower than anticipated UHI intensity can perhaps be explained by examining the rural reference measurement locations.

The airport EPW files selected for the rural reference locations in Houston, Atlanta, Seattle and Chicago are located within different built contexts than the New York rural reference location. The former airport locations (Figure 29 - Figure 32) can be classified as LCZ 08 Large, Low-Rise and are predominantly surrounded by LCZ 06 Open Low-Rise and LCZ 09 Sparsely-Built. The airport location for New York (Figure 33) can also be classified as LCZ 08 Large, Low-Rise; however, the built surroundings are predominantly LCZ 03 Compact Low-Rise. It is speculated that because the rural reference file for New York is more “urban” than it is “rural”, the UHI intensity between the urban models tested (LCZ 02 Compact Midrise and LCZ 04 Open High-Rise) and the New York reference file (LCZ 08 and LCZ 03) is less significant. If the New York reference file was in the

same contextual environment (same LCZ surroundings) as the other four climates, the magnitude of UHI intensity could be of comparable significance. A list of abridged LCZ definitions is attached in Appendix B. Local Climate Zones Abridged Definitions.

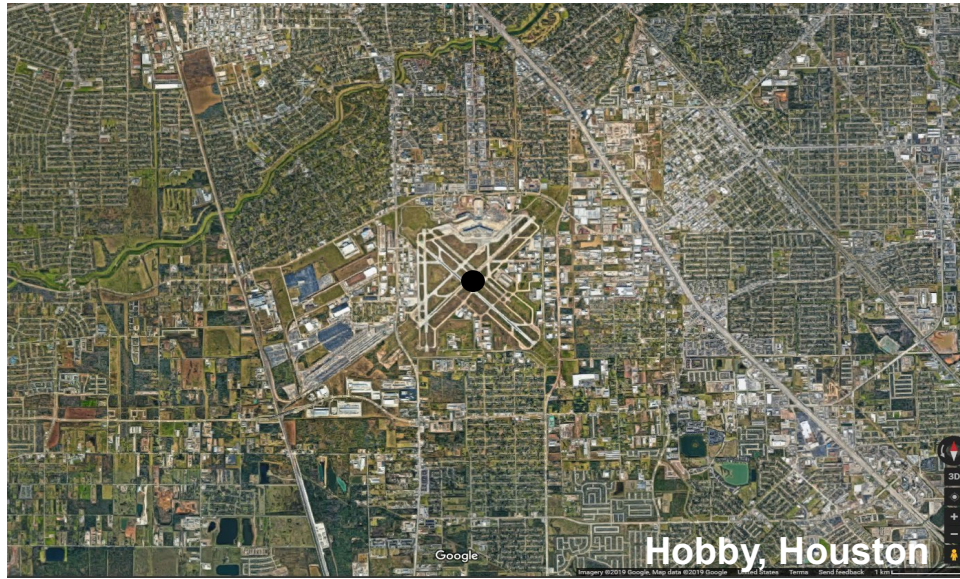


Figure 29. William P. Hobby Airport, Houston

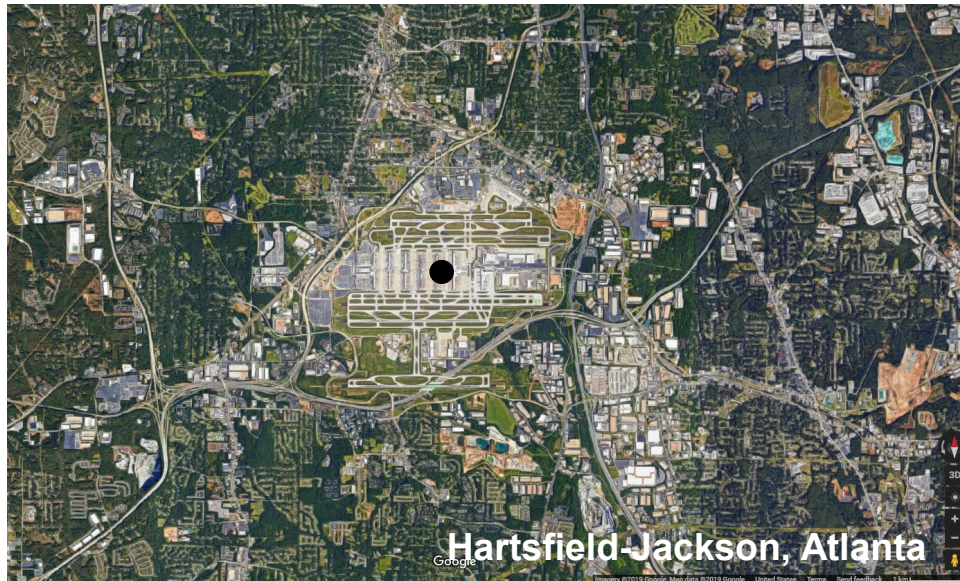


Figure 30. Hartsfield-Jackson Atlanta International Airport, Atlanta

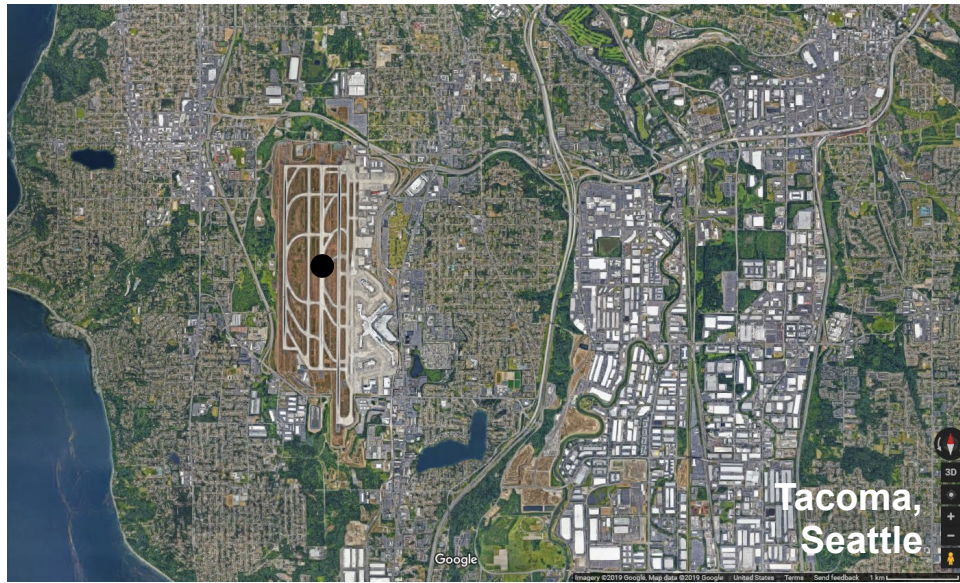


Figure 31. Seattle-Tacoma International Airport, Seattle

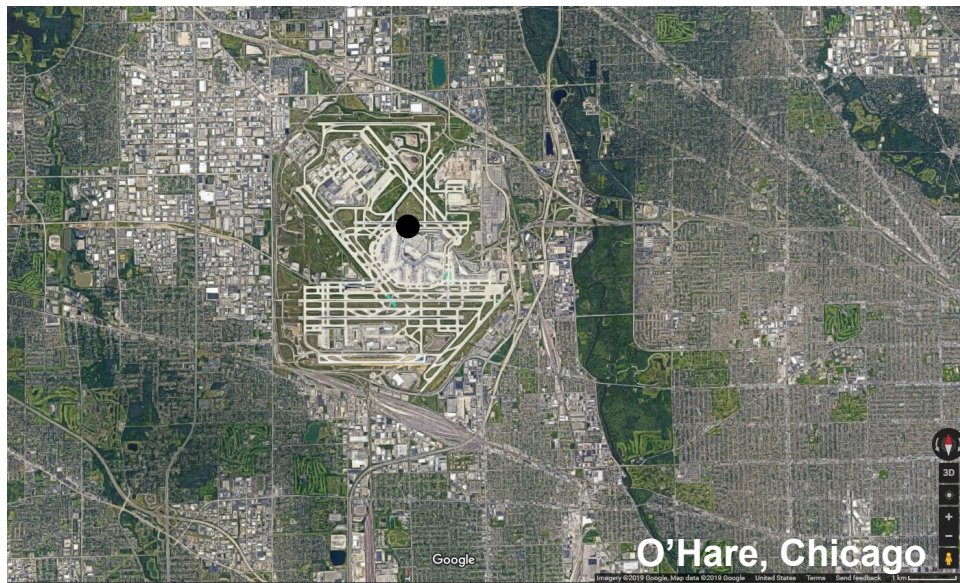


Figure 32. O'Hare International Airport, Chicago



Figure 33. LaGuardia Airport, New York

4.3.2.3. Wind and Water Observations

The presence and the effects of large bodies of water on the microclimate of the rural reference location cannot be ignored. An in-depth analysis of the impact is not considered in this study, however, a brief wind analysis is completed for the two sites affected by the presence of large bodies of water.

For Seattle, winds are prevalent from the southwesterly and northeasterly directions (Figure 34). These directions respectively point to the open corridors created by Lake Washington and the Puget Sound inlet from the Pacific Ocean, which border the city of Seattle. Since the Seattle-Tacoma airport is not isolated outside of the general city boundaries and since the city of Seattle is relatively small, wind conditions at the airport generally describe wind conditions within the city. Though not conclusive, it can be presumed that the effects of winds from the surrounding bodies of water is even throughout the city and not a special condition particular to the rural reference. This means that the rural reference file is suitable for UHI intensity studies for Seattle.

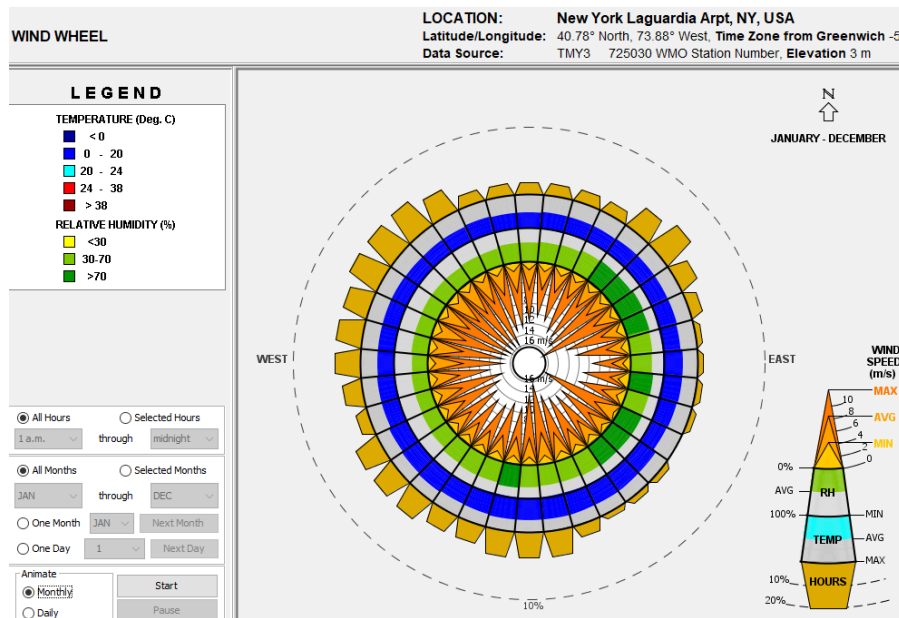


Figure 35. LaGuardia, New York Wind Wheel

4.3.3. Energy Use Intensity

The impact UHI intensity on cooling and heating EUI can be observed in section 2. Cooling and Heating Energy Use Intensity on the result sheets produced for each graph in Chapter 4.3.1.

As expected, the results indicate that the warmer the climate is, the higher the cooling EUI is, and the cooler the climate is, the higher the heating EUI is. The net change in cooling and heating EUI (Figure 36) for the tested models reveals whether UHI impact is beneficial for or detrimental to conditioning within each city and climate. The hot and humid Houston climate means that there is a consistently higher increase in conditioning EUI, relative to the other climates, ranging between approximately 1.2 kWh/m² to 1.7 kWh/m². Atlanta EUI increase is in the range of 0.80 kWh/m² to 1.3 kWh/m². New York EUI ranges between a decrease of approximately 0.25 kWh/m² for one model to increases of up to about 1.0 kWh/m² for the other models. Seattle EUI ranges between a decrease of approximately 0.15 kWh/m² to increases of up to 0.80 kWh/m². Chicago has the broadest range with a decrease of 1.65 kWh/m² in one model to about 1.9 kWh/m².

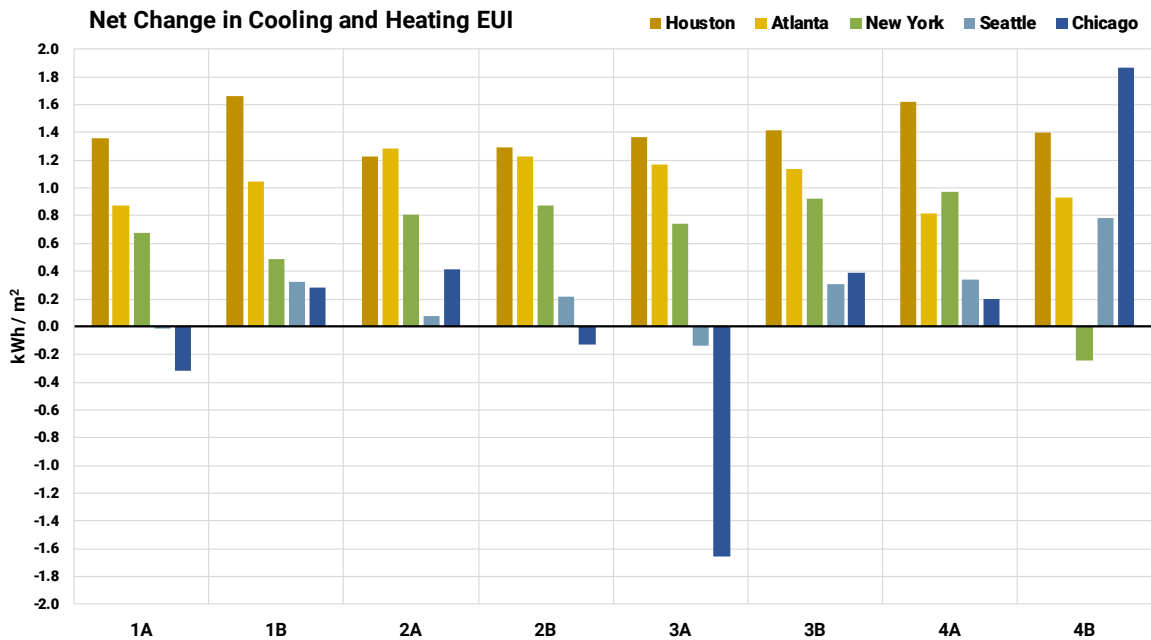


Figure 36. Net Change in Cooling and Heating EUI

Once more, UHI intensity is clearly detrimental to warmer climates proven by the higher cooling loads incurred for those cities. However, in cooler climates, UHI intensity can at times be beneficial by decreasing heating loads enough to cause a negative net change in conditioning EUI.

The EUI observations for this urban analysis also indicate an interesting point relating to the nature of this type of iterative analysis for urban areas. For warmer climates, the game revolves around picking the least harmful iteration. However, in cooler climates, the urban design iterations are able to show the most harmful and most beneficial candidates. This communicates that UHI effect could be a design intention in urban spaces. For warmer climates, the inadvertent impact can be controlled and lowered by the right urban designs and for cooler climates UHI urban spaces can be intentionally design for UHI intensity that reduces conditioning EUI.

4.3.3.1. Vegetation Impact

A hypothesis tested with these models is the impact on vegetation on UHI intensity. The vegetation variable is what causes the eight models be categorized in four sets (see Chapter 4.2.1.). The vegetation coverage ratio is varied; Group A is the LCZ 02 Compact Midrise classification with 10% vegetation cover and group B is LCZ 04 Open High-Rise classification with 30% vegetation cover. The horizontal and vertical density distribution changes accordingly.

The vegetation impact is assessed for iterations in each model set through a comparison of the cooling and heating EUI generated from the urban EPW. The results can be displayed in Figure 37 through Figure 44.

For cooling, group B consistently has a higher EUI than group A. For heating, group A has a higher EUI than group B. This can perhaps be explained by the impact of radiation on the building surfaces. Group A models have buildings that are more horizontally distributed and compact with a sky view factor of 0.45 (Table 3. LCZ Properties for used typologies (I. D. Stewart & Oke, 2012)), meaning that less façade area is exposed to the sky. Group B buildings are more vertically distributed across the site creating wider canyons with a sky view factor of 0.6 (Table 3. LCZ Properties for used typologies (I. D. Stewart & Oke, 2012)). Group B receives more solar radiation exposure on the facades and has therefore more need to cool in cooling season and less need to heat in heating season. The impact of internal load-dominated buildings is not captured by this analysis, perhaps due to the scale of the study.

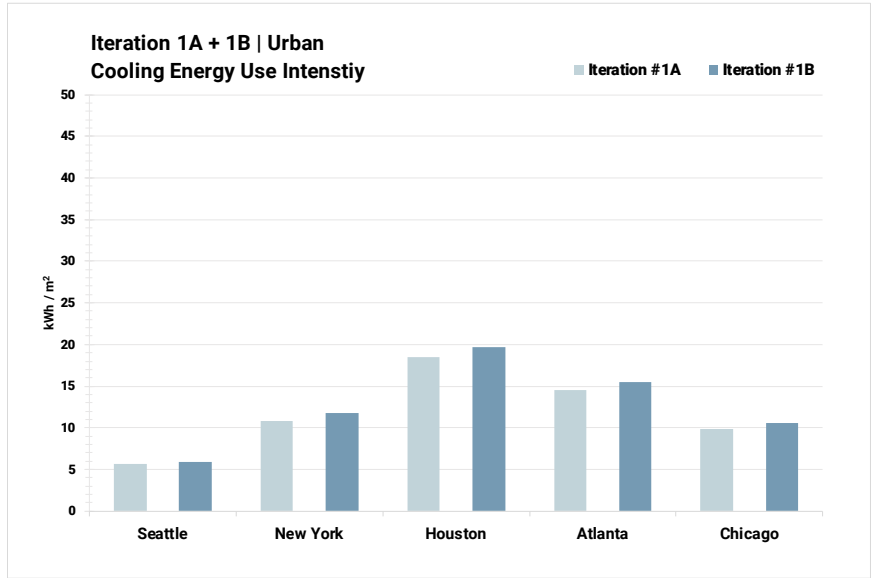


Figure 37. Model Set 1 Cooling EUI

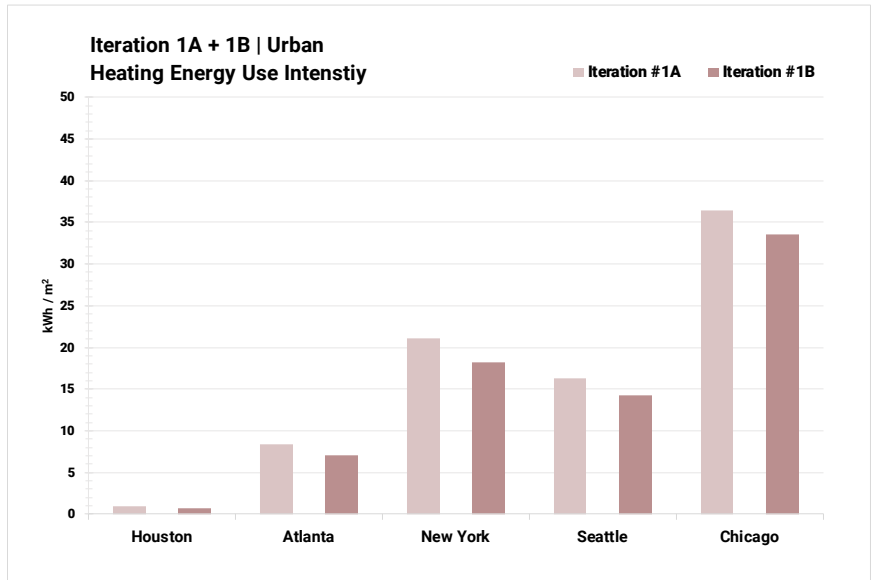


Figure 38. Model Set 1 Heating EUI

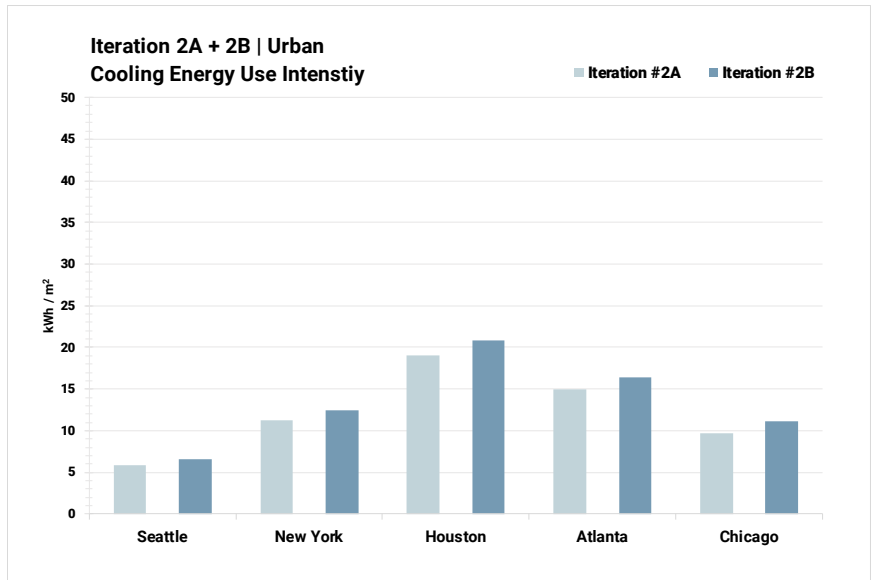


Figure 39. Model Set 2 Cooling EUI

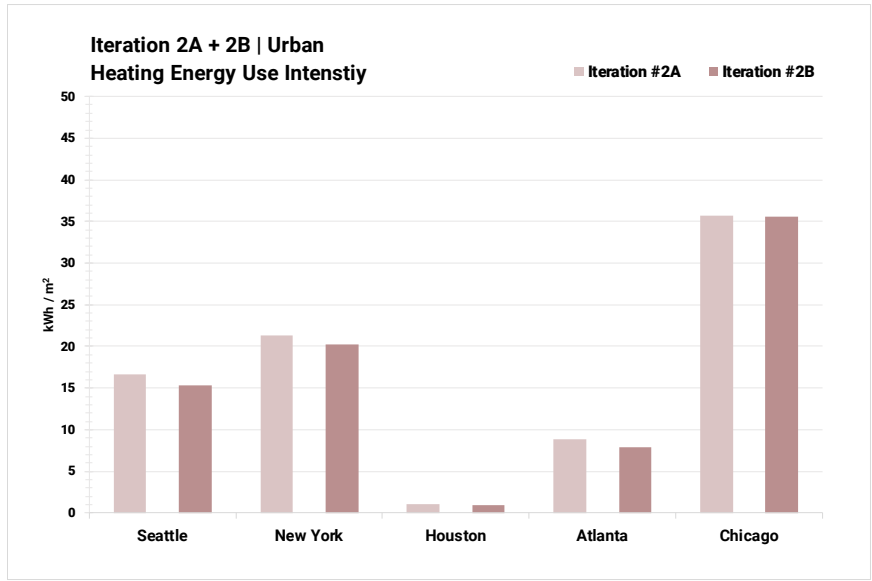


Figure 40. Model Set 2 Heating EUI

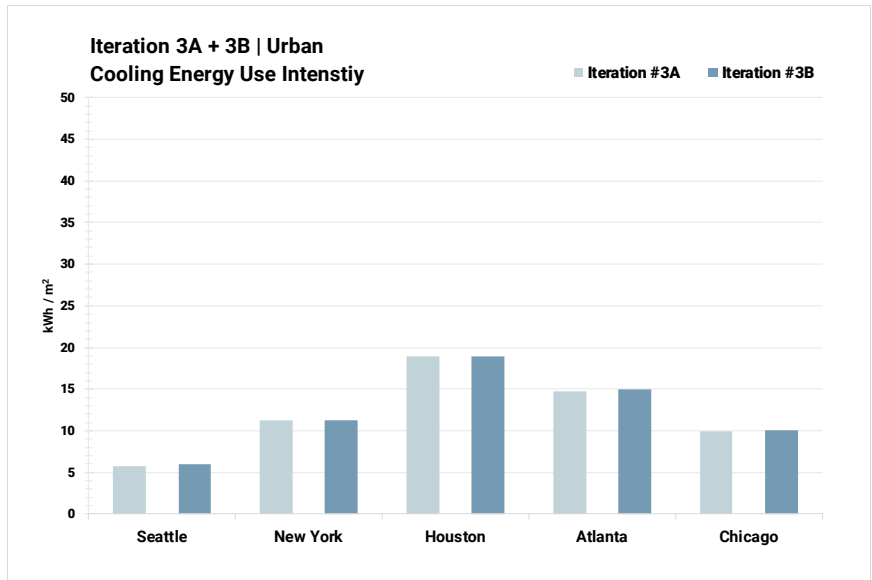


Figure 41. Model Set 3 Cooling EUI

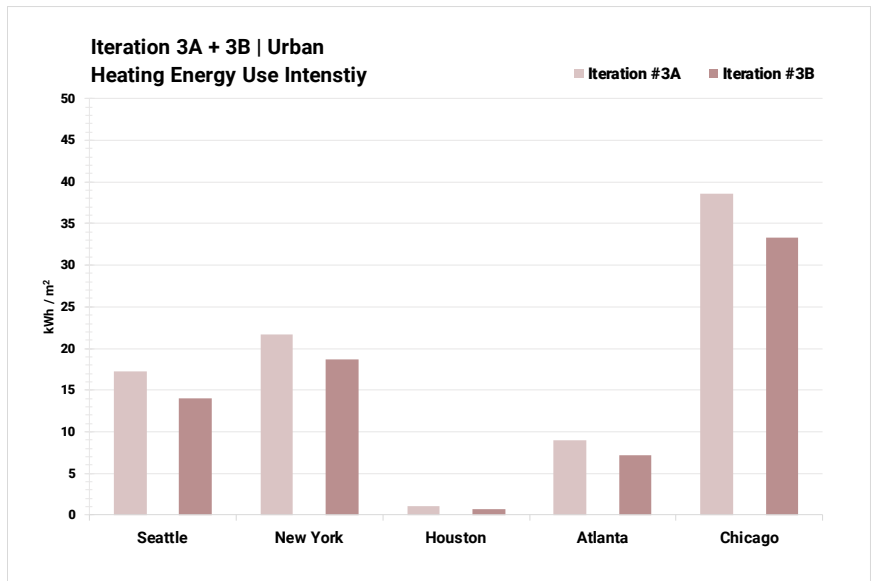


Figure 42. Model Set 3 Heating EUI

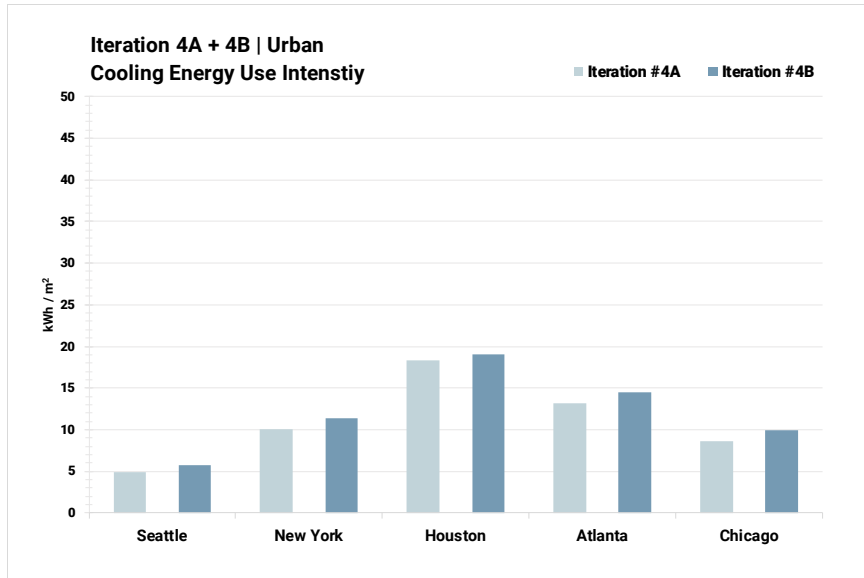


Figure 43. Model Set 4 Cooling EUI

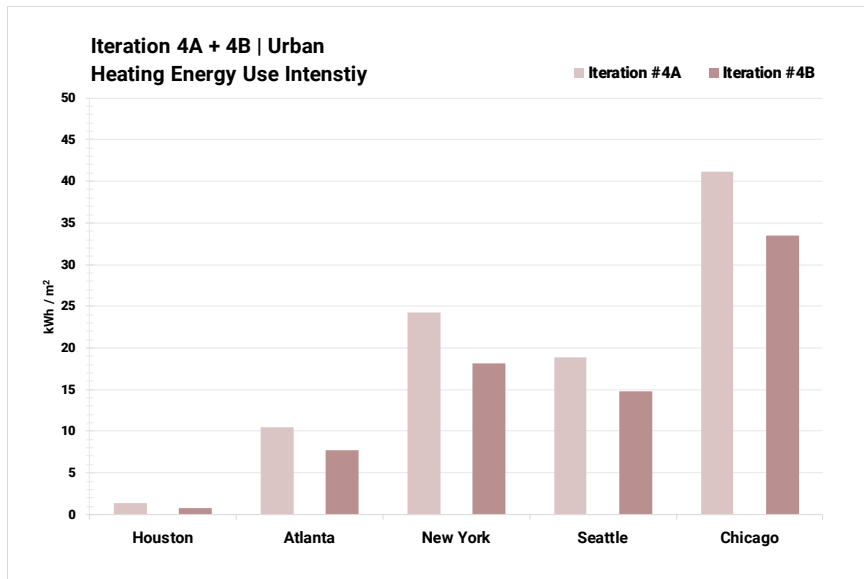


Figure 44. Model Set 4 Heating EUI

4.4. Carbon Intensity and Cost

To understand the impact of the UHI effect on the environment and on the end-use consumption of electricity, the performance of each model in each climate is evaluated by comparing calculated carbon intensity (kg/m^2) and electricity costs (cents/m^2) associated with the UHI intensity cooling and heating operations. The carbon emission factors for each city are based on 2016 state CO_2 output emission rates from the US Energy Protection Agency's (US EPA) Emissions & Generation Resource Integrated Database (eGRID) (US EPA, 2018). The electricity rates are based on 2019 state average price of electricity to ultimate customers by end-use sector (US EIA, 2019).

The results are displayed in Figure 45 through Figure 49. The best solutions, highlighted in pink, indicate the least increase or most decrease in carbon intensity and cost. However, it is not always possible to select clear solutions, or winners because in some instances, like in the case of Seattle, the differences across many of the iterations are almost negligible.

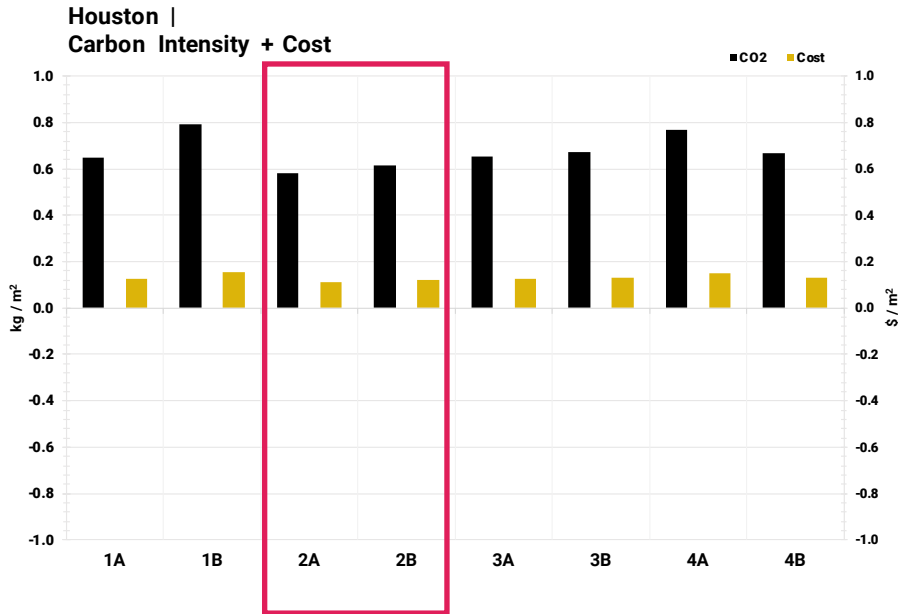


Figure 45. Houston | CO_2 Intensity and Electricity Cost

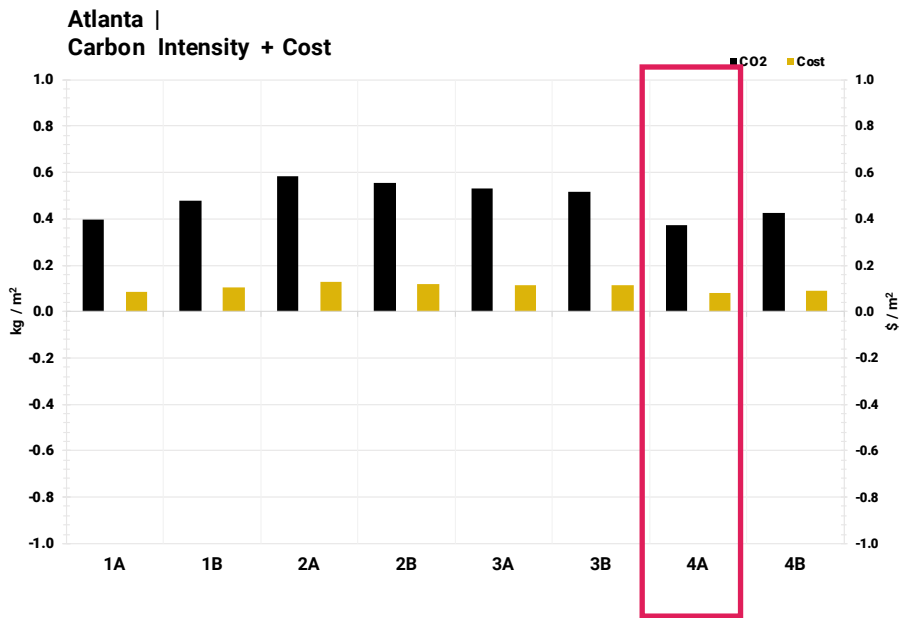


Figure 46. Atlanta | CO₂ Intensity and Electricity Cost

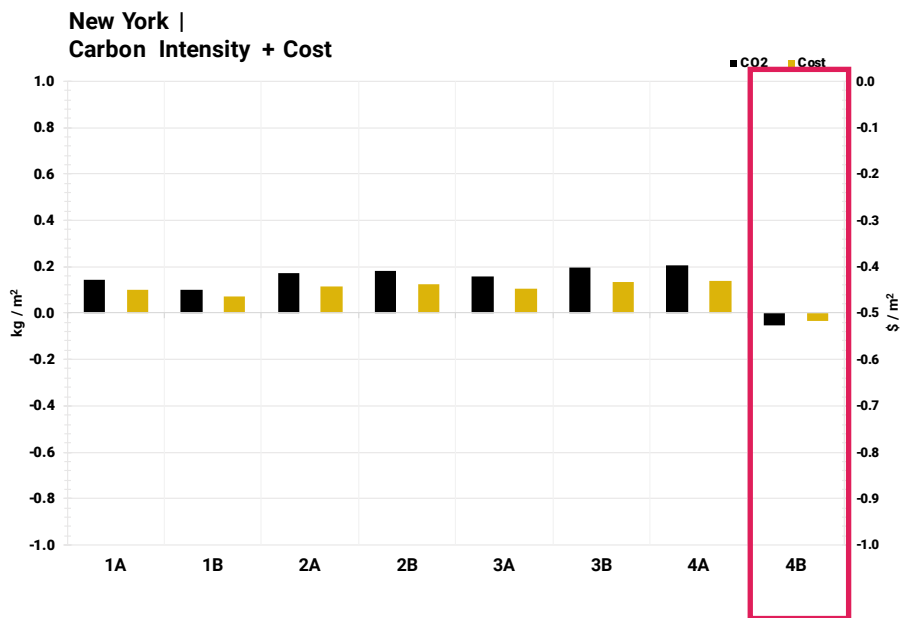


Figure 47. New York | CO₂ Intensity and Electricity Cost

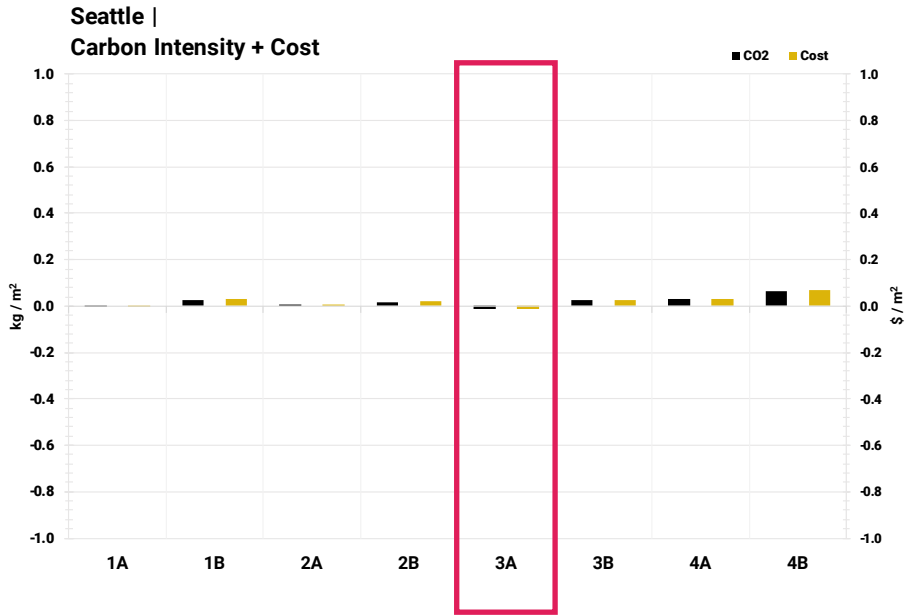


Figure 48. Seattle | CO₂ Intensity and Electricity Cost

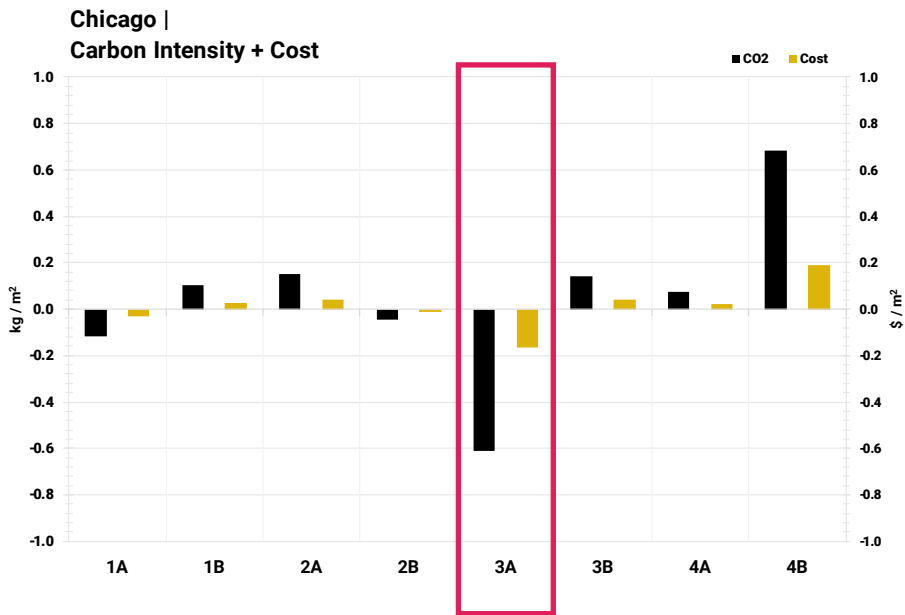


Figure 49. Chicago | CO₂ Intensity and Electricity Cost

5. Conclusion

The UHI effect implicates some of the most significant global challenges of the twenty-first century: population growth, rapid urbanization, and regional climate change. In many regions of the world, informal growth will strain local resources and pose major hindrances to sustainable urban development. Issues such as lack of infrastructure and housing, increased density and congestion, as well as inadequate planning for large-scale energy- and resource efficiency require both urgency and careful consideration in order to avoid poor planning practices that could exacerbate the adverse effects of UHI on the health, comfort and carbon footprints of cities. In order to create climate-responsive spaces and achieve better-performing cities, UHI analysis must be included in urban design practices.

The identified gap between UHI effect analysis, urban design and building performance lies in microclimate analysis. The temperature differences between rural and urban areas is typically unaccounted for due to the common practice of using rural climate files to design for urban spaces. This oversight often results in design errors for various performance metrics that are useful for benchmarking and establishing environmental performance targets at both building- and urban scales.

Existing engines that accurately evaluate UHI intensity have often not been incorporated into microclimate studies for urban environments by architects, designers, and urban planners due to prohibitively expensive computational costs, disconnected workflows within unintuitive or unfamiliar platforms, and uncertainty of difficult-to-obtain urban climatology parameters. These hindrances cause impactful delay within the design feedback loop and often generate a lack of confidence in the simulation process and output.

The objective of this research is therefore to incorporate UHI analysis into a useful and accessible design workflow that outputs in order to shape urban design practices that affect building performance.

5.1. Summary of Contributions

This thesis proposes a design integrated UHI effect analysis workflow by linking three key components:

1. Urban Weather Generator (UWG), an urban-scale climate prediction tool developed by Bruno Bueno (Bueno, 2012) to simulate microclimatic conditions of urban sites using operational weather station data.
2. Rhinoceros 3D, a conventional CAD design software.
3. Local Climate Zone (LCZ), a classification scheme developed by urban climate experts Iain Stewart and Timothy Oke as a means to standardize the quantitative physical descriptions of cities in a way that is relevant to observing urban climates.

UWG for Rhino is conceived for a simple and standard workflow that is meant to be intuitive, user-friendly and straightforward process in order to extend accessibility. The goal is to make the powerful and computationally cheap UWG engine accessible to design workflows by incorporating it as a plugin within Rhino 3D, and by coupling it with the LCZ classification scheme so that users can engage iterative microclimate analyses afforded by the computationally cheap simulations. UWG provides the method to quantify UHI effect. Rhino 3D provides a design platform that allows access to urban geometric parameters that can be automatically extracted UWG simulation, eliminating the redundancy presented in current text-based UWG workflows. The LCZ scheme provides a well-documented database and a reliable method for extracting or for estimating the difficult-to-obtain urban morphological parameters.

5.2. Future Work

This thesis is a starting point to including UHI intensity as a useful metric for multi-dimensional urban performance analyses. The limitations and the outcome of this process have provoked many research questions, specific to the scope of this thesis and in general to UHI effect.

For the workflow, it is worthwhile to further investigate and understand how various assumptions made by the UWG engine impact the engine's capability to digest various complexities of urban sites. For instance, the way in which 3D representations of vegetation are simplified for calculation, and the way in which site orientation is approximated when applying orientation specific factors like wind direction and solar radiation.

The GUI application's capabilities need to be expanded to automatically generate LCZ classification and appropriate urban morphological parameters. The GUI also needs further user testing and feedback.

For the design-integrated analysis, the consideration for colder climates is a meaningful extension to examine the impacts of other climates on the studied models. The studied iterations under each studied model set must be increased to examine the consistency of the simulation results. Lastly, the results must be studied in a multi-dimensional arena that includes other performance metrics for urban spaces in order to weigh in the impact of UHI analysis on overall urban design decision making.

References

- Bueno, B., Pigeon, G., Norford, L. K., Zibouche, K., & Marchadier, C. (2012). Development and evaluation of a building energy model integrated in the TEB scheme. *Geoscientific Model Development*, 5(2), 433–448. <https://doi.org/10.5194/gmd-5-433-2012>
- Bueno, Bruno. (2012). Study and prediction of the energy interactions between buildings and the urban climate Submitted to the Department of Architecture in Partial Fulfillment of the Requirements for the Degree of.
- Bueno, Bruno, Norford, L., Hidalgo, J., & Pigeon, G. (2012). The urban weather generator. *Journal of Building Performance Simulation*, 6(4), 269–281. <https://doi.org/10.1080/19401493.2012.718797>
- Bueno, Bruno, Roth, M., Norford, L., & Li, R. (2014). Computationally efficient prediction of canopy level urban air temperature at the neighbourhood scale. *Urban Climate*, 9, 35–53. <https://doi.org/10.1016/J.UCLIM.2014.05.005>
- Deru, M., Field, K., Studer, D., Benne, K., Griffith, B., Torcellini, P., ... Crawley, D. (2011). *U.S. Department of Energy Commercial Reference Building Models of the National Building Stock*. Retrieved from <http://www.osti.gov/bridge>
- Howard, L. (1883). *THE CLIMATE OF LONDON*. Retrieved from https://www.urban-climate.org/documents/LukeHoward_Climate-of-London-V1.pdf
- Ladybug Tools | Home Page. (n.d.). Retrieved May 20, 2019, from <https://www.ladybug.tools/>
- Mackey, C. (2017). *Urban_Weather_Generator_Workflow*. Retrieved from http://hydrashare.github.io/hydra/viewer?owner=chriswmackey&fork=hydra_2&id=Urban_Weather_Generator_Workflow&slide=0&scale=1&offset=0,0
- Mackey, C., & Roudsari, M. S. (2017). *The Tool vs. the Toolkit*. Retrieved from https://docs.google.com/presentation/d/11EqEb6TbLwhsQTzmdaGqK1daZ57IINy1mhRbXciu7ys/edit#slide=id.g26a027e876_0_115
- Mao, J. (2018). Automatic calibration of an urban microclimate model under uncertainty. Retrieved from <https://dspace.mit.edu/handle/1721.1/120873>
- Mao, J., Yang, J. H., Afshari, A., & Norford, L. K. (2017). Global sensitivity analysis of an urban microclimate system under uncertainty: Design and case study. *Building and Environment*, 124, 153–170. <https://doi.org/10.1016/j.buildenv.2017.08.011>
- Masson, V. (2000). A Physically-Based Scheme For The Urban Energy Budget In Atmospheric Models. *Boundary-Layer Meteorology*, 94(3), 357–397. <https://doi.org/10.1023/A:1002463829265>

- Nakano, A. (2015). *Urban Weather Generator User Interface Development: Towards a Usable Tool for Integrating Urban Heat Island Effect within Urban Design Process*. Massachusetts Institute of Technology.
- Nakano, A., Bueno, B., Norford, L., & Reinhart, C. F. (2015). URBAN WEATHER GENERATOR – A NOVEL WORKFLOW FOR INTEGRATING URBAN HEAT ISLAND EFFECT WITHIN URBAN DESIGN PROCESS Massachusetts Institute of Technology , Cambridge , USA Fraunhofer Institute for Solar Energy Systems ISE , Germany SIMULATION ENGINE & PLATFOR. *Building Simulation Conference*, 1901–1908. <https://doi.org/10.1016/S1091853104001594>
- National Renewable Energy Laboratory (NREL). (n.d.). Weather Data | EnergyPlus. Retrieved May 20, 2019, from <https://energyplus.net/weather>
- Oke, T. R. (1982). *The energetic basis of the urban heat island*. *Quart. J. R. Met. Soc* (Vol. 108). Retrieved from <https://rmets.onlinelibrary.wiley.com/doi/pdf/10.1002/qj.49710845502>
- Robert McNeel & Associates. (2019a). Eto Controls in Python with Python. Retrieved May 21, 2019, from <https://developer.rhino3d.com/guides/rhinopython/eto-controls-python/>
- Robert McNeel & Associates. (2019b). Rhino.Python Guides with Python. Retrieved May 21, 2019, from <https://developer.rhino3d.com/guides/rhinopython/>
- Sailor, D. J. (2011). A review of methods for estimating anthropogenic heat and moisture emissions in the urban environment. *International Journal of Climatology*, 31(2), 189–199. <https://doi.org/10.1002/joc.2106>
- Solemnia LLC | DIVA. (2019). Retrieved May 21, 2019, from <http://solemma.net/Diva.html>
- Stewart, I. D., & Oke, T. R. (2012). Local Climate Zones for Urban Temperature Studies. *Bulletin of the American Meteorological Society*, 93(12), 1879–1900. <https://doi.org/10.1175/BAMS-D-11-00019.1>
- Stewart, Iain D. (2011). Local Climate Zones: Origins, development, and application to urban heat islands. *Annual Meeting of the American Association of Geographers*, 1–16. Retrieved from <https://iainstew.files.wordpress.com/2013/01/seattle.pdf>
- U.S.DOE. (2012). Commercial Reference Buildings | Department of Energy. Retrieved May 21, 2019, from <https://www.energy.gov/eere/buildings/commercial-reference-buildings>
- UN-DESA Population Division. (2014). 2014 revision of the World Urbanization Prospects. Retrieved from <http://www.un.org/en/development/desa/publications/2014-revision-world-urbanization-prospects.html>
- UN-DESA Population Division. (2015). *World Urbanization Prospects The 2014 Revision*. Retrieved from <https://esa.un.org/unpd/wup/Publications/Files/WUP2014-Report.pdf>

- UN-DESA Population Division. (2017). *World Population 2017*. Retrieved from https://population.un.org/wpp/Publications/Files/WPP2017_Wallchart.pdf
- UN-DESA Population Division. (2018a). *World Urbanization Prospects: The 2018 Revision*. Retrieved from <https://population.un.org/wup/Publications/Files/WUP2018-KeyFacts.pdf>
- UN-DESA Population Division. (2018b). *World Urbanization Prospects - Population Division - United Nations*. Retrieved December 8, 2018, from <https://population.un.org/wup/Maps/>
- US Energy Information Administration. (2019). *Electric Power Monthly with data for February 2019*. Retrieved from www.eia.gov
- US EPA, O. (2018). Emissions & Generation Resource Integrated Database (eGRID). Retrieved from <https://www.epa.gov/energy/emissions-generation-resource-integrated-database-egrid>
- Voogt, J. (n.d.). ActionBioscience - promoting bioscience literacy. Retrieved December 12, 2018, from <http://www.actionbioscience.org/environment/voogt.html#primer>
- World Urban Database – World Urban Database and Access Portal Tools. (n.d.). Retrieved May 23, 2019, from <http://www.wudapt.org/>
- Yang, J. H. (2016). *The Curious Case of Urban Heat Island: A Systems Analysis*. MASSACHUSETTS INSTITUTE OF TECHNOLOGY.

Appendix

A. Tested Model Sets Expanded Information



1A.

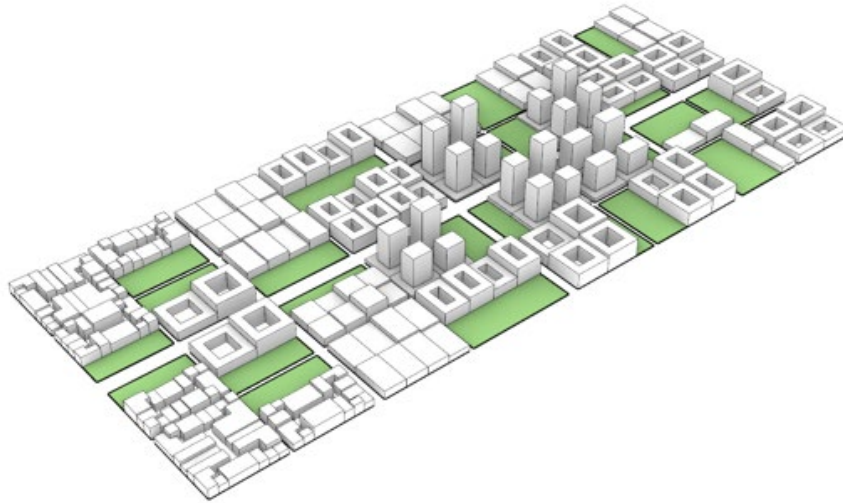


LCZ 02 | Compact Midrise

FAR 3.6 | 10% Vegetation

Commercial 60% | Residential 30% | Retail | 10%

| Parameter | Unit | Value | | |
|-------------------------|----------------|-----------------------|------------------------|-------------------|
| | | <i>Commercial 60%</i> | <i>Residential 30%</i> | <i>Retail 10%</i> |
| Average Height | m | 22.00 | 20.00 | 21.00 |
| Number of Floors | - | 6.00 | 7.00 | 4.00 |
| Floor Area | m ² | 2701768.00 | 1351525.00 | 482750.00 |
| Footprint Area | m ² | 513083.00 | 214143.00 | 146743.00 |
| Façade Area | m ² | 676933.00 | 250929.00 | 86658.00 |
| Urban Site | | | | |
| Average Building Height | m | 22.00 | | |
| Site Coverage Ratio | - | 0.69 | | |
| Facade-to-Site Ratio | - | 0.8 | | |
| Tree Coverage Ratio | - | 0.0 | | |
| Grass Coverage Ratio | - | 0.1 | | |
| Total Land Area | m ² | 1264315.36 | | |
| Total Footprint Area | m ² | 873969.00 | | |
| Total Floor Area | m ² | 4536043.00 | | |
| Floor Area Ratio | - | 3.6 | | |



1B.

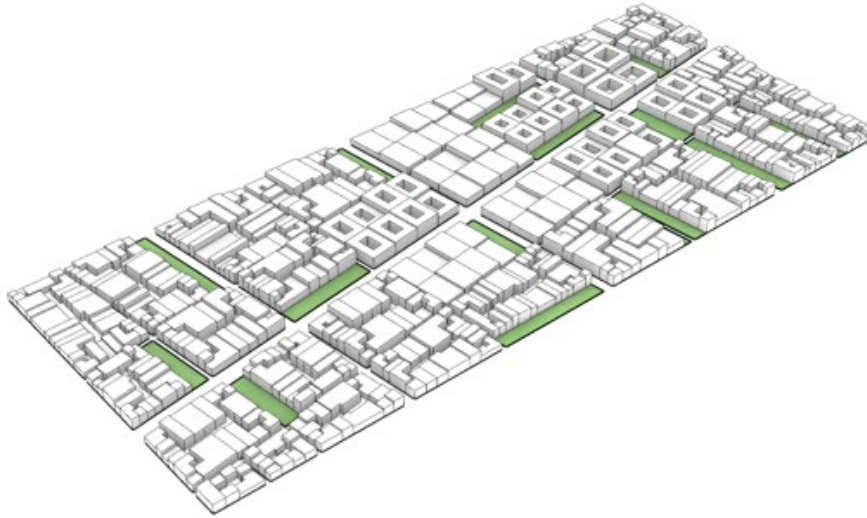


LCZ 04 | Open High-Rise

FAR 3.6 | **30% Vegetation**

Commercial 60% | Residential 30% | Retail | 10%

| Parameter | Unit | Value | | |
|-------------------------|----------------|-----------------------|------------------------|-------------------|
| | | <i>Commercial 60%</i> | <i>Residential 30%</i> | <i>Retail 10%</i> |
| Average Height | m | 27.00 | 24.00 | 34.00 |
| Number of Floors | - | 7.00 | 8.00 | 6.00 |
| Floor Area | m ² | 2684537.00 | 1365964.00 | 476484.00 |
| Footprint Area | m ² | 421400.00 | 179877.00 | 89254.00 |
| Façade Area | m ² | 744152.00 | 266931.00 | 201337.00 |
| Urban Site | | | | |
| Average Building Height | m | 27.00 | | |
| Site Coverage Ratio | - | 0.55 | | |
| Facade-to-Site Ratio | - | 0.96 | | |
| Tree Coverage Ratio | - | 0.00 | | |
| Grass Coverage Ratio | - | 0.3 | | |
| Total Land Area | m ² | 1264315.36 | | |
| Total Footprint Area | m ² | 690531.00 | | |
| Total Floor Area | m ² | 4526985 | | |
| Floor Area Ratio | - | 3.6 | | |



2A.

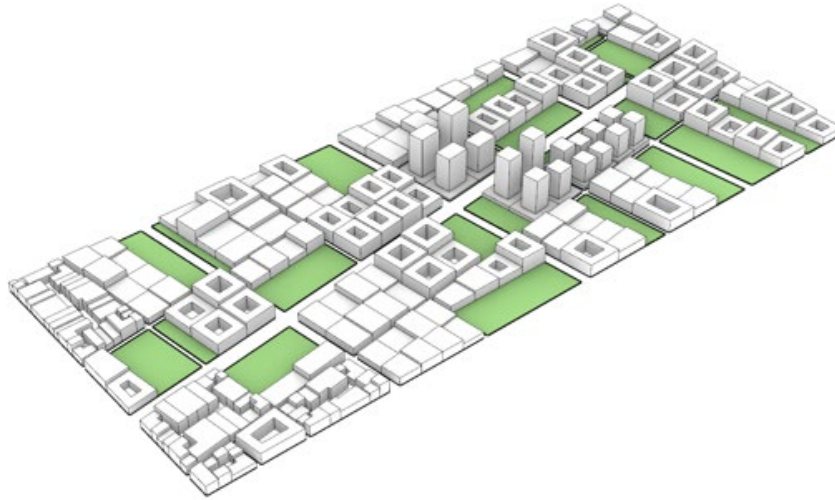


LCZ 02 | Compact Midrise

FAR 3.6 | **10% Vegetation**

Commercial 60% | Residential 30% | Retail | 10%

| Parameter | Unit | Value | | |
|-------------------------|----------------|-----------------------|------------------------|-------------------|
| | | <i>Commercial 60%</i> | <i>Residential 30%</i> | <i>Retail 10%</i> |
| Average Height | m | 23.00 | 22.00 | 21.00 |
| Number of Floors | - | 6.00 | 7.00 | 4.00 |
| Floor Area | m ² | 2742338.00 | 1391144.00 | 446006.00 |
| Footprint Area | m ² | 496679.00 | 202607.00 | 138115.00 |
| Façade Area | m ² | 728444.00 | 304844.00 | 104506.00 |
| <i>Urban Site</i> | | | | |
| Average Building Height | m | 22.00 | | |
| Site Coverage Ratio | - | 0.66 | | |
| Facade-to-Site Ratio | - | 0.90 | | |
| Tree Coverage Ratio | - | 0.00 | | |
| Grass Coverage Ratio | - | 0.1 | | |
| Total Land Area | m ² | 1264315.36 | | |
| Total Footprint Area | m ² | 837401.00 | | |
| Total Floor Area | m ² | 4579488.00 | | |
| Floor Area Ratio | - | 3.6 | | |



2B.

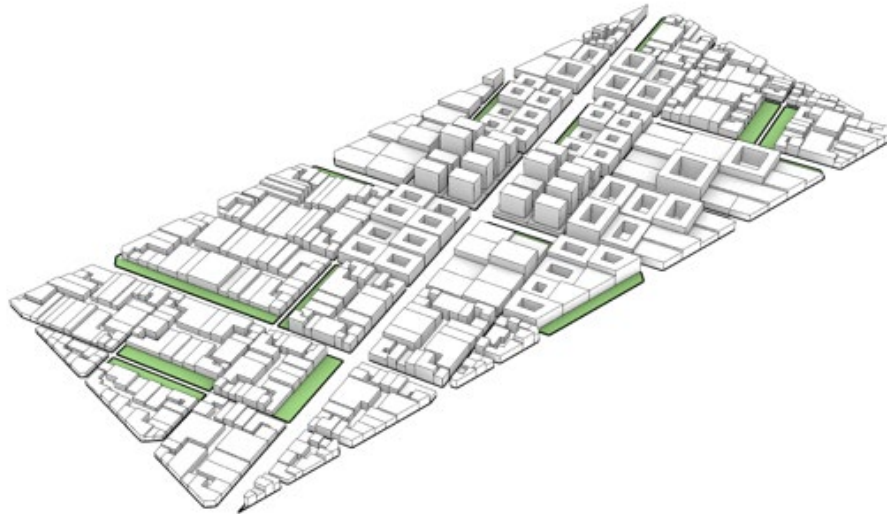


LCZ 04 | Open High-Rise

FAR 3.6 | 30% Vegetation

Commercial 60% | Residential 30% | Retail | 10%

| Parameter | Unit | Value | | |
|--------------------------|----------------|-----------------------|------------------------|-------------------|
| | | <i>Commercial 60%</i> | <i>Residential 30%</i> | <i>Retail 10%</i> |
| Average Height | m | 27.00 | 22.00 | 31.00 |
| Number of Floors | - | 7.00 | 7.00 | 5.00 |
| Floor Area | m ² | 2687972.00 | 1367571.00 | 435914.00 |
| Footprint Area | m ² | 423990.00 | 195594.00 | 91229.00 |
| Façade Area | m ² | 956302.00 | 395329.00 | 174877.00 |
| <i>Urban Site</i> | | | | |
| Average Building Height | m | 26.00 | | |
| Site Coverage Ratio | - | 0.56 | | |
| Facade-to-Site Ratio | - | 1.21 | | |
| Tree Coverage Ratio | - | 0.00 | | |
| Grass Coverage Ratio | - | 0.3 | | |
| Total Land Area | m ² | 1264315.36 | | |
| Total Footprint Area | m ² | 710813.00 | | |
| Total Floor Area | m ² | 4491457.00 | | |
| Floor Area Ratio | - | 3.6 | | |



3A.

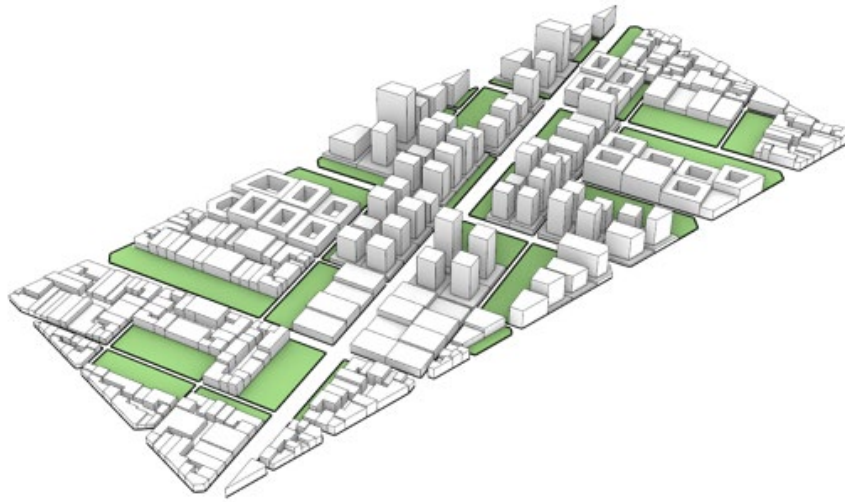


LCZ 02 | Compact Midrise

FAR 3.6 | **10% Vegetation**

Commercial 60% | Residential 30% | Retail | 10%

| Parameter | Unit | Value | | |
|-------------------------|----------------|-----------------------|------------------------|-------------------|
| | | <i>Commercial 60%</i> | <i>Residential 30%</i> | <i>Retail 10%</i> |
| Average Height | m | 23.00 | 16.00 | 28.00 |
| Number of Floors | - | 6.00 | 6.00 | 5.00 |
| Floor Area | m ² | 2679542.00 | 1332976.00 | 476450.00 |
| Footprint Area | m ² | 487735.00 | 266072.00 | 111762.00 |
| Façade Area | m ² | 635360.00 | 328037.00 | 205364.00 |
| | | Urban Site | | |
| Average Building Height | m | 22.00 | | |
| Site Coverage Ratio | - | 0.68 | | |
| Facade-to-Site Ratio | - | 0.92 | | |
| Tree Coverage Ratio | - | 0.00 | | |
| Grass Coverage Ratio | - | 0.1 | | |
| Total Land Area | m ² | 1264315.36 | | |
| Total Footprint Area | m ² | 865569.00 | | |
| Total Floor Area | m ² | 4488968.00 | | |
| Floor Area Ratio | - | 3.6 | | |



3B.



LCZ 04 | Open High-Rise

FAR 3.6 | 30% Vegetation

Commercial 60% | Residential 30% | Retail | 10%

| Parameter | Unit | Value | | |
|-------------------------|----------------|-----------------------|------------------------|-------------------|
| | | <i>Commercial 60%</i> | <i>Residential 30%</i> | <i>Retail 10%</i> |
| Average Height | m | 26.00 | 28.00 | 30.00 |
| Number of Floors | - | 7.00 | 10.00 | 5.00 |
| Floor Area | m ² | 2738641.00 | 1381221.00 | 377691.00 |
| Footprint Area | m ² | 438151.00 | 148584.00 | 76834.00 |
| Façade Area | m ² | 10127171.00 | 263570.00 | 153771.00 |
| Urban Site | | | | |
| Average Building Height | m | 27.00 | | |
| Site Coverage Ratio | - | 0.53 | | |
| Facade-to-Site Ratio | - | 1.13 | | |
| Tree Coverage Ratio | - | 0.00 | | |
| Grass Coverage Ratio | - | 0.3 | | |
| Total Land Area | m ² | 1264315.36 | | |
| Total Footprint Area | m ² | 663569.00 | | |
| Total Floor Area | m ² | 4497553.00 | | |
| Floor Area Ratio | - | 3.6 | | |



4A.

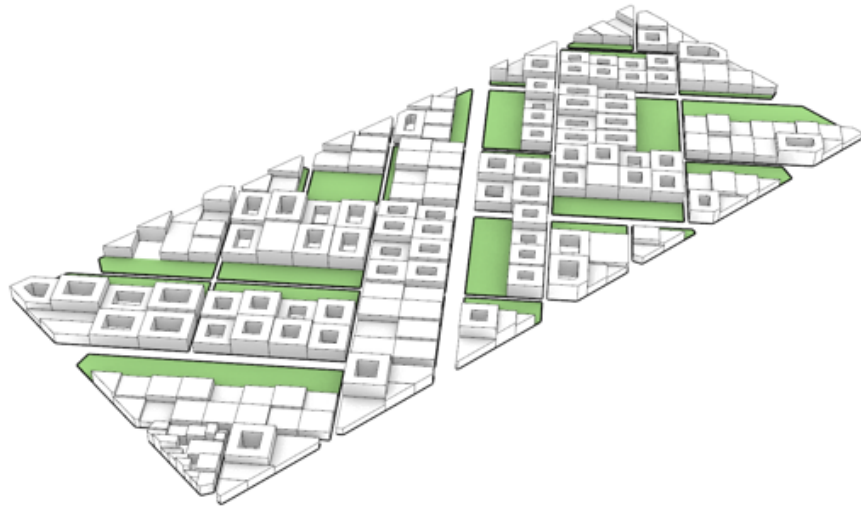


LCZ 02 | Compact Midrise

FAR 3.6 | **10% Vegetation**

Commercial 60% | Residential 30% | Retail | 10%

| Parameter | Unit | Value | | |
|-------------------------|----------------|-----------------------|------------------------|-------------------|
| | | <i>Commercial 60%</i> | <i>Residential 30%</i> | <i>Retail 10%</i> |
| Average Height | m | 20.00 | 21.00 | 24.00 |
| Number of Floors | - | 5.00 | 7.00 | 4.00 |
| Floor Area | m ² | 2641428.00 | 1380452.00 | 468943.00 |
| Footprint Area | m ² | 567751.00 | 211998.00 | 131834.00 |
| Façade Area | m ² | 550333.00 | 254342.00 | 187253.00 |
| Urban Site | | | | |
| Average Building Height | m | 20.00 | | |
| Site Coverage Ratio | - | 0.72 | | |
| Facade-to-Site Ratio | - | 0.78 | | |
| Tree Coverage Ratio | - | 0.00 | | |
| Grass Coverage Ratio | - | 0.1 | | |
| Total Land Area | m ² | 1264315.36 | | |
| Total Footprint Area | m ² | 911583.00 | | |
| Total Floor Area | m ² | 4490823.00 | | |
| Floor Area Ratio | - | 3.6 | | |



4B.



LCZ 04 | Open High-Rise

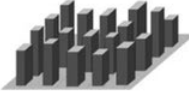
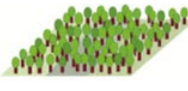



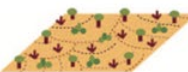











FAR 3.6 | **30% Vegetation**

Commercial 60% | Residential 30% | Retail | 10%

| Parameter | Unit | Value | | |
|-------------------------|----------------|-----------------------|------------------------|-------------------|
| | | <i>Commercial 60%</i> | <i>Residential 30%</i> | <i>Retail 10%</i> |
| Average Height | m | 26.00 | 28.00 | 30.00 |
| Number of Floors | - | 7.00 | 10.00 | 5.00 |
| Floor Area | m ² | 2745141.00 | 1389921.00 | 359591.00 |
| Footprint Area | m ² | 438151.00 | 148584.00 | 76834.00 |
| Façade Area | m ² | 10127171.00 | 263570.00 | 153771.00 |
| Urban Site | | | | |
| Average Building Height | m | 27.00 | | |
| Site Coverage Ratio | - | 0.53 | | |
| Facade-to-Site Ratio | - | 1.13 | | |
| Tree Coverage Ratio | - | 0.00 | | |
| Grass Coverage Ratio | - | 0.3 | | |
| Total Land Area | m ² | 1264315.36 | | |
| Total Footprint Area | m ² | 663569.00 | | |
| Total Floor Area | m ² | 4494653.00 | | |
| Floor Area Ratio | - | 3.6 | | |

B. Local Climate Zones Abridged Definitions

Table 4. Local Climate Zones Abridged Definitions

| Built types | Definition | Land cover types | Definition |
|--|--|---|--|
|  <p>1. Compact high-rise</p> | Dense mix of tall buildings to tens of stories. Few or no trees. Land cover mostly paved. Concrete, steel, stone, and glass construction materials. |  <p>A. Dense trees</p> | Heavily wooded landscape of deciduous and/or evergreen trees. Land cover mostly pervious (low plants). Zone function is natural forest, tree cultivation, or urban park. |
|  <p>2. Compact midrise</p> | Dense mix of midrise buildings (3–9 stories). Few or no trees. Land cover mostly paved. Stone, brick, tile, and concrete construction materials. |  <p>B. Scattered trees</p> | Lightly wooded landscape of deciduous and/or evergreen trees. Land cover mostly pervious (low plants). Zone function is natural forest, tree cultivation, or urban park. |
|  <p>3. Compact low-rise</p> | Dense mix of low-rise buildings (1–3 stories). Few or no trees. Land cover mostly paved. Stone, brick, tile, and concrete construction materials. |  <p>C. Bush, scrub</p> | Open arrangement of bushes, shrubs, and short, woody trees. Land cover mostly pervious (bare soil or sand). Zone function is natural scrubland or agriculture. |
|  <p>4. Open high-rise</p> | Open arrangement of tall buildings to tens of stories. Abundance of pervious land cover (low plants, scattered trees). Concrete, steel, stone, and glass construction materials. |  <p>D. Low plants</p> | Featureless landscape of grass or herbaceous plants/crops. Few or no trees. Zone function is natural grassland, agriculture, or urban park. |
|  <p>5. Open midrise</p> | Open arrangement of midrise buildings (3–9 stories). Abundance of pervious land cover (low plants, scattered trees). Concrete, steel, stone, and glass construction materials. |  <p>E. Bare rock or paved</p> | Featureless landscape of rock or paved cover. Few or no trees or plants. Zone function is natural desert (rock) or urban transportation. |
|  <p>6. Open low-rise</p> | Open arrangement of low-rise buildings (1–3 stories). Abundance of pervious land cover (low plants, scattered trees). Wood, brick, stone, tile, and concrete construction materials. |  <p>F. Bare soil or sand</p> | Featureless landscape of soil or sand cover. Few or no trees or plants. Zone function is natural desert or agriculture. |
|  <p>7. Lightweight low-rise</p> | Dense mix of single-story buildings. Few or no trees. Land cover mostly hard-packed. Lightweight construction materials (e.g., wood, thatch, corrugated metal). |  <p>G. Water</p> | Large, open water bodies such as seas and lakes, or small bodies such as rivers, reservoirs, and lagoons. |
|  <p>8. Large low-rise</p> | Open arrangement of large low-rise buildings (1–3 stories). Few or no trees. Land cover mostly paved. Steel, concrete, metal, and stone construction materials. | VARIABLE LAND COVER PROPERTIES | |
|  <p>9. Sparsely built</p> | Sparse arrangement of small or medium-sized buildings in a natural setting. Abundance of pervious land cover (low plants, scattered trees). | Variable or ephemeral land cover properties that change significantly with synoptic weather patterns, agricultural practices, and/or seasonal cycles. | |
|  <p>10. Heavy industry</p> | Low-rise and midrise industrial structures (towers, tanks, stacks). Few or no trees. Land cover mostly paved or hard-packed. Metal, steel, and concrete construction materials. | <p><i>b. bare trees</i></p> <p><i>s. snow cover</i></p> <p><i>d. dry ground</i></p> <p><i>w. wet ground</i></p> | <p>Leafless deciduous trees (e.g., winter). Increased sky view factor. Reduced albedo.</p> <p>Snow cover >10 cm in depth. Low admittance. High albedo.</p> <p>Parched soil. Low admittance. Large Bowen ratio. Increased albedo.</p> <p>Waterlogged soil. High admittance. Small Bowen ratio. Reduced albedo.</p> |

(I. D. Stewart & Oke, 2012)©American Meteorological Society. Used with permission.

C. Local Climate Zone Parameters

Table 5. Local Climate Zone Parameters

| Local climate zone (LCZ) | Sky view factor ^a | Aspect ratio ^b | Building surface fraction ^c | Impervious surface fraction ^d | Pervious surface fraction ^e | Height of roughness elements ^f | Terrain roughness class ^g |
|--------------------------------------|------------------------------|---------------------------|--|--|--|---|--------------------------------------|
| LCZ 1 <i>Compact high-rise</i> | 0.2–0.4 | > 2 | 40–60 | 40–60 | < 10 | > 25 | 8 |
| LCZ 2 <i>Compact midrise</i> | 0.3–0.6 | 0.75–2 | 40–70 | 30–50 | < 20 | 10–25 | 6–7 |
| LCZ 3 <i>Compact low-rise</i> | 0.2–0.6 | 0.75–1.5 | 40–70 | 20–50 | < 30 | 3–10 | 6 |
| LCZ 4 <i>Open high-rise</i> | 0.5–0.7 | 0.75–1.25 | 20–40 | 30–40 | 30–40 | >25 | 7–8 |
| LCZ 5 <i>Open midrise</i> | 0.5–0.8 | 0.3–0.75 | 20–40 | 30–50 | 20–40 | 10–25 | 5–6 |
| LCZ 6 <i>Open low-rise</i> | 0.6–0.9 | 0.3–0.75 | 20–40 | 20–50 | 30–60 | 3–10 | 5–6 |
| LCZ 7 <i>Lightweight low-rise</i> | 0.2–0.5 | 1–2 | 60–90 | < 20 | <30 | 2–4 | 4–5 |
| LCZ 8 <i>Large low-rise</i> | >0.7 | 0.1–0.3 | 30–50 | 40–50 | <20 | 3–10 | 5 |
| LCZ 9 <i>Sparse built</i> | > 0.8 | 0.1–0.25 | 10–20 | < 20 | 60–80 | 3–10 | 5–6 |
| LCZ 10 <i>Heavy industry</i> | 0.6–0.9 | 0.2–0.5 | 20–30 | 20–40 | 40–50 | 5–15 | 5–6 |
| LCZ A <i>Dense trees</i> | <0.4 | >1 | <10 | <10 | >90 | 3–30 | 8 |
| LCZ B <i>Scattered trees</i> | 0.5–0.8 | 0.25–0.75 | <10 | <10 | >90 | 3–15 | 5–6 |
| LCZ C <i>Bush, scrub</i> | 0.7–0.9 | 0.25–1.0 | <10 | <10 | >90 | <2 | 4–5 |
| LCZ D <i>Low plants</i> | >0.9 | <0.1 | <10 | <10 | >90 | <1 | 3–4 |
| LCZ E <i>Bare rock or paved</i> | >0.9 | <0.1 | <10 | >90 | <10 | <0.25 | 1–2 |
| LCZ F <i>Bare soil or sand</i> | >0.9 | <0.1 | <10 | <10 | >90 | < 0.25 | 1–2 |
| LCZ G <i>Water</i> | >0.9 | <0.1 | <10 | <10 | >90 | – | 1 |

^a Ratio of the amount of sky hemisphere visible from ground level to that of an unobstructed hemisphere

^b Mean height-to-width ratio of street canyons (LCZs 1–7), building spacing (LCZs 8–10), and tree spacing (LCZs A–G)

^c Ratio of building plan area to total plan area (%)

^d Ratio of impervious plan area (paved, rock) to total plan area (%)

^e Ratio of pervious plan area (bare soil, vegetation, water) to total plan area (%)

^f Geometric average of building heights (LCZs 1–10) and tree/plant heights (LCZs A–F) (m)

^g Davenport et al.'s (2000) classification of effective terrain roughness (z_o) for city and country landscapes. See Table 5 for class descriptions

(I. D. Stewart & Oke, 2012)©American Meteorological Society. Used with permission.